NUREG/CR-3920
SAND84-1246
R3
Printed August 1984

CORCON-Mod2: A Computer Program for Analysis of Molten-Core Concrete Interactions

R. K. Cole, Jr., D. P. Kelly, M. A. Ellis

Prepared by
Sandia National Laboratories
Albuquerque, New Mexico 87185 and Livermore, California 94550
for the United States Department of Energy
under Contract DE-AC04-76DP00789

Prepared for
U. S. NUCLEAR REGULATORY COMMISSION

Available from

GPO Sales Program
Division of Technical Information and Document Control
U.S. Nuclear Regulatory Commission
Washington, D.C. 20555

and

National Technical Information Service
Springfield, Virginia 22161

NUREG/CR-3920
SAND84-1246
R3

CORCON-MOD2: A COMPUTER PROGRAM FOR ANALYSIS OF MOLTEN-CORE CONCRETE INTERACTIONS

R. K. Cole, Jr.
D. P. Kelly
M. A. Ellis*

Thermal/Hydraulic Analysis Division

Printed: August 1984

Sandia National Laboratories
Albuquerque, New Mexico 87185
Operated by
Sandia Corporation
for the
U. S. Department of Energy

Prepared for
Division of Accident Evaluation
Office of Nuclear Regulatory Research
U. S. Nuclear Regulatory Commission
Washington, DC 20555
Under Memorandum of Understanding DOE 40-550-75
NRC FIN No. A-1019

---

*The Proteus Corp., Albuquerque, NM

ABSTRACT

CORCON is a computer code for modelling the interactions between molten core materials and concrete, such as might occur following a core meltdown accident in a Light Water Reactor. It may also be applied to experiments which simulate such accident conditions. The code predicts the behavior of the system, including heat transfer, concrete ablation, cavity shape change, and gas generation. The first version, CORCON-MOD1, was released in 1981. This report is a complete users' manual and reference for the updated version, CORCON-MOD2. The major changes are the inclusion of models for solidification of the melt and for its (non-explosive) interactions with coolant water. In addition, a number of improvements have been made in response to experience with CORCON-MOD1. The new code remains compatible with the old in the sense that MOD2 will accept any input data set which was accepted by MOD1.

CONTENTS

Page

FIGURES

TABLES

ACKNOWLEDGEMENTS

Among the many individuals who contributed to either the development of CORCON or the generation of this report, we have room to mention only a few. We wish to thank George Greene, who provided the model for the effects of gas flow on inter-layer heat transfer and the comparisons of the bubble models with experimental data. We also acknowledge our debt to several users (you know who you are!) of earlier versions of the code, whose strange interpretations of instructions and perverse choices of input parameters uncovered a number of bugs which might otherwise never have been found. Despite the extra work this caused (and our comments at the time), we must admit that both the code and its documentation were improved as a result. Finally, we would like to express our gratitude to Jan Frey for her work in preparation of the manuscript, and to Dr. Bradley Burson and Ms. Cynthia Walker of the NRC Office of Nuclear Regulatory Research for their extremely careful editing of it. If, despite their efforts, some errors or ambiguities remain, the authors assume full responsibility.

NOMENCLATURE

a	Laplace constant = $[\sigma/g(\rho_\ell-\rho_g)]^{1/2}$
A	Area
$[A]$	Aerosol concentration
c_p	Specific heat at constant pressure
C_i	Heat capacity of layer i for the new layer mass at the old temperature
f	Fraction of evolved gas entering bubbles
g	Gravitational acceleration (= 9.806 m/s^2); Gibbs free energy
h	Specific enthalpy; heat transfer coefficient
H	Total enthalpy
ΔH	Change in enthalpy; latent heat of fusion
ΔH_{abl}	Heat of ablation
k	Thermal conductivity
ℓ	Liquid layer thickness
L	Characteristic length; layer thickness
m	Mass
M	Molecular weight
Nu	Nusselt number (= hL/k)
p	Pressure
P	Power
Pr	Prandtl number (= $\mu c_p/k$)
q	Heat flux
Q	Heat flow
r	Radial coordinate
r_b	Equivalent spherical radius of a bubble

R	Radius of layer
R_o	Universal gas constant (= 8.3141 J/g-mol K)
Ra	Rayleigh number (= $g\beta\Delta T\, \ell^3/\nu\kappa$)
Re	Reynolds number (= $\rho uL/\mu$)
s	Specific entropy; slope in Shaw viscosity model
$\dot{s}$	Surface recession (ablation) rate
S	Volumetric heat source
t	Time
T	Temperature
$\bar{u}$	Average streamwise velocity in gas film
u_b	Velocity of rising bubbles
U_T	Terminal rise velocity of a single bubble
v	Molar volume
V	Volume
V_s	Superficial velocity
x	Streamwise coordinate (along gas film)
x_i	Mole fraction of species i
X_i	Layer enthalpy change in temperature units (= $\Delta H/\hat{C}$)
z	Vertical coordinate (positive downward in cavity definition)
α	Gas void (volume) fraction
β	Volumetric coefficient of expansion
δ	Gas film thickness; crust thickness
ε	Emissivity
θ	Cavity surface inclination angle
κ	Thermal diffusivity

λ	Time constant in decay power expression
μ	Dynamic viscosity
ν	Kinematic viscosity ($= \mu/\rho$)
ρ	Density
σ	Surface tension
σ_B	Stefan-Boltzmann constant ($= 5.67 \times 10^{-8}$ W/m^2K^4)
Φ	Volume fraction of solids in a solid-liquid mixture
Ω	Degree of implicitness employed in solution of inter-layer and pool surface heat transfer (fully explicit = $0 \leq \Omega \leq 1$ = fully implicit)

<u>Subscripts</u>

a	Atmosphere
abl	Ablation
B	Bubbling film
c	Concrete; convective
cln	Coolant
CHF	Critical Heat Flux
e	Elemental
f	Fluid
F	Film
fg	Vaporization
g	Gas phase
i	ith species or layer
I	Interface
ℓ	Liquid phase
L	Laminar; layer

Leid	Leidenfrost (minimum film boiling point)
p	Pool
r	Radiative; radial
R	Radial
rad_{net}	Net radiation
s	Solidification
sat	Saturation
sur	Surroundings
T	Turbulent; top
TR	Transition
W	Ablating concrete surface (wall)
z	Axial

Superscripts

k	kth temperature range in thermal equation of state
ℓ	Liquid, liquidus
m	Melting state
n	nth time level
o	Standard or unperturbed state
s	Solid; solidus
~	Projected
^	Property of new composition at old temperature

1. INTRODUCTION

A proper assessment of the risks to the public associated with the operation of nuclear power plants requires a realistic evaluation of the important accident sequences. The Reactor Safety Study[1] demonstrated that the risks associated with Light Water Reactors (LWR's) are dominated by core meltdown sequences. In these hypothetical accident sequences, loss of normal and emergency cooling systems leads to melting and slumping of the core. If uninterrupted, this is followed by failure of the pressure vessel and deposition of molten core and associated structural materials onto the concrete floor of the reactor cavity.

The interaction of the resulting pool of debris with the concrete has been identified as an important part of the accident sequence. The debris is maintained at elevated temperatures by decay heat from non-volatile fission products retained in the melt. The temperatures and heat fluxes involved are sufficient to decompose and ablate concrete; such attack could fail containment by basemat penetration. This would result in a release of radioactivity to the soil underneath the reactor building.

Potentially more important are the various mechanisms which can lead to above-ground failure of containment and release of radioactivity to the atmosphere. The most obvious of these involve the large amounts of water vapor and carbon dioxide which are produced by the decomposition of concrete. These gases, if they come into contact with molten metals, are reduced to hydrogen and carbon monoxide. (Small quantities of hydrocarbons and other species are also formed.) All four major gases contribute to the risk of eventual overpressurization of containment; hydrogen and carbon monoxide are also combustible, presenting an additional risk of sudden overpressurization if they are ignited. Also, ablative attack may cause the failure of internal structures in the containment building such as the reactor pedestal in a boiling water reactor (BWR); the resulting mechanical disruption could fail the containment itself. Finally, heat from the debris may be sufficient by itself to cause the failure of containment. This might happen, for example, by degradation of the containment penetration seals in a BWR.

A research program to investigate molten core/concrete interactions was initiated at Sandia National Laboratories in July 1975, under the sponsorship of the Reactor Safety Research Division of the U. S. Nuclear Regulatory Commission. This program was initially experimental, but its scope was soon broadened to include the development of computer models to describe the interactions. A preliminary model, based on limited data and

using untested assumptions, was quickly developed by W. B. Murfin in 1977.[2] This model, INTER1, was intended as a qualitative tool, suitable for sensitivity studies; its use for quantitative prediction was specifically discouraged by its author.[2]

Following the release of INTER1, work was begun on development of an improved computer code, CORCON. This program was intended to provide a more detailed--and more mechanistic--description of the physical processes involved in molten core/concrete interactions. The first version of the code, CORCON-MOD1,[3] was released in 1981. It lacked models for the freezing of core debris and for interactions between debris and a coolant (water), which limited its applicability to the early stages of accidents involving dry reactor cavities. Later development work has concentrated on removing these limitations. Also, as experience with the code accumulated, several deficiencies in the existing modelling became apparent and improvements were made to correct them.

It was decided that CORCON-MOD1 would be supported as originally issued. That is, errors which prevented the code from performing as intended (as indicated by the users manual) would be corrected, but improved models would not be issued until an entire new version of the code was completed. This report describes that second version of the code, CORCON-MOD2. The restrictions mentioned above have been removed by the inclusion of freezing and coolant models. Heat transfer and viscosity models have been improved, and the code has been brought into conformity with the 1977 ANSI standard for FORTRAN programming.[4]

While CORCON-MOD2 is a significant improvement over its predecessor, its predictions should not be accepted blindly for several reasons. Firstly, there are significant assumptions and simplifications in the code which can affect its applicability to certain problems. The most important of these is the quasi-steady-state model for concrete response. We believe that this is an acceptable approximation for many hypothetical reactor accident conditions and for experiments with sustained heating. However, for many transient experiments the period of ablative interaction (about 5 minutes) is not much longer than the time necessary to establish quasi-steady ablation. Secondly, some sub-models (the freezing model is an example) must be considered preliminary because the governing phenomena are not yet clearly understood. Finally, code predictions have yet to be subjected to extensive comparison with experimental data. (This situation should change as data become available from Sandia's LMF (Large Melt Facility) and the German BETA Facility.) Therefore, at least for the time being, we suggest "caveat usor".

2. PROGRAM DESCRIPTION

2.1 CORCON Phenomenology

CORCON is a general computational model describing the interactions between molten core materials and concrete. In this section, we present a brief description of the principal interaction phenomena modelled in the code. The generalizations are based in part on calculations for the "Sample Problem" of Section 7 and similar problems.

A great deal may be understood about core/concrete interactions from a very simple picture. The attack of core debris on concrete is largely thermal in a light-water reactor. Decay heat (and some heat from chemical reactions) is generated in the pool and may be lost either through its top surface or to concrete. In many experimental studies, externally-supplied induction heating is substituted for the reactor decay heat. In either case, so long as the heat source is sufficiently large, the situation rapidly approaches a quasi-steady state where these losses balance the internal sources. The partition of internally generated heat between concrete and surface is determined by the ratio of the thermal resistances of the corresponding paths. In this simple view, pool behavior is dominated by conservation of energy, with heat-transfer relations providing the most important constitutive relations.

Under most circumstances, the heat flux to the concrete is sufficient to decompose it, releasing water vapor (adsorbed and from hydroxides) and carbon dioxide (from carbonates), and to melt the residual oxides. The surface of the concrete is ablated at a rate which is typically several centimeters per hour. The molten oxides and molten steel from reinforcing bars in the concrete are added to the pool. The gases are strongly oxidizing at pool temperatures and will be reduced, primarily to hydrogen and carbon monoxide, on contact with metals in the pool. Ultimately the reacted and unreacted gases enter the atmosphere above the pool. These gases may or may not burn immediately, depending on their temperature at the time that they reach a region which is not already depleted of oxygen. Modelling of these above-pool phenomena is not included in CORCON-MOD2.

Gas released at the bottom of the pool rises through it as bubbles. In CORCON-MOD2, this process is described using a Taylor instability model[5,6] which is analogous to film boiling. Gas released at the sides of the pool is assumed to form a rising gas film between the melt and the concrete, although this is not observable and is not universally accepted. The presence of gas bubbles in the pool swells it, increasing its depth and its interfacial area with concrete. These rising gas bubbles

also result in the production of aerosols containing fission products stripped from the fuel debris. The source may be large from the point of view of consequences; in terms of reducing pool inventories, however, it is a relatively minor effect, although a few fission-product species may be completely depleted.

Because of decomposition in depth, the thermal response of the concrete is complex. The released gases produce internal pressures which drive flows of carbon dioxide, steam, and liquid water through the pores of the concrete. Experiments[7] performed at heat fluxes sufficient to ablate concrete, together with an analytic model[8] suggest that the major effect is the creation of a "wet zone" in the concrete at about 400K, with pores partially filled with liquid water. Here, adsorbed water has been freed but not vaporized, and is being driven away from the heated surface by the internal pressure. At greater temperature rises, however, the temperature profile has been shown[9] to be consistent with pseudo-steady ablation of an effectively homogeneous material. Transient concrete response is not treated by CORCON-MOD2, which uses a simple one-dimensional, steady-state ablation model.

Experimental evidence[10a,11] shows that the various oxidic species in the melt are highly miscible, as are the metallic species, but that the two groups are mutually immiscible. Buoyancy forces are usually sufficient to separate the molten debris into two phases, even in the presence of vigorous mixing by gases from the decomposition of concrete. If the oxidic phase is initially denser than the metallic phase, and settles to the bottom, a second less dense oxidic layer will form above the metal; it is composed of concrete oxides ablated by the metal (lighter than and not miscible in the metal) and steel oxides produced by chemical reaction with the concrete-decomposition gases. This three-layer configuration, oxide/metal/oxide, (if it occurs at all) does not last long; the fuel oxides become diluted by concrete oxides until the mixture is less dense than the metal and the pool "rolls over" into a configuration with all oxides in a single layer above the metal. Of course, this does not happen instantaneously; during the period when the difference in density is small, the separation is probably incomplete with substantial heterogeneous mixing. CORCON calculations, with both MOD1 and MOD2, suggest that the three-layer configuration cannot last more than about one hour. No mixing is included in the calculations.

If water is present, it will form an additional layer at the top of the pool. It is often suggested that this layer does not react violently with the molten material underneath it, but merely serves as an enhanced heat sink. This is likely to cool the top of the melt below the solidification temperature, resulting in a thin solid crust on the surface. Experiments[12] have

shown that the presence of water over simulated debris does not significantly alter the attack on concrete by the debris. Another possibility suggested[13] is that gas stirring would be sufficient to break up crusts as they form with the result that the molten pool is rather quickly converted to a (coolable) debris bed. This is supported in the referenced paper by evidence from simulant experiments using liquid nitrogen and water or Freon-11. A third possibility is the occurrence of a steam explosion. Violent interactions have been observed when water was poured onto molten bismuth or lead.[14] CORCON-MOD2 considers only the first possibility, and does not allow for either steam explosions or the reduction of a molten pool to a coolable debris bed.

As time progresses, the pool grows, its surface area increases, and decay heating decreases. Therefore, pool temperatures and heat fluxes decrease, and the possibility of refreezing arises. Substantial freezing of the metallic phase may occur. However, the large internal heating and small thermal conductivity of the oxidic phase prevent the existence of steady crusts more than a few centimeters thick. The bulk of this phase will remain liquid, probably for weeks.[10f] The question of the permeability of these crusts and solids to gases is unresolved.

Coupling between the molten pool and the rest of containment is rather one-sided; the pool serves as a source of mass and energy while being only weakly influenced by conditions in containment. (Of course, if material is falling into the pool from the cavity structure, there is another coupling, but it is one-sided in the other direction.) Containment pressure affects the properties of gases in the pool and of any water over the molten debris. However, the effects--on gas-related heat-transfer coefficients, on equilibrium gas compositions, and on the temperature and latent heat of the water--are relatively small. Heat loss from the top of the molten debris is dominated by radiation to containment structures or to the overlying water. Because of the fourth-power temperature dependence of the radiative flux, this loss is rather insensitive to containment temperatures (unless they are very high). In the absence of a water layer, the optical properties of the atmosphere may become significant. Molecular absorption by atmospheric gases is a relatively small effect,[10f] but aerosol concentrations may be great enough that the atmosphere is optically thick.[10g]

Because CORCON-MOD2 is not intended to serve as a full containment code, no attempt is made to model above-pool structures as was done by Kelly.[15] The surroundings temperature and atmospheric pressure are user specified and may be given as functions of time. In order to obtain more realistic estimates of

pool losses, the decrease in radiative heat transfer from the pool surface to the surroundings associated with atmospheric attenuation by aerosols is approximately accounted for. The calculation is based on diffusion theory for gray, infinite parallel plates, and an aerosol concentration is calculated internally for the purpose of determining the atmospheric extinction coefficient during the interaction.

2.2 Calculational Cycle

We have designed the calculational cycle in CORCON to reflect our view of the interrelationships of the various phenomena described in the preceding Section. Thus, a brief description of the calculational cycle should aid in understanding the physics involved, as well as making clear what is (and is not) modelled.

At the start of a timestep, CORCON-MOD2 has a complete "snapshot" of the problem, first from initialization and thereafter from the results of the preceding timestep. In particular, it has available the cavity shape, the stratification of the pool, and the mass, composition, and thermal state (temperature and enthalpy content) of each layer. In addition, it has all necessary transport properties, heat fluxes, ablation rates, and so forth. All of these variables are advanced to new end-of-timestep values using the calculational cycle described below, which has been modified from CORCON-MOD1.

1. Calculate a timestep. This may be constant (as in CORCON-MOD1) or variable, subject to user control.

2. Calculate the pool internal mass transport, melt/gas chemical reactions, and associated energy terms. Injection rates of concrete decomposition products (already known) are assumed to remain constant over the timestep, and the calculation proceeds in two passes. The first follows rising gases and condensed-phase materials (e.g., concrete slag entering the metal layer), layer by layer. If the material should remain in the current layer, its mass and energy are added to that of the layer; otherwise, it is equilibrated thermally with this layer and passed on to the next. Gas passing through a metal-containing layer is equilibrated chemically with the metal and the oxidic reaction products are added to the rising oxides, with any heat of reaction remaining in the layer. When the surface of the pool is reached, the rising gases are passed to an interface routine which disposes of them and initializes any downward mass flows (such as added coolant or decomposed concrete falling into the pool). As coded in CORCON-MOD2, this interface routine simply

records the gas flows for later printing and sets all downward flows to zero. However, a more general model, perhaps a full containment response code, could easily be attached through the same interface. Finally, in a second layer-by-layer pass, falling condensed-phase materials are followed downward until they are added to the appropriate layer.

3. Finish the explicit advancement of the layer energy equations. This includes addition of decay heat and subtraction of heat lost to concrete. It also accounts for interlayer heat transfer and loss from the pool surface based on start-of-timestep rates. If coolant is present and boiling, the calculation is completed here; otherwise the matrix equations for an implicit calculation of the interlayer and surface terms is set up at this time. A linearized representation of the pool thermal response, surface heat flux vs surface temperature, is then constructed.

4. Determine a (provisional) end-of-timestep value for the temperature of the surface of the pool by matching heat fluxes to and from this surface. This uses the linearized pool response and the "exact" relationships for above-pool heat transfer. If desired, the change of temperature of atmosphere and surroundings during the timestep could be included in this calculation and made consistent with the heat flux. The simple routine provided could easily become part of the interface to a more general model. Finally, a linearized representation of the above-pool thermal response, surface heat flux vs surface temperature, is constructed.

5. Complete the solution of the implicit interlayer heat transfer equations, using the provisional end-of-timestep surface temperature, to determine final layer enthalpies. Reconcile these with the known layer masses and compositions (from step 2) to determine new layer temperatures.

6. Calculate the new cavity shape, using start-of-timestep ablation rates, treated as constant over the timestep.

7. Calculate new layer densities. Determine if previous layer ordering is still appropriate; if not, flip and/or combine layers.

8. Calculate new layer transport properties (viscosity, conductivity, etc) from new compositions and temperatures.

9. Calculate bubble-rise velocities and (from known gas flow rates) pointwise void fractions in the pool. From the void fractions, the known volume of condensed phases in each layer, and the cavity shape, determine the elevation of each layer interface.

10. Evaluate decay (or externally imposed) heat sources.

11. Evaluate heat transfer between layers and resulting interlayer heat fluxes. The linearized above-pool response evaluated in step 4 is used in this calculation; the final temperature of the pool surface determined here will differ slightly from the provisional value established in step 4.

12. Calculate pointwise ablation rates along the melt-concrete interface. The thermal resistance of the gas film is calculated based on local conditions of gas flow, and the rate at which gas is entering the film. This rate is made consistent with the local heat flux and ablation rate.

At this point, we once again have a complete "snap shot" representation of the problem, appropriate to the end of the timestep. Note that at this point in the calculational cycle all calculated phenomena are at the same time level, allowing the generation of an internally consistent printed edit of the state of the system if desired at the current time. This was not the case in CORCON-MOD1, in which essentially all heat transfer coefficients and heat fluxes were one timestep out-of-date.

An examination of the main program, CORCON, will show that these steps are performed in the order 7-12, edit if required, check for end of problem, 1-6, and repeat. This is because steps 7-11 are also required as part of initialization. Performance of the calculation as part of the main transient calculation (rather than duplicating the calls in routine INITL) has a significant advantage if the code is to be overlaid, because it reduces the size of the overlay required for initialization. This has been found necessary in some cases when CORCON is coupled to a containment code.

2.3 Programming Information

CORCON-MOD2 is coded in FORTRAN which conforms with ANSI standard X3.9-1978 ("FORTRAN 77").[4] The only changes in language from CORCON-MOD1 are use of type CHARACTER for alphanumeric data, use of BLOCK IF structures in the newer routines. Fixed fields in FORMATS are still specified as nH... rather

than '...', and PARAMETER statements are not used. In cases where constants are to have full machine accuracy (e.g. pi/2), they are evaluated by execution of a short routine called SETUP. The code reads data from FORTRAN UNIT 5 and writes to UNIT 6. OPEN statements are not included; their inclusion might be desirable for some applications.

The code contains approximately 10500 source lines, including 3500 lines of COMMENTs of which 1300 are blank. It requires approximately 102 k (octal) of core for execution on the CDC CYBER-76, approximately the same as CORCON-MOD1. (In fact, the source-generated code is somewhat smaller than CORCON-MOD1, 66 k vs 70 k. The library routines for the FTN5 (FORTRAN 77) compiler appear to occupy approximately 6 k (octal) more core than those of the old FTN compiler.)

2.4 MOD2 Improvements to CORCON

CORCON-MOD2 contains many improvements over CORCON-MOD1. The most obvious are:

1. A crust-formation and freezing model has been included. This model will treat the eventual freezing of pool debris, as well as its initial melting if it is not already molten at the time of deposition.

2. A model for interaction with an overlying coolant has been included, including a full representation of the boiling curve.

3. Radiative heat transfer from the melt surface includes an approximate treatment of the opacity effects of suspended aerosols in the atmosphere. This includes a mechanistic determination of atmospheric attenuation as a function of an empirically-estimated aerosol concentration.

4. A change in the treatment of two-phase viscosities has eliminated an unphysical behavior often observed in CORCON-MOD1. With the old model, the oxidic phase could become thermally isolated from its surroundings, heat up to temperatures near 3000K, and then suddenly cool again.

5. The Bottinga-Weill viscosity model for siliceous materials has been replaced by Shaw's model. In CORCON-MOD1, discontinuities in the viscosity model were seen to trigger unphysical behavior in some cases. The new model eliminates these discontinuities, and produces results which are more reasonable.

6. In most cases, the models for heat transfer in liquids now account for bubble effects using correlations based on BNL data, rather than modified Konsetov forms. They also consider natural convection, in a form consistent with Kulacki's data, and an approximate conduction limit. (For very thin layers, CORCON-MOD1 would sometimes predict convective heat transfer rates smaller than would occur by conduction.)

7. Reactor cavity pressure may be specified by the user as a tabular function of time. This pressure affects the properties of gases within the pool, the saturation temperature of any overlying water above the debris, and the concentration of aerosols in the reactor cavity.

8. Chemical reactions of metals in the debris pool with bubbles and with gases in the film between the melt and the concrete are included. In CORCON-MOD1, only the reactions with gas bubbles were treated.

9. Variable timesteps and edit frequencies are permitted.

10. The printed output has been expanded and clarified, and all quantities are at the same time level. Input data are echoed to produce a permanent record, and the version of the code being used is identified for configuration control. The output includes gas generation rates, an approximate energy budget for the debris pool, and checks on the conservation of mass and energy.

Less obvious changes include:

11. The film heat-transfer model has been revised, and the transitions between film regimes improved.

12. The concrete recession package has been recoded to eliminate numerical problems.

13. The chemical equilibrium package has been improved to increase its efficiency and reliability.

14. Treatment of the pool surface has been modified to make it a "natural" interface for coupling to containment codes.

15. Many other routines have been simplified and clarified.

16. Calls to material property routines have been made consistent. The data contained in them have been reformatted so that the DATA statements have the form of easily-readable tables.

3. DESCRIPTION OF MODELS

The CORCON code requires models for the system components, for the various physical processes which occur, and for the material properties required to evaluate the interactions. The models in CORCON-MOD2 are described in the following sections.

3.1 System Components

The principal components of the CORCON system are the debris pool, the concrete, and the atmosphere and surroundings above the pool. The composition of each component is specified through user input in terms of a "master list" of chemical species. The list, presented in Table 3.I, is divided into four groups: oxidic compounds, metals and other elements, gases, and miscellaneous compounds. As noted in the table, not all of the species in the master list are available to the user for specification of initial compositions. The aluminates (species 12-17) are a holdover from the viscosity modelling of CORCON-MOD1 and are not used in MOD2. The fission-product pseudo species (oxides 24-28, metal 45 and gases 75-76) are used in the decay-heat generation model; the amount of each present is determined within the code, starting from the concentration of fission products in the fuel.

Although we believe that the list of available species is more than ample for describing the physical and chemical processes pertinent to the interaction of molten LWR core materials (and coolant) with concrete, blank spaces have been left in the list for future additions. Such additions to the list might be required, for example, for treatment of the sodium chemistry associated with core/concrete interactions in LMFBR accidents.

3.1.1 Debris Pool

CORCON models the debris pool as consisting of a number of layers contained in a concrete cavity. These layers are, from bottom up, a heavy oxide phase (HOX), a heavy heterogeneous mixture of oxides and metals (HMX), a metallic phase (MET), a light heterogeneous mixture (LMX), a light oxide phase (LOX), a coolant (CLN), and the atmosphere (ATM). The three-letter mnemonics are useful in describing the pool structure, and have been used in appropriate variable names throughout the code. Layer volumes, including the swelling effects of gas bubbles, determine the elevations of layer interfaces and of the pool surface.

TABLE 3.I

CHEMICAL SPLCIES INCLUDED IN CORCON MASTER SPECIES LIST

Oxides		Metals and Other Elements		Gases		Miscellaneous	
1	SiO_2	41	Fe	56	C(g)	86	H_2O evap
2	TiO_2	42	Cr	57	CH_4	87	H_2O chem
3	FeO	43	Ni	58	CO	88	$CaCO_3$
4	MnO	44	Zr	59	CO_2	89	$Ca(OH)_2$
5	MgO	45	*FpM	60	C_2H_2	90	H_2O coolant
6	CaO	46	Mn	61	C_2H_4	91-95	Blank
7	SrO	47	C(c)	62	C_2H_6		
8	BaO	48	Na	63	H		
9	Li_2O	49	**X	64	H_2		
10	Na_2O	50-55	Blank	65	H_2O		
11	K_2O			66	N		
12	$KAlO_2$			67	NH_3		
13	$NaAlO_2$			68	N_2		
14	$BaAl_2O_4$			69	O		
15	$CaAl_2O_4$			70	O_2		
16	$MgAl_2O_4$			71	OH		
17	$MNAl_2O_4$			72	CHO		
18	Fe_2O_3			73	CH_2O		
19	Al_2O_3			74	$CrO_3(g)$		
20	UO_2			75	*$FpMO_2(g)$		
21	ZrO_2			76	*$FpMO_3(g)$		
22	Cr_2O_3			77-85	Blank		
23	NiO						
24	*$FpMO_2(c)$						
25	*$FpMO_3(c)$						
26	*FpOx						
27	*FpAlkMet(c)						
28	*FpHalogn(c)						
29	Fe_3O_4						
30	Mn_3O_4						
31	PuO_2						
32-40	Blank						

*Pseudo species representing four condensed phase fission product groups.

**Inert oxidic species treated as an element "X" in melt/gas-phase equilibrium calculation.

Aluminates, species 12-17, not used in CORCON-MOD2.

These seven layers are always present in the data structure, but may be "empty" in the sense of containing no material. In particular, the heterogeneous mixtures HMX and LMX have been included in anticipation of further model improvements but are always empty: although most of the coding relating to these layers is included in CORCON-MOD2, there is currently no provision for introducing material into them. Note that the coolant (CLN) is treated as another layer, on the same footing as debris-containing layers.

Within this system, a one-layer pool (not counting a possible coolant) would only have material in HOX or MET. A two-layer pool would have material in MET, and in HOX or LOX depending on the relative densities of oxide and metal. A three-layer pool can be formed with material in HOX (primarily fuel oxides), in MET, and in LOX (primarily concrete and steel oxides). The code allows for the possibility that the oxidic phase (fuel) may initially be denser than the metallic phase. It is important to note that this is not externally imposed: the code tests relative densities and relocates the contents of HOX into LOX as soon as $\rho_{HOX} < \rho_{MET}$.

An overlying coolant layer can be added to any of these configurations; its composition must be specified as water (H_2O).

3.1.2 Concrete Cavity

The concrete cavity containing the core debris is assumed to be axisymmetric. Two simple geometries are available to describe its initial shape, as a cylinder with either a flat base or a hemispherical base. The shape of the cavity is represented and tracked by the position of a number of points, termed "body points", on its surface. A general (axisymmetric) initial shape may also be defined by specifying the initial position of each body point.

The composition of the concrete must also be specified, and may be chosen as one of the three built-in default concretes. These are referred to as "basaltic aggregate concrete", "limestone aggregate common sand concrete", and "generic southeastern United States concrete". The last is the so-called "CRBR concrete". The compositions of these concretes are given in Table 3.II; they are based on measured compositions reported by Powers.[10b] The solidus and liquidus temperatures for these concretes, also included in internal data, are given in Table 3.III; the user must specify an ablation temperature somewhere between these limits.

TABLE 3.II

CHEMICAL COMPOSITIONS OF DEFAULT CONCRETES
(Values in w/o)

Species	Species No.	Basaltic Aggregate Concrete	Limestone Aggregate-Common Sand Concrete	CRBR Concrete
SiO_2	1	54.84	35.80	3.60
TiO_2	2	1.05	0.18	0.12
MnO	4	0.00	0.03	0.01
MgO	5	6.16	0.48	5.67
CaO	6	8.82	31.30	45.40
Na_2O	10	1.80	0.082	0.0078
K_2O	11	5.39	1.22	0.68
Fe_2O_3	18	6.26	1.44	1.20
Al_2O_3	19	8.32	3.60	1.60
Cr_2O_3	22	0.00	0.014	0.004
CO_2	59	1.50	21.154	35.698
H_2O evap	86	3.86	2.70	3.94
H_2O chem	87	2.00	2.00	2.00

TABLE 3.III

MELTING RANGES OF DEFAULT CONCRETES

	Temperature (K)	
Concrete	Solidus	Liquidus
Basaltic Aggregate	1350	1650
Limestone Aggregate-Common Sand	1420	1670
CRBR	1690	1875

Alternatively, provision is made for the user to define a "non-standard" concrete. In this case, its composition and melt range must be user-specified, in addition to the ablation temperature. The concrete composition may be specified either in terms of $CaCO_3$ and $Ca(OH)_2$, or as their decomposition products, CaO, CO_2, and H_2OCHEM (chemically bound water). The latter form is used internally, with the code performing the conversion if necessary.

Steel reinforcing bar in the concrete is also permitted; if present, it is assumed to be pure iron (Fe). Concrete, with or without reinforcing steel, is treated as a homogeneous material.

3.1.3 Atmosphere and Surroundings.

The atmosphere above the pool and its surroundings serve as sinks for mass (evolved gases) and energy (convection and radiation from the pool surface). CORCON-MOD2 contains very simple models for these components. The atmosphere is described by a specified (constant) temperature and (time-dependent) pressure. The surroundings are described by a specified (time-dependent) temperature and (time- or temperature-dependent) emissivity. Within the code, the pool surface (bottom of the atmosphere) is treated as a major computational interface. Very limited information, restricted to mass flows and (linearized) heat transfer relations, is passed across the interface. Thus, because the interface is well defined and actively used in the stand-alone code, a more-detailed above-pool model--or a full containment response code--could be easily substituted.

Heat transfer from the pool surface is by convection and radiation, with the latter mode ordinarily dominant. Convective heat transfer is calculated using the atmosphere temperature, while radiative heat transfer uses the surroundings temperature. If desired, CORCON-MOD2 computes atmospheric aerosol concentration for the purpose of estimating the optical thickness of the cavity atmosphere above the pool.

3.2 Physical Processes

A number of physical processes are included in the modelling of molten-fuel/concrete interactions; these include internal energy generation, mass and heat transfer, chemical reactions, concrete response, and bubble phenomena. The models are described in the following subsections. The level of detail is intended to be sufficient for understanding of the basic concepts and the code implementation; for details, the reader should consult the references. In several cases, one or more phenomena

are tightly coupled and must be considered simultaneously. For example, concrete response determines gas generation, which affects heat transfer and the heat flux to concrete, which in turn feeds back to determine concrete response. We will note such coupled interactions in the discussion which follows.

3.2.1 Energy Generation

The entire fuel/concrete interaction process is driven by decay heat generated in the pool, including actinides, decay products and irradiated structural materials. Because of the loss of some of the more volatile fission products before the pool is formed, use of the ANS Standard decay curve is not appropriate. While decay heating could be calculated using detailed decay chains, as described in the Users' Manual for CONTAIN,[16] the isotopic information is not needed for fission-product tracking in CORCON-MOD2. Therefore, we have included a much simpler decay heat model in the code.

Bennett[17] has shown that the decay power for typical reactor cores in the 1-hour to 10-day time-frame is nearly proportional to operating power and relatively insensitive to burnup. Therefore, a SANDIA-ORIGEN[18] calculation was performed for a reference core representative of a large PWR core at equilibrium burnup (3320 MWt and 33000 MWD/MTU). From the results of this calculation, we identified 27 elements (excluding noble gases) which account for essentially all the heat production in the reference core in the time-frame of interest. We assume that the initial intact-core inventory is proportional to core operating power, as specified by the user. The initial pool inventory of fission products is then determined by the fraction of the core contained in the melt, as given by the mass of UO_2 and the user-specified core size, multiplied by a "retention fraction" for each element. These retention fractions account for partial loss of the more volatile species during the early phases of meltdown. The elements, their assumed chemical forms[19] and concentrations in the core, and the default retention fraction for each species[1] are given in Table 3.1V. The retention fractions may be overridden by the user if desired.

The decay power is calculated using the further assumption that the specific decay power (W/g-atom) associated with each element is a simple function of time after SCRAM. The values of the decay power associated with each element (also taken from the reference SANDIA ORIGEN calculation) were fit in the form

$$P(t) = m_e \, C \, e^{-\lambda t} \qquad (3.2\text{-}1)$$

where $P(t)$ is the decay power (W)
t is the time after SCRAM (days)
m_e is the elemental mass (gram-atoms)
and C (W/gram-atom)
λ (day $^{-1}$)

are the fit coefficients. Four time intervals are used with breaks at 0, 0.1, 0.6, 2.2, and 20 days. The different fit coefficients for each time period reflect the changing isotopic compositions of the elements.

There may be further losses from the melt during the interaction due to further vaporization, and to mechanical sparging and aerosol generation driven by concrete decomposition gases. We found that, based on Powers' data,[10d] aerosol generation was not a significant factor in material loss or reduction of decay power. Therefore, only vaporization of alkali metals and halogens is considered in the present model. It is extremely unlikely that either group will be present in elemental form because the alkali metals boil (at one atmosphere) slightly below 1000K and the halogens boil below 500K. The halogens will probably be present as alkali halides (e.g. CsI) with boiling points of 1500-1600K. Under ordinary conditions, the melt will contain more alkali metal than halogen; the excess will most probably occur as hydroxides with boiling points comparable to the halides. However, the retention fractions may be specified such that the amount of halogen present exceeds the amount of alkali metal. If this occurs, the model in CORCON-MOD2 will eliminate the excess halogen during initialization; an appropriate message is written to the output file. The remaining halogens and alkali metals are then removed exponentially in time with an arbitrary but reasonable half-life of 10 minutes.

Except in the decay model, the fission products and actinides are grouped as four pseudo elements, as follows:

FpM - metals which may oxidize, and whose oxides may volatilize
FpOx - chemically inert oxides
FpAlkMet - alkali metals
FpHalogn - halogens.

Thus, the composition of the melt is represented in terms of these four pseudo elements which are resolved into actual elements only for the calculation of decay power.

3.2.2 Pool Layer Heat Transfer

Heat is removed at the boundaries of the pool, which are its top surface and its interface with concrete. As discussed in Section 2, the internal temperature of the pool adjusts rather

TABLE 3.IV

DECAY-HEAT ELEMENTS AND GROUPINGS

Pseudo-Element	Element	Mass Concentration [g-atom/MW(thermal)]	Retention Fraction[1]
FpM			
Metals	Mo	.6053	.97
	Tc	.1545	.97
	Ru	.3885	.97
	Rh	.0690	.97
	Sb	.00244	.85
	Te	.0627	.85
FpOx			
Monoxides	Sr	.2155	.90
	Ba	.1915	.90
Dioxides	Zr	.7352	.99
	Ce	.3870	.99
	Np	.0422	.99
	Cm	.00204	.99
	Nb	.01139	.99
	Pu	.7921	.99
	Am	.00593	.99
Sesquoioxides	Y	.1099	.99
	La	.1662	.99
	Pr	.1446	.99
	Nd	.4638	.99
	Sm	.0539	.99
	Eu	.01705	.99
FpAlkMet			
Alkali Metals	Rb	.0819	.19
	Cs	.3776	.19
FpHalogn	Br	.00530	.10
Halogens	I	.0320	.10
UO_2	U	user input	
Zr, ZrO_2	Zr (Structural)	user input	

quickly so that these heat losses balance the internal heat generation and the heat transfer approaches a steady state. Therefore, we have developed quasi-steady models for heat transfer in CORCON-MOD2. The principal advantage of quasi-steady models is that heat fluxes at any time depend on the current state of the pool and not on its history. For example, fully developed flow is assumed in convective correlations and the temporal development of boundary layers is not considered.

In CORCON-MOD2, we employ a multi-layered pool model (Section 3.1.2) for which it is convenient to consider heat transfer one layer at a time. Given a trial set of interfacial temperatures, a solution is found (independently) for each layer. Newton's iteration is then used to revise the interfacial temperatures to satisfy the requirement that the heat flux must be continuous at all interfaces between layers. The solutions for the individual layers are repeated at each step. The heat-transfer model allows for several possible configurations in each layer: the layer may be completely molten; it may have a solid crust on one or more surfaces, or it may be completely solid. In this section, we will address heat transfer in a liquid layer or the liquid portion of a partially-solidified layer. The modifications necessary to account for crusting or freezing will be described in the next section.

Heat transfer coefficients are required from the interior of a liquid layer to its surfaces. If the layer were a right circular cylinder there would be three such coefficients, to the upper, lower, and radial surfaces. In CORCON-MOD2, these three heat transfer coefficients are evaluated for a cylinder whose thickness and volume match those of the layer. Boundaries with other layers are assumed to be horizontal, and the corresponding heat transfer coefficients employed directly. For the boundary with concrete, an appropriate combination is constructed, as described in Section 3.2.4, to account for the actual inclination of the surface.

The analysis includes the effects of the passage of concrete decomposition gases through the liquid. A number of models have been proposed for heat transfer in the presence of bubble agitation or injection. In CORCON-MOD1, heat transfer was based on the Konsetov model,[20] as modified by Blottner,[21] with a different expression for each surface. In CORCON-MOD2, this model has been retained only for the radial (vertical) surface, in the form

$$h = k\,(Pr\,g/\nu^2)^{1/3}\,(0.05\alpha)^{1/3} \qquad (3.2.2\text{-}1)$$

where Pr is the Prandtl number of the liquid, ν is its kinematic viscosity, g is the acceleration of gravity, and α is the void fraction. This resembles a (turbulent) natural convection correlation with a bubble buoyancy term, $\rho\alpha$ replacing the thermal-expansion buoyancy term, $\rho\beta\Delta T$. (In CORCON-MOD1, another term was included in the bracket to produce the appropriate natural-convection limit as the superficial velocity goes to zero. In CORCON-MOD2, this limit is separately imposed, as described below.)

Since the release of CORCON-MOD1, Ginsberg and Greene[22] have compared simulant data for horizontal liquid/liquid interfaces subjected to a gas flux with the predictions of several models and concluded that the Konsetov forms of CORCON-MOD1 "seriously underpredict...the data." Both Greene's data and those of Werle,[23,24] were included. Therefore, heat transfer coefficients for horizontal surfaces are calculated in CORCON-MOD2 from Greene's correlation of the experimental data

$$h = 5.05 \frac{k}{r_b} \left(\frac{\rho_\ell V_s r_b}{\mu_\ell} \right)^{1/2} P_r^{0.8} \qquad (3.2.2\text{-}2)$$

Here r_b is the effective radius (based on volume) of the bubbles in the layer. This resembles the Szekely model,[25] which may be put in the form of Equation 3.2.2-2 with the Prandtl number raised to the 0.5 power and the coefficient replaced by 1.69. Szekely's model may be derived from the idea that heat is transferred by transient conduction with bubbles periodically disrupting the developing thermal gradients. It is therefore referred to as a "surface renewal" model.

Ginsberg and Greene also noted that further enhancement of heat transfer by entrainment effects became significant at rather modest gas superficial velocities on the order of 1 cm/s. This is not considered in CORCON-MOD2 because the heat transfer coefficients are already so large that their exact values are not critical--the pool is almost isothermal, and the losses of heat from its boundaries are primarily controlled by other thermal resistances.

For the coolant layer, boiling heat transfer is also included. The model in CORCON-MOD2 includes the full boiling curve, based on standard pool boiling correlations as summarized by Bergles.[26] No correction is made for the effects of gas injection at the melt/coolant interface. The various correlations involved are not used directly in CORCON-MOD2. This is possible because the boiling heat transfer coefficient for a given fluid, water in this case, is a function of pressure and temperature only, with all of the detailed dependence of material properties on temperature and

pressure contained in the one function. A series of calculations was performed outside the code, using thermal and transport properties from the Steam Tables,[27] to generate tables of values. These were then fit by simple analytic forms, which reproduce the tables within 3% over the pressure range of 10kPa to 10MPa (saturation temperatures from 320K to 580K). The principal advantage of using these fits is that the extensive libraries of water properties themselves need not be included in the code.

Nucleate boiling is treated by using the Rohsenow[28] correlation for the temperature rise and the Zuber[29,30] correlation (with Rohsenow's coefficient[31] for the critical heat flux to calculate the values of q_{CHF} and of $T_w - T_{sat}$ at the point of critical heat flux. These are represented as

$$q_{CHF} = \frac{1.50 \times 10^{-6} (10^{-5} p)^{0.415}}{1.0 + 5.97 \times 10^{-3} (10^{-5} p)^{1.117}} \qquad (3.2.2\text{-}3)$$

$$(T_w - T_{sat})_{CHF} = \frac{1.71 \times 10^{3}\ C_{sf}\ (10^{-5} p)^{0.894}}{1.0 + 7.58 \times 10^{-3}\ (10^{-5} p)^{0.965}} \qquad (3.2.2\text{-}4)$$

in S.I. units (q in W/m^2K, p in Pa, and T in K); the surface coefficient, C_{sf}, is taken as 0.01. The nucleate-boiling portion of the boiling curve is then represented as

$$q = q_{CHF}\ [(T_w - T_{sat})/(T_w - T_{sat})_{CHF}]^{3.03} \qquad (3.2.2\text{-}5)$$

where the exponent is that attributed to Rohsenow in Reference 26.

The effect of subcooling on nucleate boiling is included using the expression recommended by Ivey.[32]

$$q_{CHF,sub}/q_{CHF,sat} = 1 + C_{Ivey}\ (T_{sat} - T_b) \qquad (3.2.2\text{-}6)$$

where T_b is the bulk temperature of the fluid and the coefficient C_{Ivey} is given by

$$C_{Ivey} = 0.1 \left(\frac{\rho_\ell}{\rho_v} \right)^{3/4} \frac{c_\ell}{h_{fg}} \qquad (3.2.2\text{-}7)$$

This coefficient is calculated as a function of pressure from the fit

$$C_{Ivey} = \frac{4.77 \times 10^{-2} \, (10^{-5} p)^{-0.683}}{1.0 - 6.29 \times 10^{-3} \, (10^{-5} p)^{0.862}} \qquad (3.2.2\text{-}8)$$

The film boiling regime is based on the Berenson correlations[33] for the the heat-transfer coefficient in film boiling and for the temperature difference at the Leidenfrost (minimum film-boiling point). These have been fit for use in CORCON-MOD2 as

$$q_{Leid} = \frac{1.88 \times 10^{4} \, (10^{-5} p)^{0.894}}{1.0 + 7.58 \times 10^{-3} (10^{-5} p)^{0.956}} \qquad (3.2.2\text{-}9)$$

and

$$(T_w - T_{sat})_{Leid} = \frac{8.56 \times 10^{1} (10^{-5} p)^{0.848}}{1.0 + 1.38 \times 10^{-1} (10^{-5} p)^{.0750}} \qquad (3.2.2\text{-}10)$$

Above the Leidenfrost point, the total heat flux including radiation is represented, in accordance with Equation 7.45 of Reference 26, as

$$q = q_c \, (q_c/q)^{1/3} + q_r \qquad (3.2.2\text{-}11)$$

Here q_c is the convective heat flux in the absence of radiation, and the factor $(q_c/q)^{1/3}$ accounts for the fact that the total heat flux contributes to the vaporization rate, which determines the thickness and thermal resistance of the vapor film. The heat flux q_c has an explicit variation with temperature as the 3/4 power of $(T_w - T_{sat})$. We assume that this dominates the implicit temperature dependence through material properties, so that q_c may be calculated as

$$q_c = q_{c,Leid} \left[(T_w - T_{sat})/(T_w - T_{sat})_{Leid} \right]^{0.75} \quad (3.2.2\text{-}12)$$

The radiative contribution, q_r, is given for infinite parallel gray walls by

$$q_r = \frac{\sigma_B (T_w^4 - T_{sat}^4)}{1/\varepsilon_w + 1/\varepsilon_f - 1} \quad (3.2.2\text{-}13)$$

where ε_w is the emissivity of the wall and ε_f that of the fluid.

The transition-boiling regime is represented by a simple linear interpolation in ℓn P vs ℓn T between the point defined by Equations 3.2.2-4 and -5 and the point defined by Equations 3.2.2-9 and -10.

At sufficiently low gas velocities, heat transfer in molten debris or coolant is dominated by natural convection. This process is modelled in CORCON-MOD2 by conventional Nusselt-Rayleigh correlations in the form.[34]

$$Nu = \max (0.54\ Ra^{1/4},\ 0.14\ Ra^{1/3}) \quad (3.2.2\text{-}14)$$

for axial heat transfer in an unstable thermal gradient, and

$$Nu = \max (0.59\ Ra^{1/4},\ 0.10\ Ra^{1/3}) \quad (3.2.2\text{-}15)$$

for radial heat transfer. Here

$$Nu = h\ell/k \quad (3.2.2\text{-}16)$$

is the Nusselt number, based on the layer thickness ℓ, and

$$Ra = g\beta\Delta T\ell^3/\nu\kappa \quad (3.2.2\text{-}17)$$

is the Rayleigh number. ΔT is the temperature difference, fluid to boundary. In Equations 3.2.2-14 and -15, the first expression in parentheses corresponds to laminar (low Rayleigh number) convection and the second to turbulent (high Rayleigh number) convection.

We have previously shown[10d] that axial heat transfer in a fluid layer with known average and boundary temperatures could be described using these conventional convective heat transfer relations, combined with conservation of energy. This approach is used in CORCON-MOD2. The heat transfer coefficient at a surface where the temperature gradient is stable is calculated directly from Equation 3.2.2-15. If the temperature gradient is stable at one interface but unstable at the other, convective flows driven by the unstable gradient steepen the stable gradient. To account for the resulting increase in heat transfer, the heat transfer coefficient for the stable gradient is then calculated from

$$Nu_{stable} = 1 + (1 + 2\, Nu_{unstable} |\Delta T_{unstable}| / |\Delta T_{stable}|)^{1/2} \qquad (3.2.2\text{-}18)$$

Kulacki and co-workers[35-37] have developed correlations for convective heat transfer in internally heated fluid layers. Our model has been used to reproduce the various correlations with a maximum error of 30% and an average error closer to 10%, so that CORCON-MOD2 may be said to be reasonably consistent with the Kulacki results. Further discussion may be found in Reference 10e.

The natural convection limit is imposed in CORCON-MOD2 by choosing the greater of the Nusselt numbers calculated for bubble-enhanced and for natural convection. The actual implementation assumes that Equation 3.2.2-18 may be applied even when $Nu_{unstable}$ is evaluated for bubble-enhanced convection.

For very thin or very viscous layers, the natural convection correlations above can yield smaller heat fluxes than would result from simple conduction. Therefore, an approximate conduction limit is imposed in CORCON-MOD2, again in the form of a lower limit on the Nusselt number. The formulation is based on the average temperature of the liquid layer, T_ℓ, which is consistent with CORCON usage and is normal practice for convective heat transfer. For convection, there is a (usually unstated) assumption that the boundary layers are thin and that the local temperature is essentially equal to the average temperature almost everywhere. The assumption fails at or near the conduction limit, where the temperature profile is quadratic (for a uniform volumetric source). This is the reason that we have chosen an "approximate" limit rather than an "exact" one. A full discussion is contained in Reference 10e.

In the radial direction, the exact conduction result for a quadratic temperature profile is

$$Nu_R + q_R \ell/[k(T_\ell - T_R)] = 4 \ell/R \qquad (3.2.2\text{-}19)$$

expressed as Nusselt number based on layer thickness. This provides the desired lower bound on radial heat transfer.

The exact axial conduction result is

$$q_T = 2k [T_\ell - T_T + (-T_B + 2T_\ell - T_T)]/\ell \qquad (3.2.2\text{-}20)$$

$$q_B = -2k [T_\ell - T_B + (-T_B + 2T_\ell - T_T)]/\ell \qquad (3.2.2\text{-}21)$$

where the fluxes are positive up, and "B" and "T" refer to the bottom and top surfaces, respectively. Note that q_B in Equation 3.2.2-20 does not necessarily have the same sign as $(T_B - T_\ell)$ (and similarly for q_T and $(T_\ell - T_T)$ in Equation 3.2.2-21), which would greatly complicate an attempt to impose the "exact" limit. In order to avoid this, we have employed the approximations

$$q_T \approx 2k \{T_\ell - T_T + 2 [\max ((T_\ell - T_T)(T_\ell - T_B), 0)]^{1/2}\}/\ell \qquad (3.2.2\text{-}22)$$

$$q_B \approx -2k \{T_\ell - T_B + 2 [\max ((T_\ell - T_T)(T_\ell - T_B), 0)]^{1/2}\}/\ell \qquad (3.2.2\text{-}23)$$

which have the desired sign properties, and the same values as Equations 3.2.2-20 and -21 for the limiting cases of no internal heating ($T_\ell = (T_B + T_T)/2$) and of large internal heating ($T_B - T_\ell = T_T - T_\ell$). In fact, as discussed in Reference 10e, the approximation errs only in the temperature at which steady state is achieved for given boundary temperatures and volumetric heating. This error is unavoidable if we wish the heat fluxes to have the same sign as the temperature differences. In any case, if the conduction limit in a liquid is reached, the layer must be relatively thin and the maximum error in the average temperature, one third of the temperature difference across the layer,[10e] must be relatively small. It represents only a minor error in the sensible heat content of the layer and has no other consequences.

Equations 3.2.2-22 and -23, rewritten in the form of Nusselt numbers based on layer thickness, are employed in CORCON-MOD2 as lower bounds on the Nusselt numbers in a liquid layer.

3.2.3 Crust Formation and Freezing

After some period of interaction, pool temperatures will fall to the point where solidification begins. In the early stages, we assume that crusts will form at one or more interfaces with the interior of the layer remaining liquid. (This is not the only possibility: the crusts may be unstable, or the entire melt may form a slurry.) At later times, considerable freezing may occur. If part or all of a layer becomes frozen, heat can be removed from it by conduction only, which is ordinarily far less effective than convection. Because of internal heating and the fact that cooling cannot continue unless heat losses exceed sources, freezing is largely self-limiting. Substantial freezing of the metallic layer may occur, but in the layer containing fuel oxides the volumetric heating is much greater and the thermal conductivity much lower so that only thin crusts can form.

For some accident scenarios, the core debris may initially be solid or partially solid. If the degree of solidification is such that internally-generated heat cannot be removed, the debris temperature will rise and material will melt until convective heat transfer is sufficient to allow a balance to be achieved. In general, melting will proceed outward from the center of the debris.

A complete formulation of the problem involves transient, two-dimensional heat transfer with conduction, convection, and change of phase. The spatial resolution must be sufficient to resolve centimeter-thick crusts on layers with dimensions of meters. A numerical solution of the full problem would be very difficult, if not impossible.

A major effect of the presence of solid crusts on heat transfer is the limitation of convective losses because the boundary temperature of the liquid cannot fall below the solidification temperature. Also, a crust provides an additional thermal resistance between the interior of the pool and its surroundings. Both effects tend to reduce heat losses and slow internal cooling rates (or force reheating) so that a steady state is approached. Therefore, we have developed[38] a relatively simple quasi-steady-state model for inclusion in CORCON-MOD2.

The model is formulated in terms of the average temperature of the layer, which is known from its mass and energy content, although it assumes the existence of a temperature profile within the layer. The basic approach is to construct a steady-state

solution to the heat-transfer equations in a right circular cylinder whose average temperature, boundary temperatures, thickness, and volume all match those of the actual layer. The resulting heat fluxes at the boundaries are then used at the corresponding boundaries of the actual layer. As described above, the state of a layer will evolve toward a situation where heat losses balance internal heat generation. The average temperature and the boundary heat fluxes at this steady state are determined by the internal heating and the boundary temperatures for the layer.

As a further simplification, the problem is reduced to two independent one-dimensional problems, one axial and one radial, by performing radial and axial averages, respectively, of the full two-dimensional problem. This is a familiar approximation for convective heat transfer in an almost isothermal liquid layer with thin thermal boundary layers, and its accuracy is seldom questioned. It might be expected to be less accurate in the opposite limit of conduction in a solid. Therefore, we have tested the approximate model by comparing its predictions with the exact solution for steady-state conduction in a right circular cylinder with uniform volumetric heating and specified surface temperatures.[10h] The quantities compared were the resulting average temperature of the layer and the partition of internally generated heat among upward, downward, and radial heat flows. The agreement between the two calculations is good: differences in the partition of heat and in the effect of boundary temperatures on the average temperature are less than 10%, and the calculated temperature rises due to internal heating differ by less than 20%. This is true for any anticipated height-to-diameter ratio of the cylinder. Therefore, we believe that the one-dimensional simplification is sufficiently accurate for use in a code such as CORCON-MOD2.

Within a one-dimensional calculation, a layer may be entirely liquid, entirely solid, or liquid with a solid crust. For the axial case, a crust may exist on the top, on the bottom, or both. In liquid regions, heat transfer is by convection (natural or bubble-enhanced) with a conduction limit as described in Section 3.2.2. In solid regions, it is by conduction. The all-liquid case employs the results of Section 3.2.2 directly, while the all-solid case uses the analytic results for steady-state conduction with a constant volumetric source which follow from

$$q_z = - k \, dT/dz \qquad (3.2.3\text{-}1)$$

$$dq_z/dz = S_z \qquad (3.2.3\text{-}2)$$

$$q_r = -\,k dT/dr \qquad (3.2.3\text{-}3)$$

$$d(rq_r)/dr = rS_r \qquad (3.2.3\text{-}4)$$

Here the heat flux, q, is positive upward or outward and S is the volumetric heat source. These relations lead to familiar quadratic temperature profiles. In terms of boundary and average temperatures, the heat fluxes are

$$q_B = k\,(-4T_B + 6\bar{T} - 2T_T)/L \qquad (3.2.3\text{-}5)$$

$$q_T = k\,(-2T_B + 6\bar{T} - 4T_T)/L \qquad (3.2.3\text{-}6)$$

$$q_R = 4\,k\,(\bar{T} - T_R)/R \qquad (3.2.3\text{-}7)$$

with subscripts B, T, and R referring to the bottom, top, and radial surfaces. Here $\bar{T}$ is the average temperature of the layer, and L and R are its thickness and radius, respectively. Note that the volumetric source does not appear in these results; the implications of this are further discussed in Reference 10h.

In the case of a liquid with crusts, the liquid sub-layer is solved first using assumed values of its average temperature and thickness or radius, T_ℓ and ℓ or R_ℓ, and appropriate boundary temperatures. For any surface at which a crust exists, the boundary temperature is assumed to be the solidification temperature. Conduction in a crust is again governed by Equations 3.2.3-1 through -4, and the temperature profile is again quadratic within the crust. We require continuity of the heat flux at the interface with the liquid, and set the volumetric source in the crust equal to that in the liquid.

$$S_z = (q_T - q_B)/\ell \qquad (3.2.3\text{-}8)$$

$$S_r = 2q_r/R_\ell \qquad (3.2.3\text{-}9)$$

This leads to crust thicknesses and average temperatures of

$$\delta_B = 2k(T_S - T_B)/\left[\left(q_{B\ell}^2 + 2k(T_S - T_B)S_z\right)^{1/2} - q_{B\ell}\right] \qquad (3.2.3\text{-}10)$$

$$\delta_T = 2k(T_S - T_T)/\left[\left(q_{T\ell}^2 + 2k(T_S - T_T)S_z\right)^{1/2} + q_{T\ell}\right] \qquad (3.2.3\text{-}11)$$

$$\delta_R = 2k(T_S - T_R)/\left[\left(q_{R\ell}^2 + k(T_S - T_R)S_r\right)^{1/2} + q_{R\ell}\right] \qquad (3.2.3\text{-}12)$$

$$\bar{T}_B = (2T_S + T_B)/3 + q_{B\ell}\,\delta_B/6k \qquad (3.2.3\text{-}13)$$

$$\bar{T}_T = (2T_S + T_T)/3 - q_{T\ell}\,\delta_T/6k \qquad (3.2.3\text{-}14)$$

$$\bar{T}_R = (T_S + T_R)/2 \qquad (3.2.3\text{-}15)$$

for those crusts which are present. Here T_S is the solidification temperature, $\bar{T}_x$ is the average temperature of crust x, and $q_{x\ell}$ is the heat flux at its interface with the liquid, where "x" may be B, T, or R. In some cases, one or more of Equations 3.2.3-10, -11, and -12 may have no real solution. For this to happen the effective source (divergence of the heat flux) must be negative, which may occur if a layer is being heated by an adjacent layer. The solution is to repeat the calculation with the source made less negative by increasing the assumed liquid temperature and/or dimensions.

In general, neither the total layer thickness (or radius) nor the overall average temperature thus determined will be correct for the layer. This requires an iteration on the thickness and temperature of the liquid sublayer. A two-variable form of Newton's iteration has been found effective for this. A "bound-and bisect" backup has been included for reliability.

3.2.4 Melt/Concrete Heat Transfer

There is no consensus concerning either the exact nature of the interface between the melt and the concrete or the mechanisms by which heat is transported across it. This region, into which gases and molten or partially molten oxides from concrete decomposition are injected, is too thin to be seen either visually or with x-rays.[39] There are a number of competing models for prediction of heat transfer through the interface: examples are described in References 5, 21, 40, 41, and 42.

Because there is no convincing experimental evidence to confirm or reject any of the models, and the alternate models do not give answers which are greatly different, we have retained (with some modifications) the model from CORCON-MOD1. This model assumes that the boundary region is dominated by a gas film, and that on horizontal and near-horizontal surfaces the Taylor instability leads to formation of bubbles which enter the melt, while on more-steeply inclined surfaces the gas forms a flowing film.

For a gas film on a nearly horizontal surface, heat transfer is computed from a mechanistic model based on momentum balance in a Taylor-instability bubbling cell.[40] The result may be cast in the form of a Nusselt number based on film thickness as

$$Nu_B \equiv h_B \delta_B / k_g = 0.804, \qquad (3.2.4\text{-}1)$$

where h_B is the heat-transfer coefficient, δ is the film thickness, and k_g is the thermal conductivity of the gas. The factor 0.804 is the fraction of the surface not occupied by bubble sites and therefore available for heat transfer. The film thickness satisfies

$$\delta_B^3 = 15.05\ Re_B L^3. \qquad (3.2.4\text{-}2)$$

Here L is a material property

$$L = \{\mu_g^2/[g\rho_g(\rho_l - \rho_g]\}^{1/3} \qquad (3.2.4\text{-}3)$$

where g is the acceleration of gravity, subscripts l and g refer to pool material and film properties, respectively, and

$$Re_B = \rho_g V_s a/\mu_g \qquad (3.2.4\text{-}4)$$

is the Reynolds number based on the Laplace constant

$$a \equiv [\sigma/g\ (\rho_l - \rho_g)]^{1/2} \qquad (3.2.4\text{-}5)$$

and the superficial velocity V_s with which gas enters the film. It is worth noting that if the process modelled were really film boiling, the equations would be closed through the relations

$$q = h_B \Delta T = \rho_g V_s h'_{fg} \qquad (3.2.4\text{-}6)$$

where h'_{fg} is the effective heat of vaporization. Relatively simple manipulation can then be used to reduce the present model to the form of Berenson's[33] correlation for boiling on a flat plate

$$h = 0.67 \left[\frac{k_g^3 g h'_{fg}\ (\rho_\ell - \rho_g)}{\mu_g\ \Delta T\ 2\ \pi a} \right]^{1/4} \qquad (3.2.4\text{-}7)$$

with a coefficient of 0.68 rather than 0.67.

The bubble model is used for inclinations less than 15° in CORCON-MOD2. Above 30° we use a flowing-film model, and consider both laminar and turbulent films. The transition model used between 15° and 30° will be described later. The film models are mechanistic, based on momentum balances in an inclined flowing film, with Reynolds analogy used for heat transfer in the turbulent case. The results, expressed as Nusselt numbers, are

$$Nu_{LF} \equiv h_{LF}\delta_{LF}/k_g = 1 \qquad (3.2.4\text{-}8)$$

$$Nu_{TF} \equiv h_{TF}\delta_{TF}/k_g = 0.325 Pr^{1/3} Re_F^{\ 3/4}\ , \qquad (3.2.4\text{-}9)$$

where Pr is the Prandtl number for the film, and Re_F is the Reynolds number based on film thickness

$$Re_F = \rho_g \bar{u} \delta / \mu_g. \qquad (3.2.4\text{-}10)$$

with $\bar{u}$ the average flow velocity in the film. The film thicknesses satisfy

$$\delta_{LF}^3 = 5.61\ Re_F L^3 / \sin\theta \qquad (3.2.4\text{-}11)$$

$$\delta_{TF}^3 = 0.0469\ Re_F^{7/4}\ L^3 / \sin\theta \qquad (3.2.4\text{-}12)$$

where θ is the inclination from the horizontal.

In CORCON-MOD2 we have abandoned the Persh transition[43] between laminar and turbulent regimes because it was based on external flows. Instead, we employ a much simpler "transition" which will ensure continuity of film thickness and heat-transfer coefficient with the appropriate limits:

$$\delta_F = \max\ (\delta_{LF}, \delta_{TF}) \qquad (3.2.4\text{-}13)$$

$$Nu_F = \max\ (Nu_{LF}, Nu_{TF}) \qquad (3.2.4\text{-}14)$$

$$h_F = Nu_F\ k_g / \delta_F \qquad (3.2.4\text{-}15)$$

where the various film thicknesses and Nusselt numbers have been defined above.

A transition between the bubbling model and the film-flow model is also required. We have incorporated a mechanistic model[10g] based on a momentum balance with a fraction f of injected gas going into bubbles and the rest into establishing the film. The results have the form

$$\delta^3 = \delta_F^3 + f(\sin)\ 15^o / \sin\theta)\ \delta_B^3 \qquad (3.2.4\text{-}16)$$

$$h = [f Nu_B + (1 - f) Nu_F]\ k_g / \delta \qquad (3.2.4\text{-}17)$$

A transition is achieved by decreasing f linearly with $\sin\theta$ from 1 at 15° to 0 at 30°.

Because of the high temperatures involved, heat transfer by radiation across the gas film must also be included. The radiative component accounts for about one half of the total heat flux in many CORCON calculations. We use the form for a transparent gas between infinite parallel gray walls

$$q_{rad_{net}} = \frac{\sigma_B \, (T_A^4 - T_W^4)}{(1/\varepsilon_p + 1/\varepsilon_W - 1)} \qquad (3.2.4\text{-}18)$$

Here σ_B is the Stefan-Boltzmann constant, T_A and T_W are the temperatures of the pool side of the gas film and of the ablating concrete surface, respectively, and ε_p and ε_W are the corresponding emissivities.

The convective heat-transfer coefficients above involve the superficial velocity of gas entering the interface region and, in film flow regions, the film-wise mass flow. The latter is determined by the entering gas flow at all upstream points. The superficial gas velocity is determined by the concrete response which is determined by the total heat flux. This, in turn, involves the heat-transfer coefficients themselves. A self-consistent solution has been found advisable for numerical stability; this is obtained through a simple iteration.

Note that $\rho_g \bar{u} \delta$ is the mass flow per unit width of film, which satisfies

$$\frac{d}{ds} (r \rho_g \bar{u} \delta) = r f \rho_g V_s \qquad (3.2.4\text{-}19)$$

where r is the local radius of the cavity, s is the path length, measured along the film, and f is the interpolation factor which imposes the transition from bubbling to film flow. In CORCON-MOD2, we solve this equation by use of a simple predictor-corrector method. An inner iteration, as described above, is required to solve the non-linear (because of radiation) energy balance at each point. In cases where the spacing between body points is too great to resolve the development of the gas film, intermediate points are considered by the integration routine. They are not saved, unlike the "integration points" in CORCON-MOD1.

Heat transfer through the gas film is formulated in terms of the temperatures of its surfaces. On the pool side, this temperature, T_A, is determined implicitly by the requirement that the heat flux be continuous. The subroutine SURFEB is used to perform a surface energy balance at the interface between the melt and the gas film and evaluate its temperature at each spatial point. The nonlinear equation

$$q_p = q_{rad_{net}} + h_f (T_A - T_W) \qquad (3.2.4\text{-}20)$$

is solved for T_A using Newton's iteration. A complete solution, including the full evaluation of pool-side heat transfer within the iteration loop, would be extremely expensive in computer time because the energy balance is typically performed at hundreds of points along the pool/concrete interface.

In CORCON-MOD1,[3] the pool-side heat flux is represented in terms of a heat transfer coefficient, whose dependence on T_A (if any) is ignored in the iteration. The value for the last previous evaluation of within-pool heat transfer is used. The crust-formation model in CORCON-MOD2 introduces a discontinuity in behavior when T_A passes through the solidification temperature T_S. The qualitative dependence of q_p on T_A is shown in Figure 3.1. When T_A is slightly greater than T_S, no crust exists and the derivative dq_p/dT_A is given by a convective heat-transfer coefficient which is typically large. When T_A is slightly less than T_S, a crust must be present and the derivative is small because a small change in surface temperature merely changes the (steady) crust thickness with very little change in the heat flux. The discontinuity in slope must be accounted for to prevent unphysical results or failure of the iteration which determines T_A.

In CORCON-MOD2, we use a piecewise-linear approximation to q_p as a function of T_A. There are two cases, as shown in Figure 3.2, depending on whether a crust was present (T_A was less than T_S) when within-pool heat transfer was last evaluated. If so, q_p is evaluated as

$$q_p = q_p^{old} + \frac{dq_p}{dT_A} (T_A - T_A^{old}) \quad , \qquad (3.2.4\text{-}21)$$

for $T_A \leq T_S$. For $T_A > T_S$, q_p is extrapolated linearly to zero at $T_A = T_M$, where T_M is currently taken as the temperature of the liquid center of the layer. This is illustrated in Figure 3.2A. If, on the other hand, no crust was previously present (T_A was greater than T_S), Equation 3.2.4-21 is used to evaluate q_p for $T_A \geq T_S$. For $T_A < T_S$, the heat flux q_p is assumed to be constant as shown in Figure 3.2B.

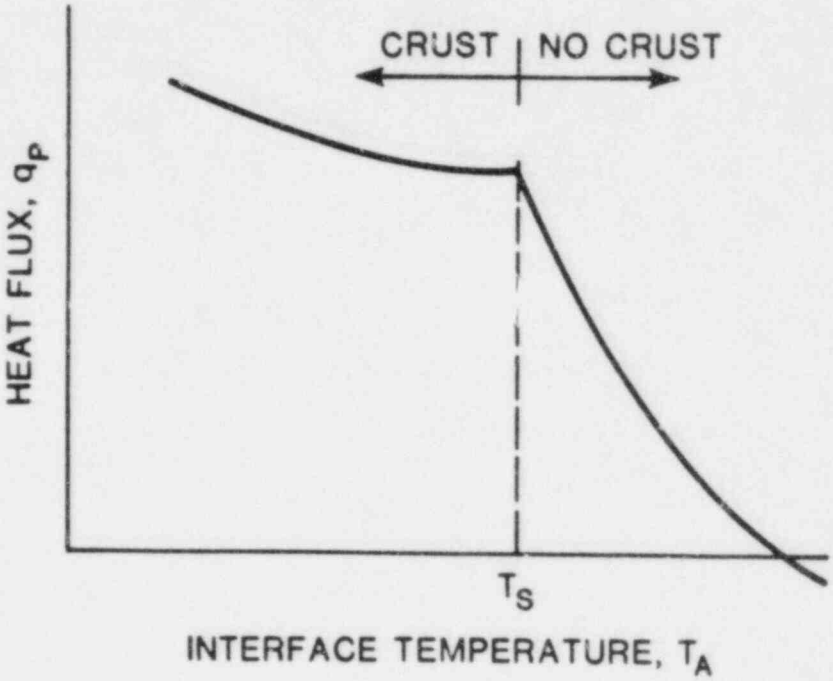

Figure 3.1 Dependence of Heat Flux on Surface Temperature

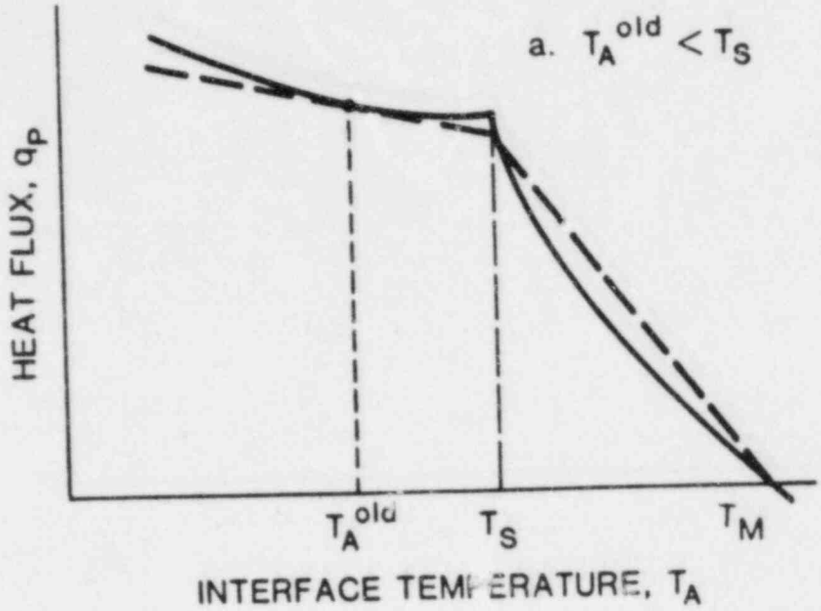

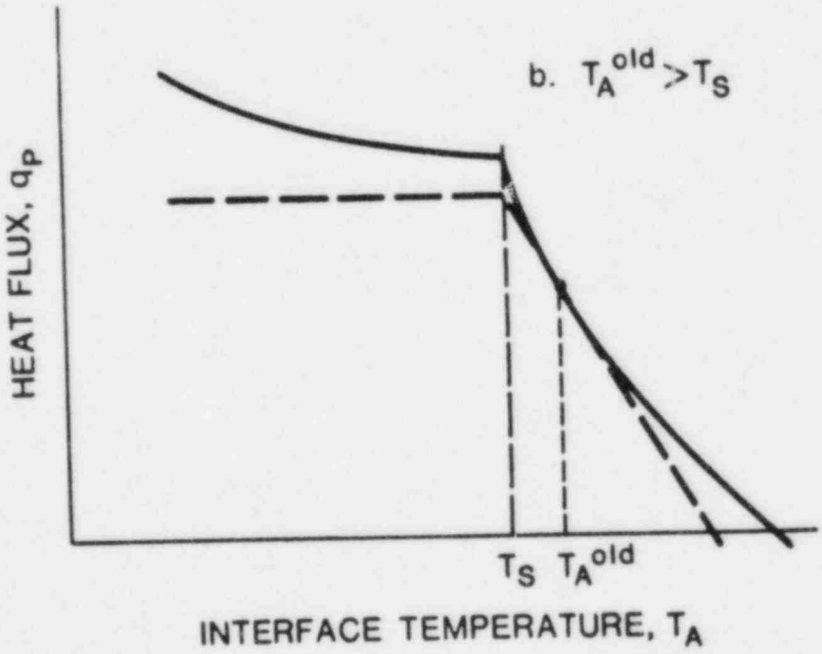

Figure 3.2 Approximation to Heat Flux as a Function of Interface Temperature

3.2.5 Pool Surface Heat Transfer

We anticipate that CORCON-MOD2 will be coupled to containment response codes such as MARCH[44] and CONTAIN.[16] To simplify such efforts, the pool surface has been treated as a major computational interface in CORCON-MOD2, with limited information passed in a well-defined way between above- and below-surface modules. Otherwise, these modules are quite independent; in particular, the need for simultaneous solution of above-surface and below-surface heat transfer relations has been avoided.

Each half of the problem (above- and below-surface) defines an upward heat flow, Q_S, as a function of the surface temperature, T_S. An energy balance at the surface of the pool requires finding that T_S for which these heat flows are equal; this generally involves solution of a nonlinear--and perhaps very complicated--equation. This may be viewed somewhat differently: for each half of the problem, the boundary condition at the pool surface is the heat flow vs temperature characteristic of the other half, and the object is to find a simultaneous solution. Each "half-problem" is solved with a boundary condition representing the response of the other half, linearized about the most-recently-calculated surface temperature. The calculation is described in more detail below.

First, the end-of-timestep response of the pool, linearized about its start-of-timestep value, T_S^n,

$$Q_S = Q_S^o\Big|_{Pool} + \frac{dQ_S}{dT_S}\Big|_{Pool} (T_S - T_S^n), \qquad (3.2.5\text{-}1)$$

is calculated in ENRCN1 and passed to the above-pool module, ATMSUR. This response includes contributions from the implicit terms in the pool energy equation, involving the change in layer temperatures with change in end-of-timestep heat loss from the surface. In ATMSUR, it is used as a boundary condition for the full nonlinear problem involving atmosphere and surroundings, resulting in a provisional end-of-timestep surface temperature, $\tilde{T}_S^{n+1}$. This, together with the linearization of above-surface response about T_S^{n+1},

$$Q_S = Q_S^o\Big|_{sur} + \frac{dQ_S}{dT_S}\Big|_{sur} (T_S - \tilde{T}_S^{n+1}), \qquad (3.2.5\text{-}2)$$

is passed back to the below-surface modules. The linearization ultimately serves as a boundary condition for another non-linear calculation which results in the final end-of-timestep value T_S^{n+1}. This procedure has advantages with respect to the energy-conservation equations, as will be discussed in Section 3.2.9.

In the version of ATMSUR included in CORCON-MOD2 for stand-alone use, heat loss from the pool surface includes convective heat transfer to the atmosphere and radiative heat transfer to the surroundings. Thermal radiation is the dominant mechanism. If desired, the radiative effects of aerosols in the atmosphere may be included in the calculation, with an atmospheric opacity determined from estimated aerosol concentrations as described in Section 3.2.11. Once the optical thickness of the atmosphere is known, the one-dimensional diffusion equation is applied for infinite, parallel, optically gray plates giving

$$q_{rad_{net}} = \frac{\sigma_B \left(T_s^4 - T_{sur}^4\right)}{1/\varepsilon_s + 1/\varepsilon_{sur} - 1 + 0.75\ KL} \qquad (3.2.5\text{-}3)$$

where T_s is the surface temperature, T_{sur} is the surroundings temperature, K is the extinction coefficient, L is an average path length for radiation in the cavity atmosphere, and ε_s and ε_{sur} are the surface and surroundings emissivities, respectively. Note that Equation 3.2.5-3 reduces to the transparent atmosphere equation as either the extinction coefficient or the average path length approaches zero.

Convection produces additional heat transfer from the pool surface. Unless the atmosphere is truly transparent, however, convection and radiation are strongly coupled; the radiation tends to increase thermal stability and reduce convection.[45] Further discussion, together with references, may be found in Reference 10g. Therefore, we have included only a very simple convection model in CORCON-MOD2. The convective heat transfer from the pool surface to the atmosphere is given by

$$q_{conv} = h_a \left(T_s - T_a\right) \qquad (3.2.5\text{-}4)$$

where T_a is the bulk temperature of the atmosphere. The heat transfer coefficient, h_a, is assumed to be a constant 10 W/m^2 K.

Therefore, the total heat flux from the surface (interface) is given by

$$q_s = q_{rad_{net}} + q_{conv} \qquad (3.2.5\text{-}5)$$

This equation is solved for T_s simultaneously with the linearized pool response, Equation 3.2.5-1, to determine the provisional end-of-timestep surface temperature $\tilde{T}_s^{n+1}$.

3.2.6 Concrete Decomposition and Ablation

The response of concrete exposed to high heat fluxes is complex. Concrete is an inhomogeneous material which undergoes changes in composition as it is heated. The most important of these changes are the vaporization of interstitial and adsorbed water at about 400 K, the decomposition of calcium hydroxide near 700 K, and that of calcium carbonate between about 1000 and 1100 K. (Actually, several rate processes are involved, but the temperature ranges quoted are typical.) The carbon dioxide, water vapor, and liquid water produced within the solid concrete flow through the pores of the remaining matrix in response to pressure gradients. Finally, the remaining oxide matrix melts, at a temperature which ranges from about 1500 K to 1900 K for representative concretes. Because the matrix is a mixture of compounds, the melting actually takes place over a range of temperatures (and the rates of several chemical processes are also involved). In the context of molten-core/concrete interactions, the molten and semi-molten materials are removed from the surface into the pool, as the surface recedes.

A detailed treatment of the in-depth response of the concrete is available in codes such as USINT[8] and SLAM.[46] In CORCON-MOD2, we employ a drastically simplified model, based on a steady-state one-dimensional energy balance. If a steady temperature profile exists in the concrete, a simple heat balance at the concrete surface yields

$$q = \rho_c \Delta H_{abl}\, dx_a/dt \qquad (3.2.6\text{-}1)$$

where q is the net heat flux to the concrete, ρ_c is the density of concrete, ΔH_{abl} is the ablation enthalpy of concrete (a material property), and x_a is the position of the concrete surface. The heat flux q must, of course, be reconciled with the melt/concrete heat transfer model of Section 3.2.4. In general, this procedure will involve an iteration to determine the temperature of the pool side of the interfacial gas film, allowing for the fact that the thermal resistance of that film may depend on the gas generation which results from the ablation. If this temperature is below the ablation temperature, the concrete is treated as an adiabatic boundary with q (and dx_a/dt) set equal to zero.

We emphasize that the pseudo-steady temperature profile, which is used to justify Equation 3.2.6-1, does not appear in the equation. The sensible heat and chemical energy (and changes in these quantities) associated with the temperature profile are ignored. This is not a problem in cases where the pool contains a

high temperature liquid melt: studies by ACUREX, using a more complex ablation code, have shown that the ablation processes reaches a quasi-steady state within about 1 minute.[47] At very late times, or early times with initially solid debris, the inaccuracies could be greater.

The quasi-steady model is also used to calculate the generation of decomposition gases; that is, the mass generation rate of each gas is taken as its partial density in the concrete times the ablation rate. Gas released in advance of the ablation front is thus ignored; this assumption neglects the initial burst of gases associated with establishing a steady profile in the concrete by a hot molten pool. The model is also in error at early times for solid debris, because no gas is generated before ablation begins, as well as at late times if ablation ceases.

The ablation energy for concrete in Equation 3.2.5-1 is calculated internally, and consists of both sensible and chemical energies. The sensible energy is computed as described in Section 3.3.1. It includes the energy necessary to raise gaseous decomposition products to the concrete ablation temperature to account for the so-called "transpiration cooling" effect. The chemical energy is included using experimentally determined heats of decomposition for three reactions: evaporation of free water (11 kcal/mole), release of chemically bound water from hydroxides (25 kcal/mole), and release of CO_2 from carbonates (40 kcal/ mole). The enthalpy of limestone aggregate/common sand concrete (including decomposition products where appropriate) is illustrated in Figure 3.3 as a function of temperature.

The ablation temperature of concrete is not precisely defined because ablated material may not be completely molten. In CORCON-MOD2, we consider a melting range defined by the concrete liquidus and solidus temperatures, with the ablation temperature ordinarily chosen to lie between them. The choice affects the calculated heat of ablation, as may be seen from Figure 3.3. Concrete decomposition products enter the gas film or the pool at the ablation temperature, with the enthalpy appropriate to that temperature. Therefore, because all enthalpies are computed from the same data base, the choice of ablation temperature has no effect on overall conservation of energy.

If the concrete contains reinforcing steel, the energy necessary to raise it to the concrete ablation temperature is included in the "concrete" ablation enthalpy.

3.2.7 Chemical Reactions

The principal chemical reaction involved in core/concrete interactions is the oxidation of metals in the pool by concrete-decomposition gases. These gases, water vapor and carbon dioxide, are reduced in the process, primarily to hydrogen and carbon

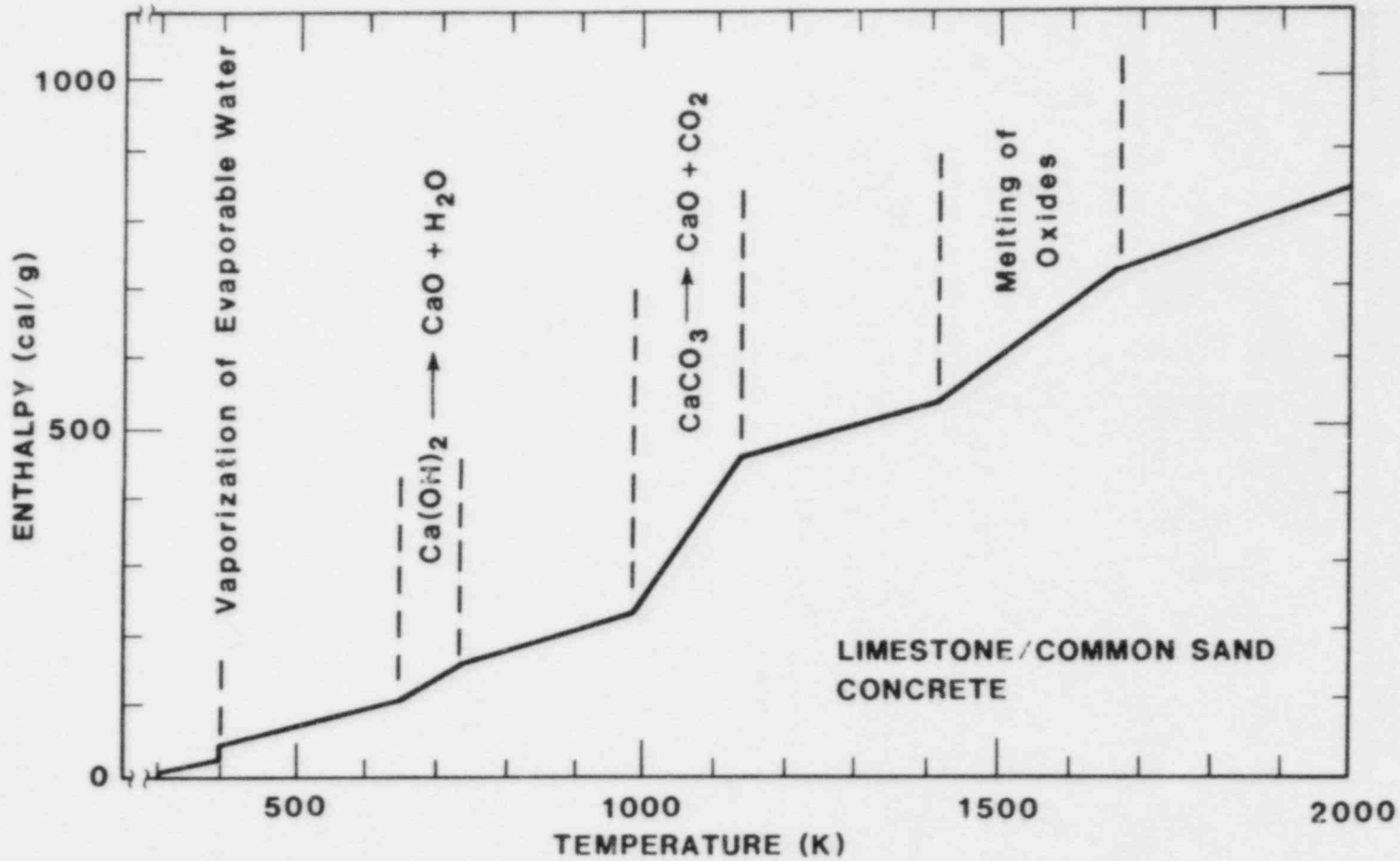

Figure 3.3 Enthalpy of Concrete and its Decomposition Products

monoxide. It is possible to further reduce carbon monoxide to atomic carbon. This is predicted in CORCON-MOD1 in many cases involving metallic zirconium. In CORCON-MOD2, we treat the reactions of metals in the pool with gases in the gas film as well as those with rising gas bubbles which were included in CORCON-MOD1. Because of possible differences in temperatures, these are treated as separate reactions.

A second reaction, the reduction of oxides at the pool surface by the oxygen-poor atmosphere above the melt, was included in CORCON-MOD1.[3] This feature was tested, but was bypassed in released versions of the code because of the incomplete treatment of the atmosphere. We have retained it, still bypassed, in CORCON-MOD2.

The calculation is based on minimization of the Gibbs function for 38 chemical species composed of 11 elements. These species include all relevant condensed species (the metals, their oxides, and condensed carbon), the principal gaseous species of water vapor, hydrogen, carbon dioxide, and carbon monoxide, and a variety of less-important gases such as light hydrocarbons. The subroutine employed, MLTREA, has evolved from an implementation by Powers[10c] of the method of Van Zeggeren and Storey.[48] It performs a simple first-order steepest descent minimization of the Gibbs function subject to constraints on mass conservation and on non-negativity of concentrations. The version included in CORCON-MOD2 has been heavily modified and is described in detail in Reference 10f, to which the reader is referred for details.

The procedure has a number of significant advantages: (1) it is extremely general; (2) reactions need not be specified; (3) convergence does not require a good initial guess (although it is much faster if one is available); and (4) the resulting FORTRAN code is relatively small for the number of species considered. The metallic reactants and oxidic products are treated as mechanical mixtures in MLTREA; that is, entropy-of-mixing and heat-of-solution terms are neglected in their chemical potentials. The result is that the metals are oxidized, to depletion, in the order zirconium, chromium, iron, nickel.

The thermodynamic-properties package (Section 3.3.1) employs the standard thermochemical reference point of separated elements in their standard states. With this reference point, heats of formation of all species are automatically included, and all heats of reaction are implicitly contained in the enthalpy data. In fact, they are calculated only for edit purposes.

3.2.8 Mass Transfer and Associated Heat Effects

Processes involving mass transfer are of considerable importance in the modelling of molten core/concrete interactions. These include injection of concrete decomposition products (condensed and gaseous) into the pool and, in principal, further additions of core materials, structural materials, or coolant entering from above. It is convenient to include chemical reactions in the same calculational structure, because these reactions affect the nature of transferred masses.

These transport processes modify both the mass inventories and the energy contents of the various pool layers. The corresponding terms in the mass and energy equations are evaluated in subroutine MHTRAN. The structure of this routine closely mirrors our picture of the physical processes it models, as described in the following paragraphs.

The masses and enthalpies of all pool layers are updated for mass transfer and associated heat transfer in two passes. The first pass, upward through the pool, follows the rising gases and rising condensed-phase materials from concrete decomposition or melt/gas reactions. The direction of motion is, of course, determined by the density relative to the local layer material. The compositions and enthalpies of these rising materials are followed and modified for chemical reactions. The materials are thermally equilibrated with any layers they pass through, and their energy is ultimately added to the layer where they remain. This final layer is assumed to be the first oxide-containing layer encountered for oxides, the first metal-containing layer for metals, and the atmosphere for gases. Any heat of reaction remains with the layer where the reaction occurred. The second calculational pass, the downward pass, is similar: it follows any material entering the pool from above in addition to sinking reaction and concrete ablation products.

Figures 3.4 through 3.6 show this in more explicit detail. In these figures, Q denotes thermal equilibration, M/G refers to the metal/gas oxidation reaction, and O/A to an oxide/atmosphere reduction reaction included in the code structure but disabled in released versions. The "mixture" layers, containing heterogeneous mixtures of metals and oxides, are also present in the code structure but disabled. The total heat capacity of a layer is assumed to be much greater than that of materials passing through it so that thermal equilibration takes place at the start-of-timestep layer temperature. The associated change in layer enthalpy is given by

$$\Delta H_L = H(m_{in}, T_{in}) - H(m_{out}, T_{out}) \qquad (3.2.8\text{-}1)$$

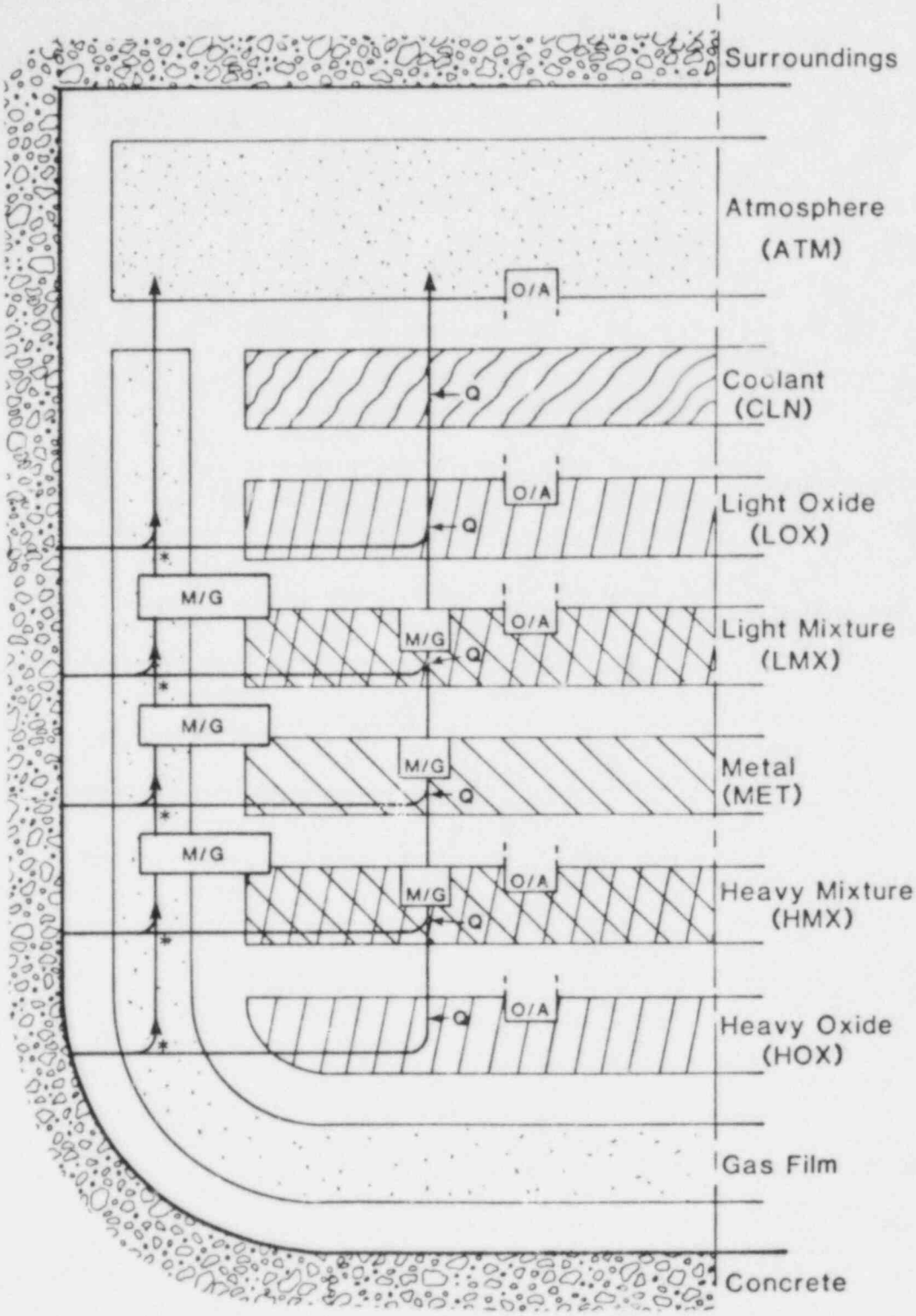

Whether gas enters the pool or rises up through the gas film at each * is determined by the local surface inclination angle. Q in the pool layers denotes thermal equilibration.

Figure 3.4 Path of Gas through Pool

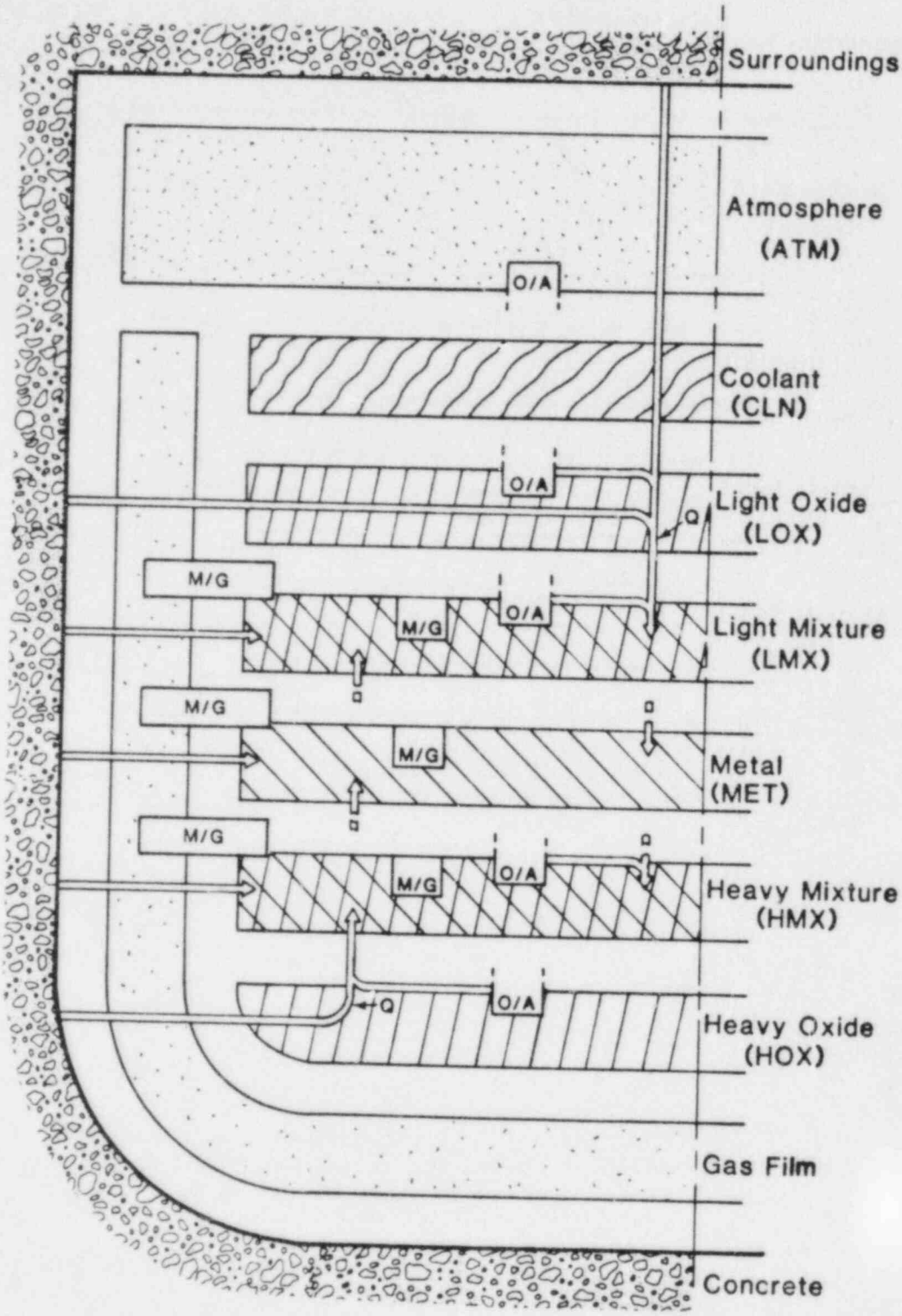

Figure 3.5 Path of Metal through Pool

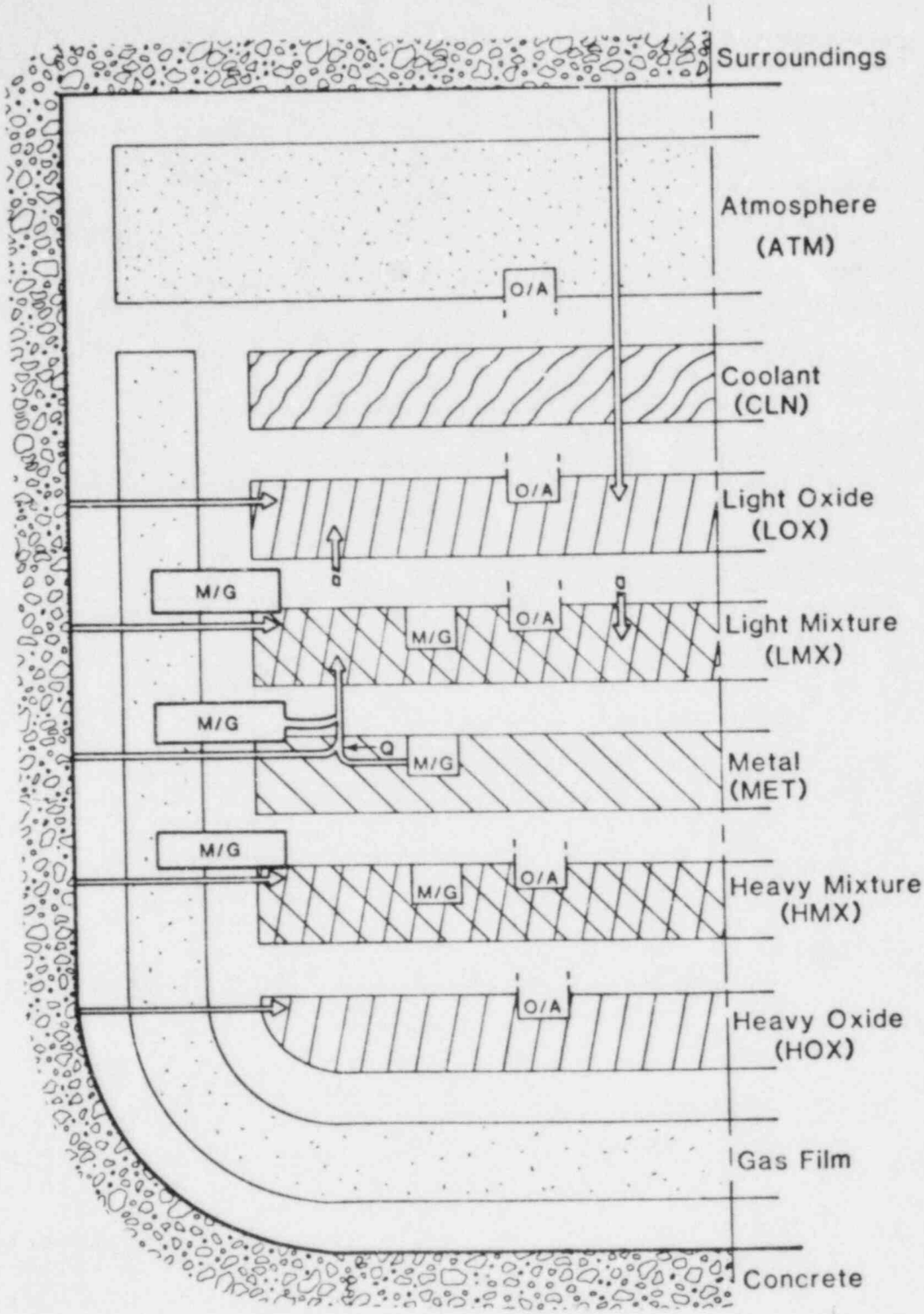

Figure 3.6 Path of Oxide through Pool

where H is enthalpy, T is temperature, m is mass (including composition), and the subscripts "L", "in", and "out" refer to the layer, to material entering it, and to material leaving it, respectively. Because the enthalpy package employs the standard thermochemical reference point of separated elements in their standard states, this equation will also hold including the effects of chemical reactions. If, for example, the composition of the gas which leaves the layer differs from that of the gas which entered, the the entire energy effect is accounted for through the different compositions associated with m_{out} and m_{in}.

3.2.9 Energy Conservation

The energy equation to be solved for each layer of the pool is given by

$$H_i^{n+1} = H_i^n + \Delta H_{enter\ i} - \Delta H_{leave\ i} + \Delta H_{react\ i} \qquad (3.2.9\text{-}1)$$

$$+ \Delta H_{source\ i} - Q_{abl\ i} + Q_{Bi} - Q_{Ti}$$

Here H_i^n is the total enthalpy of layer i at time level n

$\Delta H_{enter\ i}$ is the enthalpy of materials entering during the time-step

$\Delta H_{leave\ i}$ is the enthalpy of materials leaving during the time-step

$\Delta H_{react\ i}$ is the enthalpy gain from chemical reactions

$\Delta H_{source\ i}$ is the enthalpy gain from decay heat sources

$Q_{abl\ i}$ is the heat loss to ablate concrete

Q_{Bi} is the heat transferred from the bottom surface (zero for the bottom layer where this is part of Q_{abl})

and Q_{Ti} is the heat transferred to the top surface.

As discussed in Section 3.2.8, the "entering", "leaving", and "reaction" terms are naturally associated. The "reaction" term is included implicitly in the other two for the thermochemical reference point employed. These terms are calculated in subroutine MHTRAN as discrete changes, involving all of the material which moves during a time-step as the result of concrete ablation or addition from above. Residence times are not considered--all materials which result from ablation are assumed to be completely relocated during the same timestep.

Decay heat power changes slowly. Therefore, the corresponding term in the energy equation is evaluated explicitly (in the numerical-methods sense) as a beginning-of-timestep power multiplied by Δt. The remaining three terms in Equation 3.2.9-1 involve heat flows which are driven by temperature differences. The heat loss to concrete is also evaluated explicitly, but the remaining terms are treated using a linearized-implicit algorithm. These terms involve the axial heat flows to the upper and lower surfaces of the layer (with the exception of the bottom layer for which the lower surface is adjacent to concrete), and are taken as weighted averages of the values at time n and the linearly-projected values at time n+1. This results in the equation

$$H_i^{n+1} = H_i^{n+1(\text{explicit})} + \Omega\Delta t[(\tilde{Q}_{Bi}^{n+1} - Q_{Bi}^{n}) - (\tilde{Q}_{Ti}^{n+1} - Q_{Ti}^{n})] \tag{3.2.9-2}$$

where the tilde "~" denotes the linearized projection described below, and, of course, $H_i^{n+1(\text{explicit})}$ includes the terms $(Q_{Bi}^{n} - Q_{Ti}^{n})\Delta t$. The implicitness factor Ω is programmed as a variable, but is set equal to 1.

We calculate the projected end-of-timestep heat fluxes from

$$\tilde{Q}_{Ti}^{n+1} - Q_{Ti}^{n} = A_I \left[\frac{\partial q_T}{\partial T_L}\bigg|_i \tilde{\Delta}T_i + \frac{\partial q_T}{\partial T_T}\bigg|_i \tilde{\Delta}T_I \right] \tag{3.2.9-3}$$

$$= \tilde{Q}_{Bi+1}^{n+1} - Q_{Bi+1}^{n} = A_I \left[\frac{\partial q_B}{\partial T_B}\bigg|_{i+1} \tilde{\Delta}T_I + \frac{\partial q_B}{\partial T_L}\bigg|_{i+1} \tilde{\Delta}T_{i+1} \right]$$

if i is not the top layer in the pool, or from

$$\tilde{Q}_{Ti}^{n+1} - Q_{Ti}^{n} = A_I \left[\frac{\partial q_T}{\partial T_L}\bigg|_i \tilde{\Delta}T_i + \frac{\partial q_T}{\partial T_T}\bigg|_i (\tilde{T}_S^{n+1} - T_S^{n}) \right] \tag{3.2.9-4}$$

$$= Q_S^{n} + \frac{dQ_S}{dT_S}\bigg|_{sur} (\tilde{T}_S^{n+1} - T_S^{n})$$

if it is. Here $q_{T(B)i}$ is the upward heat flux at the top (bottom) of layer i, T_i is the temperature of layer i, T_I is the temperature of the interface, A_I is its area, and Q_S^n and dQ_S/dT_S sur define the linearization of above-pool heat transfer described in Section 3.2.5. The subscripts B, T, and L refer to the bottom and top of a layer, and to the layer average, respectively. It is important to note that dq_{Ti}/dT_{Ti} may not equal $-dq_{Ti}/dT_i$. An example of this occurs for a primarily molten layer with a thin crust. An increase in the average temperature increases the liquid temperature and the heat flux to the crusted surface, while an increase in the surface temperature merely decreases the crust thickness with little change in heat flux (under the quasi-steady assumptions of CORCON-MOD2).

The temperatures of the interfaces (other than the top surface) are eliminated, and the change in the temperature of layer i during the timestep approximated in terms of the change in enthalpy by

$$\tilde{\Delta}T_i \approx X_i \equiv (H_i^{n+1} - \hat{H}_i)/\hat{C}_i \quad . \qquad (3.2.9\text{-}5)$$

Here $\hat{H}_i$ is the total enthalpy at temperature T_i^n of the contents of the layer at time n+1, and $\hat{C}_i$ is the corresponding heat capacity. When coolant is present, Equation 3.2.9-5 is valid only so long as the coolant remains subcooled. When boiling occurs, T_i^{n+1} must be the saturation temperature T_{sat}, and the final enthalpy of the coolant will determine what fraction of it has vaporized during the time-step. This is handled by initially treating H_{cln}^{n+1} and T_{cln}^{n+1} as independent variables.

Equations 3.2.9-2 through -5 result in a set of linear equations for the layer enthalpies at time n+1. As coded in subroutine ENRCN1, the equations are written in terms of the X's (which may be thought of as enthalpy changes in temperature units) in the form

$$\sum_j A_{ij} X_j = b_i^{(1)} + b_i^{(2)} (\tilde{T}_S^{n+1} - T_S^n) + b_i^{(3)} \tilde{\Delta}T_{cln} \qquad (3.2.9\text{-}6)$$

They are solved as

$$X_i = X_i^{(1)} + X_i^{(2)} (\tilde{T}_S^{n+1} - T_S^n) + X_i^{(3)} \tilde{\Delta}T_{cln} \qquad (3.2.9\text{-}7)$$

with $(T_S^{n+1} - T_S^n)$ and $\tilde{\Delta}T_{cln}$ left undetermined.

If no coolant is present, so that all the $X_i^{(3)}$ are 0, the heat flow at the top surface, including the effects of all implicit terms in the energy equation, now has the form

$$Q_s^{n+1} = Q_s^n + \left.\frac{dQ_s}{dT_s}\right|_{pool} (\tilde{T}_s^{n+1} - T_s^n) \quad . \qquad (3.2.9\text{-}8)$$

This is the linearized pool response mentioned in Section 3.2.5. Specifically, the derivative is

$$\left.\frac{dQ_s}{dT_s}\right|_{pool} = \left.\frac{dQ_T}{dT_T}\right|_{top\ i} + \left.\frac{dQ_T}{dT_L}\right|_{top\ i} X^{(2)}_{top\ i} \qquad (3.2.9\text{-}9)$$

This is solved simultaneously with the above-pool thermal response in subroutine ATMSUR to determine $\tilde{T}_s^{n+1}$. The final evaluation of layer enthalpies and the corresponding layer temperatures is then performed in subroutine ENRCN2. This allows the implicit nature of the equations to be maintained across the pool surface even though above- and below-surface heat transfer are not evaluated simultaneously. It is the stabilizing effect of the implicit algorithm which makes possible the relatively long timesteps routinely employed in the code.

If coolant is present but remains subcooled, H_{cln}^{n+1} and $\tilde{\Delta}T_{cln}$ are related through Equation 3.2.9-5, and $\tilde{\Delta}T_{cln}$ may be eliminated from both Equations 3.2.9-7 and -8 through the relationship

$$\tilde{\Delta}T_{cln} = \left[X^{(1)}_{cln} + X^{(2)}_{cln} (\tilde{T}_s^{n+1} - T_s^n)\right] \Big/ (1 - X^{(3)}_{cln}) \qquad (3.2.9\text{-}10)$$

This possibility is tested, using the above-pool thermal response from the beginning of the timestep

$$Q_s^{n+1} = Q_s^n + \left.\frac{dQ_s}{dT_s}\right|_{sur} (\tilde{T}_s^{n+1} - T_s^n) \qquad (3.2.9\text{-}11)$$

to close the set of equations. If this results in a T_{cln}^{n+1} below saturation, the elimination of ΔT_{cln} is accepted, and the solution proceeds as for the no-coolant case. If, on the

other hand, this calculation results in a T_{cin}^{n+1} above saturation, we assume that sufficient boiling occurred during the timestep to hold the temperature to saturation and set T_{cin}^{n+1} equal to T_{sat}. In this case, we use the above-pool thermal response from the start of the timestep, Equation 3.2.9-11, to complete the solution in subroutine ENRCN1. The resulting enthalpy of the coolant corresponds to a liquid/vapor mixture at the saturation temperature. The partition of mass between the two phases is evaluated, and the vapor component is added to the gases which left the pool during the timestep. As before, the calculation is completed through ATMSUR and ENRCN2, but with the derivative dQ_s/dT_s set very large (negative). This procedure assures that ATMSUR will determine a value for T_s^{n+1} very near to T_{sat}.

A special case arises when the coolant layer is totally depleted during a timestep, and the calculation just described results in a layer enthalpy greater than that for saturated vapor. In this case, we assume that all vapor was generated at saturation and decrement the mass and energy of the coolant layer accordingly, but we do not update the enthalpies of other layers at this time. The entire calculation is repeated, with the coolant layer now absent. Because of the detailed balance of heat-flow terms in Equation 3.2.9-2, energy is conserved exactly. Although the total enthalpy of the coolant is not zero at the start of the recalculation, its final enthalpy must be zero. Inspection of the equation will show that the result of the implicit calculation is to force the net heat delivered to the coolant layer during the timestep to be exactly sufficient to vaporize it at its saturation temperature.

The major approximation in this treatment of the coolant is the use of saturation conditions at the beginning of the timestep rather than at the end. This could result in an apparently superheated liquid coolant or in one which is apparently subcooled but boiling. In practice, no significant problems have been observed.

3.2.10 Bubble Phenomena

Gas which rises through the pool as bubbles influences heat transfer, as des ribed in Section 3.2.2. In addition, the volume of the pool is inflated by the volume of the gas bubbles, a phenomena referred to as "level swell". We calculate a void fraction, the volume fraction of gases within the pool. This depends on the flow of gases and on the residence time of bubbles in the pool; the latter is determined by their rise velocity. The resulting relationship is

$$\alpha = V_s/u_b \qquad (3.2.10\text{-}1)$$

where α is the void fraction, u_b is the bubble velocity, and V_s is the superficial velocity (volumetric flux) of gas through the pool. The bubble velocity is assumed to be related to the terminal velocity of a single bubble in infinite fluid, U_T, by

$$u_b = (1 - \alpha)^n U_T \qquad (3.2.10\text{-}2)$$

where n is taken as -1, corresponding to churn-turbulent bubbly flow.[49] This results in a void fraction of

$$\alpha = V_s/(V_s + U_T) \quad . \qquad (3.2.10\text{-}3)$$

The void fraction is limited to 0.42 as suggested by Blottner.[21]

The terminal velocity of single bubbles is a function of their size and of fluid properties. There are several regimes to be accounted for. We consider three cases: small bubbles in Stokes flow, with terminal velocity

$$U_{T_1} = \frac{2}{9} \rho_\ell g r_b^2/\mu_\ell \; ; \qquad (3.2.10\text{-}4)$$

medium-sized bubbles with

$$U_{T_2} = 1.53 \, (ga)^{1/2} \quad ; \qquad (3.2.10\text{-}5)$$

and large, spherically capped bubbles for which

$$U_{T_3} = (g r_b)^{1/2} \quad . \qquad (3.2.10\text{-}6)$$

For a given bubble size, the terminal velocity is taken as

$$U_T = \min \, [U_{T_1}, \max \, (U_{T_2}, U_{T_3})] \qquad (3.2.10\text{-}7)$$

In Equation 3.2.10-5, "a" represents the Laplace constant defined in Equation 3.2.4-5.

The size of bubbles entering the pool is predicted from the Taylor-instability bubbling model, which has the form

$$r_b = Ca \qquad (3.2.10\text{-}8)$$

Here CORCON-MOD2 uses C = 3.97 based on the experimental data of Hosler and Westwater.[50] In the development of CORCON, two other gas-velocity/bubble-size regimes were investigated: the analogs of nucleate and of patchy bubbling. They were rejected because the small bubble sizes predicted (on the order of 1 millimeter) did not agree with observation of prototypic melt/concrete experiments.

The bubble size is recalculated at each layer interface; allowance is made for the effects of chemistry and the changes in temperature and pressure, but not for coalescence. The average of the radius of bubbles entering and that of bubbles leaving is used to calculate a single terminal velocity for each layer.

The predictions of this model for the terminal velocities of single bubbles are compared with experimental data[51,52] in Figure 3.7. Greene and Ginsberg compared the predicted void fractions with Greene's simulant data.[53] The results are shown in Figure 3.8, taken from the Reference.

We calculate a gas flux at the elevation of each body point by using the local cross-sectional area and the total gas flow from lower in the pool. A local void fraction is then calculated, and the elevations of layer interfaces determined from the integral of the non-gas volume.

$$\int_{z_{BOT}}^{z_{TOP}} dz \quad (1 - \alpha\,(z))\, A(z) = m_L/\rho_L \,. \qquad (3.2.10\text{-}9)$$

Finally, layer-averaged void fractions are computed from

$$\bar{\alpha}_L = 1 - m_L/\rho_L V_L \,. \qquad (3.2.10\text{-}10)$$

Terms are defined in Figure 3.9.

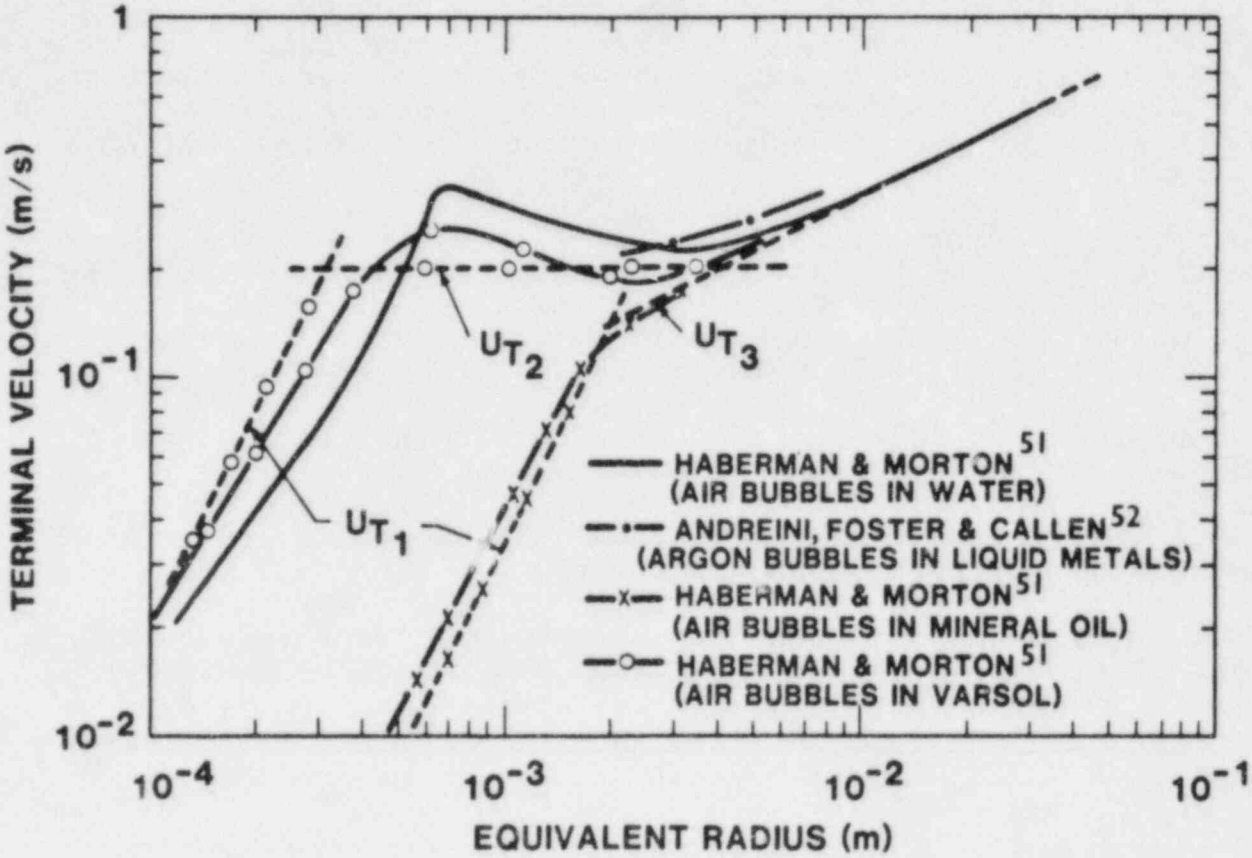

Figure 3.7 Terminal Velocity Variations for Single Bubbles Rising through Several Liquids

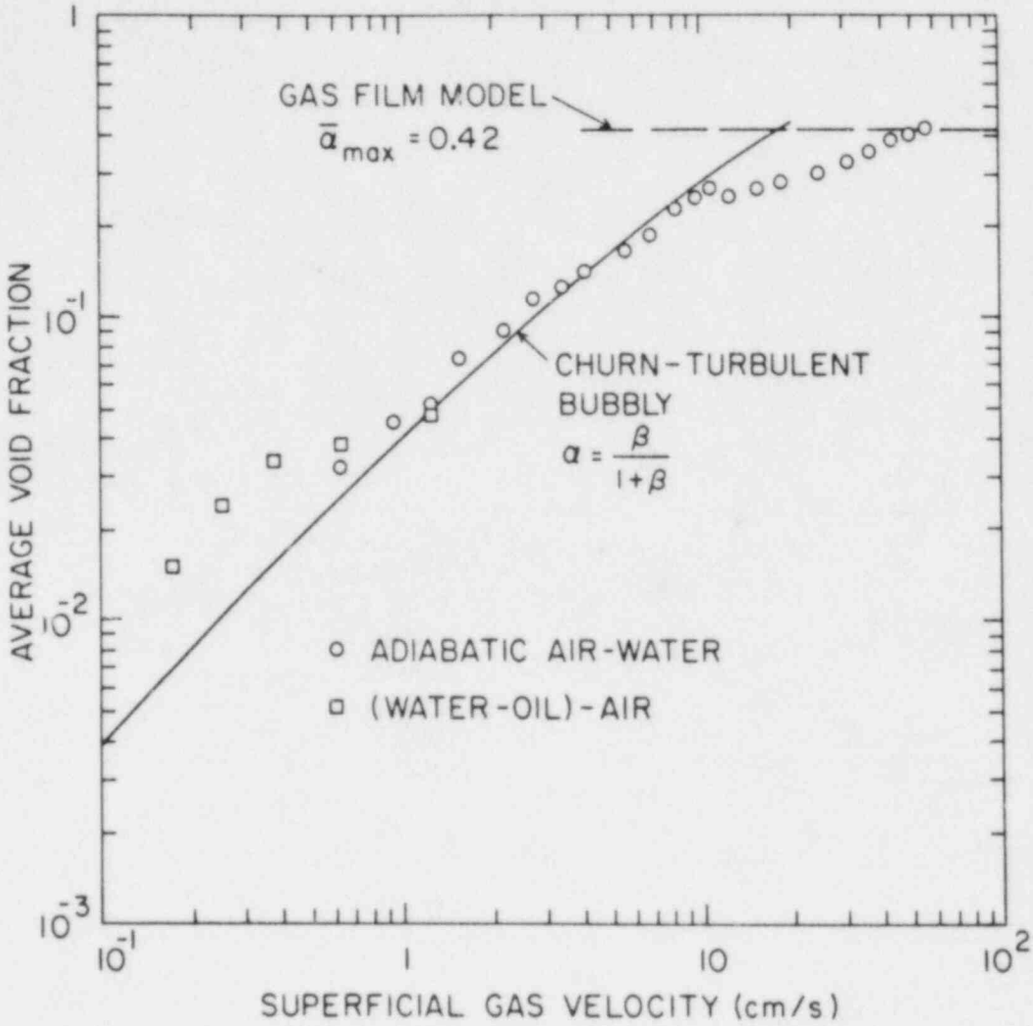

Figure 3.8 Comparison of Void Fraction Model with Data of Greene and Ginsburg

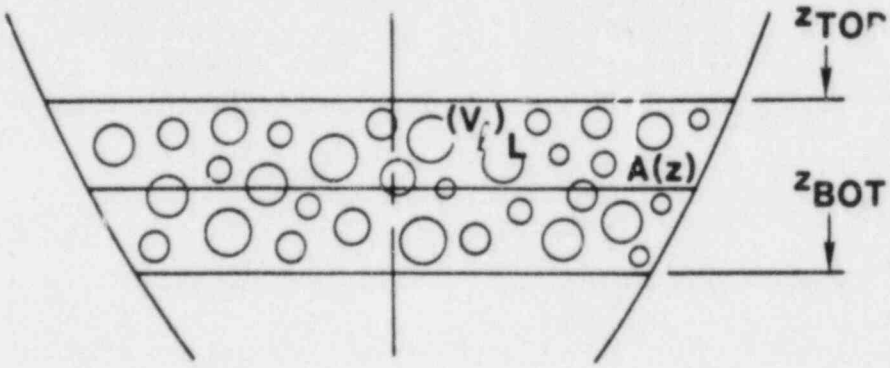

Figure 3.9 Melt Layer L

3.2.11 Atmospheric Opacity

As gases from decomposition of concrete pass through the melt and leave the pool, aerosols are generated by mechanisms such as sparging and bubble bursting. These aerosols are observed in experimental work, and an empirical source term has been developed based on a limited number of experiments[10d] which is given by

$$[A] = (33. + 240.V_s)\ \exp(-19000K/T) \qquad (3.2.11\text{-}1)$$

where [A] is the concentration (g/m^3 STP) of aerosol in the evolved gas, T is temperature of the melt (K), and V_s is the superficial gas velocity (m/s STP). It must be emphasized that both the superficial velocity and the concentration in this expression have been reduced to standard temperature and pressure (STP). The melt temperature affects only the exponential activation term. This is unclear in the cited reference, but has been confirmed by Powers.[54]

The temperature T in Equation 3.2.11-1 is assumed to be the temperature of the top layer of the melt. The gas flow (in bubbles) through the pool is converted to a superficial velocity at STP, and the aerosol concentration is adjusted to the temperature and pressure directly above the pool, with the temperature taken as that of the top layer. If coolant is present, we assume that it is effective in scrubbing aerosols from the evolved gases, and set the concentration in the atmosphere equal to zero.

This aerosol concentration is calculated solely for the purpose of determining the radiative properties of the atmosphere; no composition is calculated for it, and its mass is not charged against the pool inventory.

3.2.12 Cavity Shape Change

The shape of the cross-section of the cavity is defined for computational purposes by a series of "body points." These are the intersections of a fixed series of rays with the cavity surface as shown in Figure 3.10. Given the cavity geometry at the start of a timestep, the shape change procedure provides a new cavity shape at the end of the timestep. The normal recession rate is used at each body point, as calculated by the concrete ablation model. The methods used have evolved from the CASCET model written by ACUREX/Aerotherm Corporation,[47] under contract to Sandia, for CORCON-MOD1. We first assume that the concrete recession follows the local normal at each body point and then project the resulting surface points back onto the rays. The projection is performed by passing a circle through

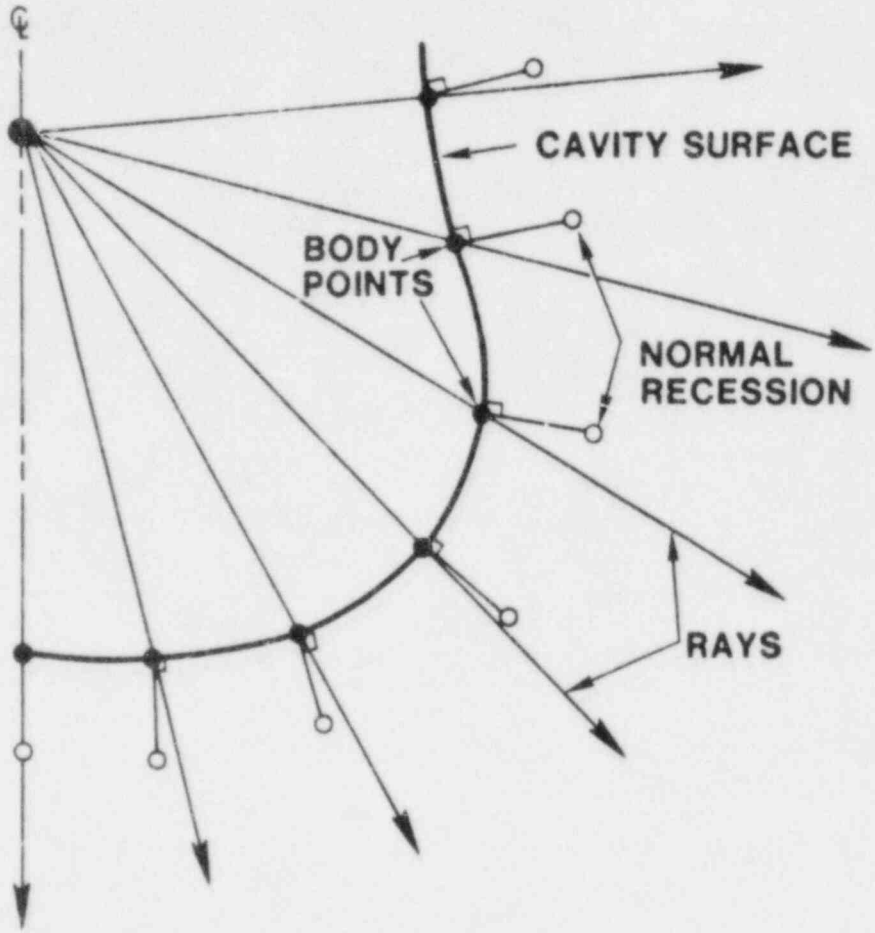

Figure 3.10 Normal Surface Recession

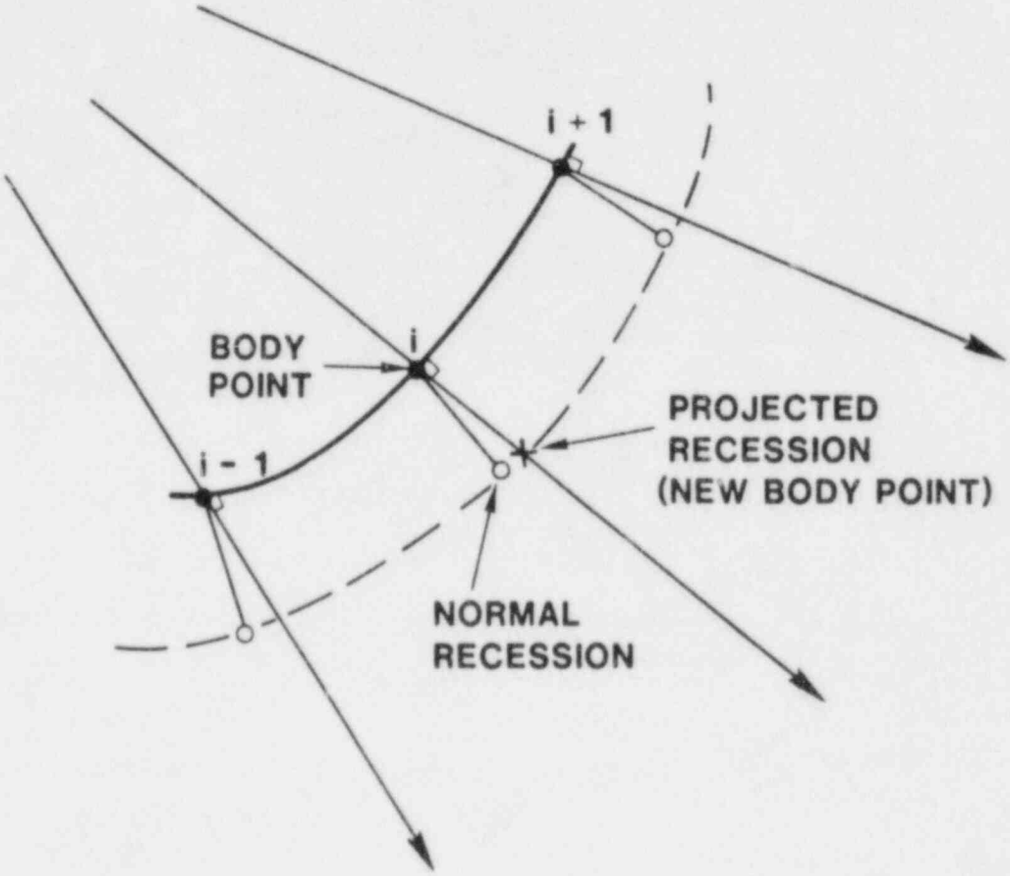

Figure 3.11 Circle Intersection Projection Method

each normally-receded point and its two nearest neighbors, and defining the new body point as the intersection of this circle with the corresponding ray as shown in Figure 3.11. A solution will exist so long as no body point is allowed to cross the neighboring ray during a timestep. In fact, there are two solutions, and we pick the one which is nearer to the normally-receded point. Because of numerical difficulties encountered in CORCON-MOD1, the equations have been reformulated and the solution procedure recoded.

With one exception, the rays emanate from an origin on the vertical axis of symmetry of the cavity. We have retained the so-called "tangent ray" from CASCET. This is a single ray, parallel to the axis, which defines the edge of the flat bottom of the cavity. Because the corresponding body point moves vertically, the bottom is constrained to remain flat as is required by the ablation model. When the cavity surface passes through a point where the tangent ray crosses an ordinary ray, the ordering of the body points is changed appropriately.

In these calculations, the "normal" at each body point is chosen as the bisector of the angle formed by lines from the body point to its nearest neighbors on each side. A more-general definition from CASCET was used in CORCON-MOD1. It was found that, although it gave slightly better results for smooth shapes, the CASCET form occasionally led to pathological geometries where the simpler model does not. Another modification was made to prevent numerical sharpening of corners projecting into the cavity. In this case, shown in Figure 3.12, if the normal ablation during a timestep is $\Delta s = s\Delta t$, the point defining the corner moves $\Delta s/\cos(\gamma/2)$. (Projection back onto the ray system is not included in this Figure.) In CORCON-MOD2, the correction is made for recession of all body points for which $\gamma>0$.

3.3 Material Properties

Calculation of the physical processes described in the preceding sections requires values for a wide range of thermodynamic and transport properties. These properties are treated as functions of composition and of temperature. However, the dependence is not always explicitly included in the CORCON-MOD2 model; for example, the values used for surface tensions are independent of temperature.

In most cases, properties are required for the mixtures of species which make up the components of the CORCON system, although the calculation of chemical equilibrium requires the chemical properties of the individual species. With a few exceptions, such as the viscosity of oxide mixtures with large silica contents, mixture properties are calculated from those of the constituent species.

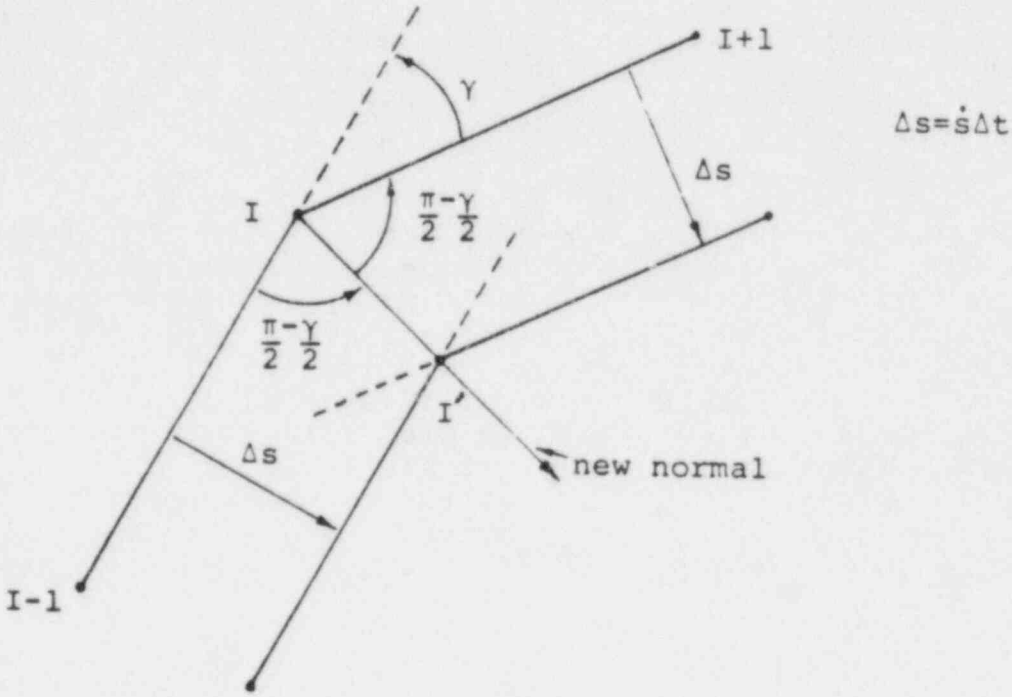

Figure 3.12 Enhanced Recession for Inside Corner Point

3.3.1 Thermodynamic Properties

The thermodynamic properties calculated are density, specific heat, enthalpy, and chemical potential.

Density - ρ (kg/m^3)

Condensed phases:

Mixture densities are computed from

$$\rho_m = 10^3 \, m_m / \sum_i (m_i v_i / M_i) \qquad (3.3.1\text{-}1)$$

where the molar volumes of the individual species are given by

$$v_i = v_i'[1 + c_i(T - 1673K)]. \qquad (3.3.1\text{-}2)$$

Values for v_i' and c_i applicable to the liquid phase are stored in subroutine DENSTY for all condensed species.[55-57] The temperature range of the data from which this relationship was generated varies considerably for the different species. For many of the oxides, it is from 1200 - 1800 C, while for others it covers the entire range from melting to boiling. However, Equation 3.3.1-2 is applied at all temperatures. This disregards the change in density which accompanies freezing.

Gaseous phase:

Densities are computed from the ideal gas relationship

$$\rho_m = 10^3 p M_m / R_o T \qquad (3.3.1\text{-}3)$$

where M_m is the mixture molecular weight ($\sum_i x_i M_i$).

Specific Heat - c_p (J/kg K)

The specific heat of any species, condensed or gaseous, is represented in the form

$$c_{p_i} = A_i + 10^{-3} B_i T + 10^{-6} C_i T^2 + 10^5 D_i / T^2. \qquad (3.3.1\text{-}4)$$

Within the calculation, units are ca /mol K, reflecting the original data sources; a convers on to S.I. (J/kg K) is made before return from the calculational package. Values of the constants A_i, B_i, C_i, and D_i are tabulated in subroutine CONFND, with one or more temperature ranges for each species. A single range is used for all gaseous

species, and the fits are valid from 298.15 to 6000K. The fits for condensed species include both the liquid and one or more solid phases; in some cases, two ranges are defined for a single phase. Thus, each species requires from two to five sets of coefficients. The upper limit of validity is above 2500K in most cases, although it is as low as 2000K in others.[57-61] In any case, the data for the highest temperature range included are used for all temperatures above the minimum for this range. Mixture specific heats are computed by mass averaging as

$$c_{p_m} = 4186.8 \sum_i (m_i c_{p_i})/m_m \qquad (3.3.1\text{-}5)$$

where the constant provides the conversion to S.I. units.

<u>Enthalpy</u> - h (J/kg)

Species enthalpies are computed from integrals of the corresponding specific heats. The conventional thermochemical reference point of separated elements in their standard states (25°C, 1 atm) is employed; i.e., the enthalpies correspond to the JANAF tables. The result may be expressed in the form

$$\begin{aligned} h_i(T) &= h_i(T^1) + \int_{T^1}^{T} dT' c_{p_i}(T') \\ &= K_{hi}^k + A_i^k (T - T_i^k) + 10^{-3} B_i^k (T^2 - T_i^{k2})/2 \qquad (3.3.1\text{-}6) \\ &\quad + 10^{-6} C_i^k (T^3 - T_i^{k3})/3 - 10^5 D_i^k (1/T - 1/T_i^k) \end{aligned}$$

for T in the kth temperature range for species i (i.e. $T_i^k < T < T_i^{k+1}$). The $\{T_i^k\}$ are the break points in the specific heat fits. The first is 298.15K and the last is treated as infinite. Thus, the first integration constant, K_{hi}^1, is the standard enthalpy of formation of species i. Any others required are computed internally, subject to the condition that the discontinuity in enthalpy at T_i^k be the appropriate heat of transition, $\Delta H_{i,TP}^k$, if a phase change occurs at T_i^k and zero otherwise. Subroutine CONFND contains tables of these heats of formation and of transition. The integration constants are evaluated internally during an initial call to CONFND from routine SETUP in order to assure full-word accuracy on machines of different word length. This is done to avoid the possibility of negative discontinuities in h(T), which could cause numerical problems. At this time, the discontinuities in enthalpy are also replaced by smooth transitions over an arbitrary temperature range of 10K. As with specific heat, the enthalpy of a mixture is computed by mass averaging:

$$h_m(T) = 4186.8 \sum_i [m_i h_i(T)]/m_m. \qquad (3.3.1\text{-}7)$$

Mass-averaging of specific heats (Equation 3.3.1-5) and enthalpies (Equation 3.3.1-7) is really appropriate only for mechanical mixtures in which each species is unaffected by the others. Because of mutual solubilities, actual mixtures of metallic or oxidic species form one or more phases. The principal effect is a change in melting behavior; rather than the individual species melting independently at their own melt points, the entire mixture melts over a range of temperatures.

We account for this effect--at least partially--in CORCON-MOD2. The melting range, defined by the liquidus and solidus temperatures, is prescribed by external models for mixtures of condensed species. Specific heat and enthalpy are calculated in three ranges:

1. For $T < T^s$, the calculation is as described above with the exception that extrapolated solid properties are used for any species which would ordinarily be liquid. This is simply accomplished by ignoring the presence of the sets of coefficients and integration constants for temperature ranges in which the species is liquid, so that the last set describing a solid continues to be used above the melting point.
2. For $T^l < T$, extrapolated liquid properties are used for any species which would ordinarily be solid by ignoring the presence of data for the solid.
3. For $T^s < T < T^l$, linear interpolation in enthalpy is used between the liquidus and solidus. The constant slope is returned as the specific heat. The effect of this construction is indicated in Figure 3.13

<u>Chemical Potential</u> - g (J/kg K)

Chemical potentials for the species are required in the calculation of chemical equilibrium, and are computed from the molar Gibbs function

$$g_i = h_i - Ts_i \qquad (3.3.1\text{-}8)$$

where s is the entropy and may be computed at temperature T and at the reference pressure of one atmosphere from

$$\begin{aligned} s_i(T) &= S_i(T^l) + \int_{T^l}^{T} dT' c_{p_i}(T')/T' \\ &= K_{si}^k + A_i^k \ln (T/T_i^k) + 10^{-3} B_i^k (T - T_i^k) \qquad (3.3.1\text{-}9) \\ &\quad + 10^{-6} C_i^k (T^2 - T_i^{k2})/2 - 10^5 D_i^k (1/T^2 - 1/T_i^{k2})/2 \end{aligned}$$

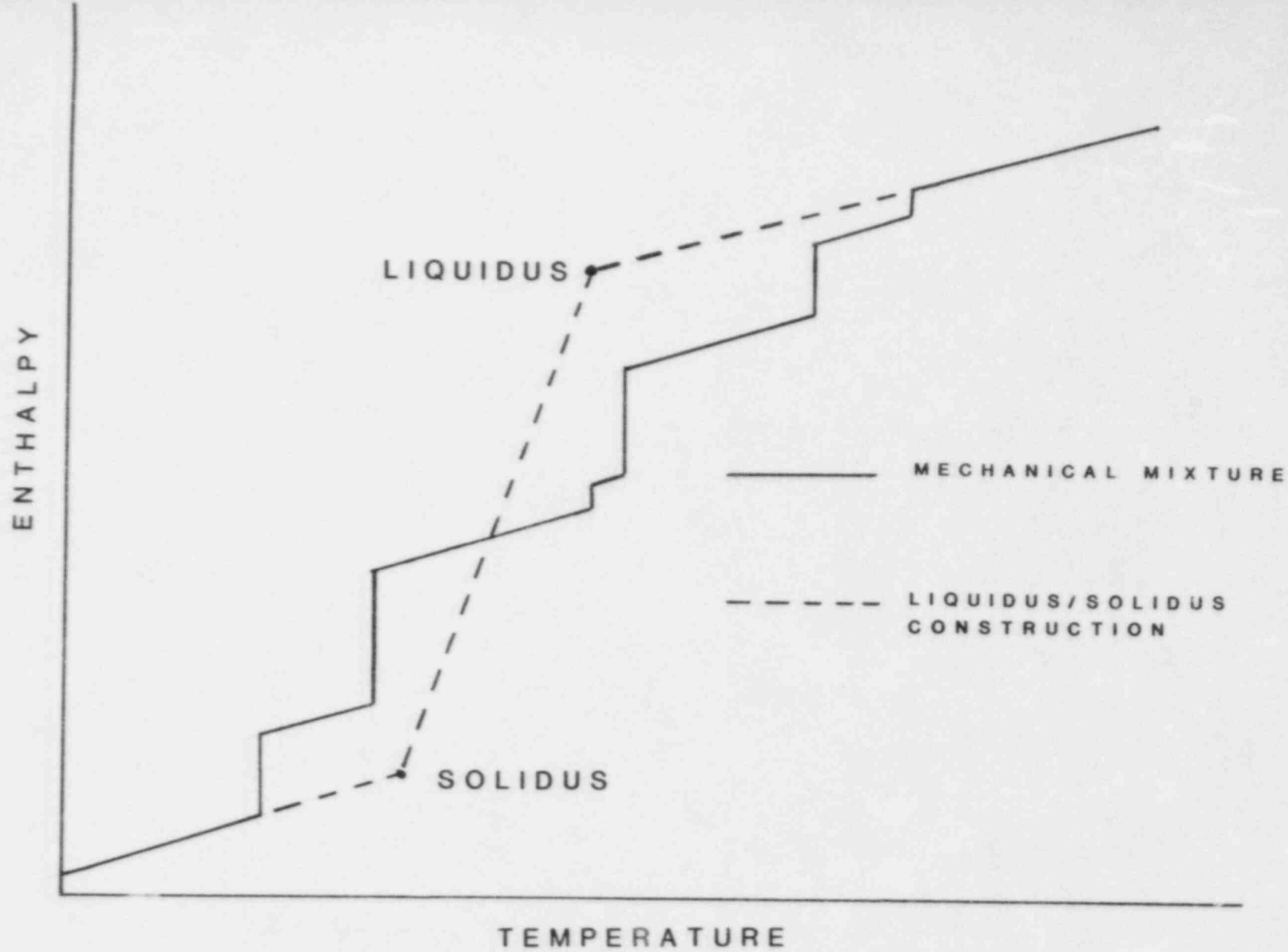

Figure 3.13 Two-Phase Construction for Mixture

for T in the kth temperature range for species i (i.e. $T_i^k < T < T_i^{k+1}$). The first integration constant, K_{Si}^1, is the standard entropy of formation of species i and, as with the enthalpy, any others required are computed internally, subject to the condition that the discontinuity in enthalpy at T_i^k be the appropriate entropy of transition $\Delta H_{i,TR}^k/T_i^k$, if a phase change occurs at T_i^k and zero otherwise. Again, subroutine CONFND contains the necessary data tables and calculates integration constants during the initial call from SETUP. The chemical potentials, evaluated in subroutine CHEMPO, are used only as internal variables in the chemical equilibrium sub-routine MLTREA, which employs chemists' units of cal/mole. Therefore, no conversion to S.I. is made. MLTREA itself converts the standard chemical potentials for pure gases at one atmosphere pressure to mixture conditions using the ideal gas result

$$g_i\ (p,T) = g_i^o(p,T) + R_oT\ \ln\ (p_i) \qquad (3.3.1\text{-}10)$$

where p_i is the partial pressure of gaseous species i. No pressure correction is made for condensed species.

3.3.2 Transport Properties

The transport properties computed in CORCON-MOD2 are the dynamic viscosity, the thermal conductivity, the surface tension, and the emissivity. Detailed models are included for condensed-phase species and mixtures only. Gas-phase viscosity and thermal conductivity (required for calculation of heat-transfer coefficients at the melt/concrete interface) are treated as constants using representative values defined in subroutine GFLMPR.

Dynamic Viscosity - μ (kg/m s)

Oxidic phase:

The viscosity of molten oxides is quite complex, particularly when significant amounts of silica (SiO_2) are present. For low-silica mixtures, the viscosity is computed from the Kendell-Monroe expression.[56,62]

$$\mu_m = [\sum_i X_i \mu_i^{1/3}]^3. \qquad (3.3.2\text{-}1)$$

The viscosities of the species are determined using an Andrade form[61]

$$\mu_i = \mu_i^o \exp\ [\alpha_i/T] \qquad (3.3.2\text{-}2)$$

where the constants μ_i^o and α_i are determined by empirical correlation.

Values of these coefficients are included (in subroutine VISCTY) for only a limited number of species. The values for FeO, Al_2O_3, and UO_2 are based on published data;[56,59] that for CaO is based on our own unpublished theoretical estimate. The values for ZrO_2 and Cr_2O_3 are based on analogy with UO_2 and FeO respectively. These are important contributors to the viscosity because they may be dominant species in either the fuel-oxide layer or the light-oxide (slag) layer. Only these species are considered in the Kendell-Monroe calculation, and the resulting composition is renormalized.

For mixtures with a higher silica content, the viscosity can be greatly increased by the formation of strongly bonded chains of SiO4 tetrahedra. The viscosity is calculated from a model proposed by Shaw.[63] This was originally generated as a fit to the correlation developed by Bottinga and Weill based on geologic data,[64] and was shown to give good agreement with it within the original data base. (The Bottinga-Weill correlation, as implemented in the VISRHO model,[55] was used in CORCON-MOD1, where it was found to give unrealistic values for viscosity when extrapolated to some of the compositions and temperatures encountered in code calculations.) Shaw's model has an extremely simple form, for which good extrapolation properties are built in:

$$\mu = \exp[s\ (10^4/T - 1.50) - 6.40]. \qquad (3.3.2\text{-}3)$$

Here the viscosity, μ, is in poise (1.0 poise = 0.1 kg/m s) and s is a function of mixture composition given by

$$s = (\sum_i n_i x_i s_i^o / \sum_i n_i x_i)\ x_{SiO_2}. \qquad (3.3.2\text{-}4)$$

Data are included in subroutine VISCTY for TiO_2, FeO, MgO, CaO, Li_2O, Na_2O, K2O, Fe_2O_3, and Al_2O_3; these values are taken from Shaw's paper. Also included are data for UO_2 and ZrO2 based on an assumed analogy with TiO_2, and for Cr_2O_3 based on an assumed analogy with Fe_2O_3. Again, the composition in terms of these species is re-normalized for use in Equation 3.3.2-3.

The Shaw model is restricted to mixtures with relatively high silica contents; it is matched to the low-silica Kendell-Monroe form by simply accepting the greater of the two values calculated from Equations 3.3.2-1 and -3. The transition, where the two values are equal, is typically at a composition of 20 to 30 percent silica.

Metallic Phase:

We assume that the viscosity of the metallic phase can be represented by the viscosity of iron (the major constituent) as given by the expression[56,65]

$$\mu_m = 1.076 \times 10^{-3} \exp(3313/T). \qquad (3.3.2\text{-}5)$$

Two-Phase, Solid-Liquid Slurry:

CORCON-MOD1 contained a model for the enhancement of viscosity by suspended solids, in the form

$$\mu_{sl} = \mu_m \left[\frac{1 + \phi/2}{(1 - \phi)^4} \right] \qquad (3.3.2\text{-}6)$$

where μ_{sl} is the slurry viscosity, μ_m is the viscosity of the pure liquid mixture, and ϕ is the volume fraction of solids. This form was suggested by Kunitz[66] for slurries containing less than 50 percent solids by volume. In CORCON-MOD1, the expression was assumed to apply up to 90 percent solids, with the solids fraction computed by linear interpolation between the mixture liquidus, T^l, and the mixture solidus, T^s, as

$$\phi(T) = \frac{T^l - T}{T^l - T^s} \qquad \text{for } T^s < T < T^l. \qquad (3.3.2\text{-}7)$$

Although the Kunitz model is retained in CORCON-MOD2, it has been disabled there because of problems observed in CORCON-MOD1. For all calls to the subroutine VIS2PH which evaluates the two-phase multiplier, the fraction of solids, ϕ, is set to zero in the calling subroutine.

Thermal Conductivity - k (W/m K)

Values of thermal conductivity[56,57,59,61,67] for condensed-phase species are stored in subroutine VISCTY. No temperature dependence is included. Mixture values are computed from the species values by mole-fraction averaging.

Surface Tension - σ (N/m)

Values of surface tension[56,57,59,61] for condensed-phase species are stored in subroutine SIGMY. No temperature dependence is included. Mixture values are computed from the species values by mole-fraction averaging.

Emissivity - ϵ (-)

The calculation of radiative heat transfer requires emissivities for the radiating surfaces. In the CORCON-MOD2 code, only the emissivity of water (coolant) is stored as internal data. Values are input by the user for the ablating concrete surface, for the oxidic and metallic melt phases, and for the surroundings above the pool. The first is specified as a constant, while the last three may be input as functions of either surface temperature or time.

3.3.3 Liquid-Solid Phase Transition

In order to model solidification effects, we must be able to determine the liquidus and solidus temperatures for metallic and oxidic mixtures. Melting temperatures and latent heats of fusion are readily available for a wide range of materials. Values for all the condensed-phase species in the CORCON Master List (Table 3.I) are contained in the thermodynamic property tables described in Section 3.3.1. The situation is quite different for the mixtures encountered in melt/concrete interactions; data are lacking, and the mixtures are too complex for detailed analysis. Therefore, we have developed relatively simple procedures for estimating the liquidus and solidus temperatures of the various mixtures encountered in CORCON-MOD2. These temperatures are also used in the construction of a single melt transition in the enthalpy of such mixtures, as described in Section 3.3.1

Concrete:

The melting of concrete is strongly influenced by the presence of trace species such as alkali oxides. However, melting ranges for typical concretes have been determined experimentally, and are included as part of the internal data in CORCON-MOD2 for the three built-in concrete varieties. For user-specified concretes, the liquidus and solidus temperatures must also be input by the user; the values for the built-in concretes, Table 3.III, should provide some guidance.

Metallic Mixtures:

For metallic mixtures (at least late in the accident when solidification is likely) the principal constituents should be Cr, Fe, and Ni from stainless steel. Therefore, we have constructed a simple fit to the iron-chromium-nickel ternary phase diagram,[68] with due consideration to the associated binary phase diagrams. The liquidus and solidus temperatures are fit as

$$T^{\ell} = \min\,(2130 - 510W_{Fe} - 1140W_{Ni},\ 1809 - 90W_{Cr} - 440W_{Ni},\ 1728 - 200W_{Cr} - 40W_{Fe},\ 1793 - 230W_{Cr} - 130W_{Ni}) \qquad (3.3.3\text{-}1)$$

$$T^{s} = \min\,(2130 - 730W_{Fe} - 3310W_{Ni},\ 1809 - 90W_{Cr} - 560W_{Ni},\ 1728 - 250W_{Cr} - 100W_{Fe},\ 1783 - 310W_{Cr} - 140W_{Ni},\ 1613) \qquad (3.3.3\text{-}2)$$

where W_{Cr}, W_{Fe}, and W_{Ni} are the weight fractions of Cr, Fe, Ni, respectively. These expressions agree with the original curves within a few tens of degrees. The corresponding contour maps are shown in Figure 3.14. As implemented in CORCON-MOD2, the presence of other elements is ignored, and the weight fractions of chromium, iron, and nickel are renormalized so that $W_{Cr} + W_{Fe} + W_{Ni} = 1.0$.

Oxidic Mixtures:

The melt behavior of oxidic mixtures is far more complicated. The major constituents of concrete, CaO, SiO_2, and Al_2O_3, form a complicated ternary system (see, e g, Reference 56). The fuel oxides, UO_2 and ZrO_2, appear to form a relatively simple system, but it is really a single-line in the far more complicated uranium-oxygen-zirconium ternary system. Because consideration of the complete phase diagram for concrete oxides plus fuel oxides seems to be out of the question, the melting behavior of oxidic mixtures is based on a simple analytic model. We treat the mixture as a pseudo-binary system in which the fuel oxides form one "component" with concrete and steel oxides form the other; the two components are assumed to form ideal solutions in both liquid and solid phases. This results in implicit equations for the liquidus and solidus temperatures

$$x_1 \exp\left[-\frac{\Delta H^1}{R_o}\left(\frac{1}{T_1^m} - \frac{1}{T^{\ell}}\right)\right] + x_2 \exp\left[-\frac{\Delta H^2}{R_o}\left(\frac{1}{T_2^m} - \frac{1}{T^{\ell}}\right)\right] = 1 \qquad (3.3.3\text{-}3)$$

$$x_1 \exp\left[\frac{\Delta H^1}{R_o}\left(\frac{1}{T_1^m} - \frac{1}{T^{s}}\right)\right] + x_2 \exp\left[\frac{\Delta H^2}{R_o}\left(\frac{1}{T_2^m} - \frac{1}{T^{s}}\right)\right] = 1 \qquad (3.3.3\text{-}4)$$

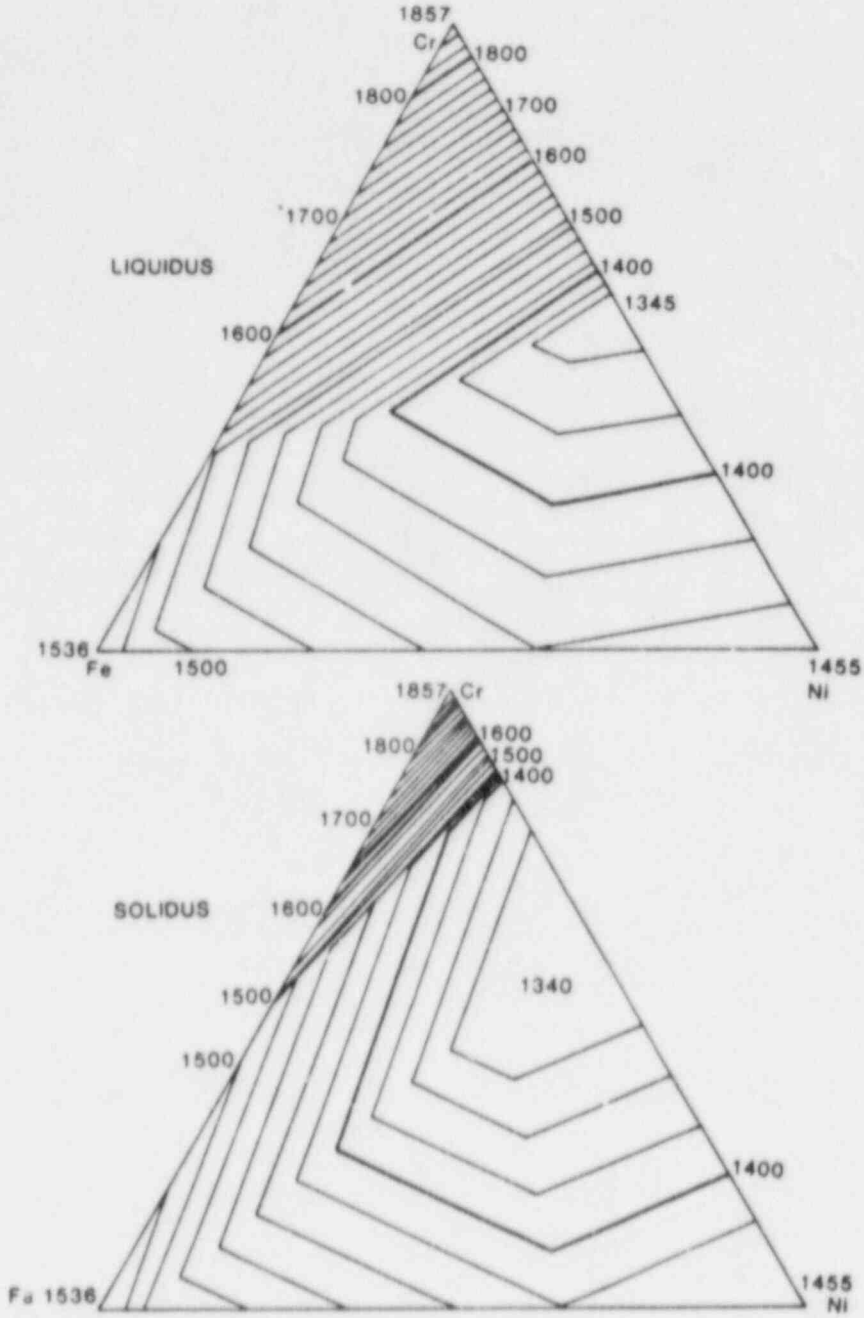

Figure 3.14 Liquidus and Solidus Temperature Fits for Cr-Fe-Ni System

where x_i is the mole-fraction of component i, T_i^m is its melting temperature, and ΔH_i is its heat of fusion. This formalism may be applied to a mixture of mixtures by treating T_i^m as T_i^ℓ, the liquidus temperature of mixture i, in the liquidus equation (3.3.3-3) and as T_i^s, the solidus temperature of mixture i, in the solidus equation (3.3.3-4). This procedure is not rigorous, but appears to yield reasonable results.

The melt properties for the fuel oxides (UO_2 + ZrO_2) are taken as [22]

$$\Delta H = 20800x + 17700\ (1 - x) - 5050\ x\ (1 - x) \qquad (3.3.3\text{-}5)$$

$$T^s = T^l = \Delta H/(20800x/2950 + 17700\ (1 - x)/3123) \qquad (3.3.3\text{-}6)$$

where ΔH is the component latent heat in cal/mole, T^s and T^l are in K and x is the mole fraction of ZrO_2 in the UO_2 + ZrO_2 mixture. For the second mixture, concrete oxides + steel oxides, we use concrete properties with T^s and T^l from either built in data (for the three default concretes) or from user input data (for a non-standard concrete). The mixture latent heat, ΔH, is internally calculated from built-in enthalpy data as

$$\Delta H = \bar{h}^l\ (\bar{T}) - \bar{h}^s\ (\bar{T}) \qquad (3.3.3\text{-}7)$$

where

$$\bar{T} = 1/2\ (T^s + T^l) \qquad (3.3.3\text{-}8)$$

and

$$\bar{h}^{\ell,s}\ (\bar{T}) = \sum_i m_i \bar{h}_i^{\ell,s}\ (\bar{T})/m \qquad (3.3.3\text{-}9)$$

Here $h_i^{\ell,s}(\bar{T})$ are the enthalpies of the liquid and solid phases of the constituent species, extrapolated, if necessary, as described in Section 3.3.1.

An example of the resulting phase diagram, for UO_2 + 35 mol/o ZrO_2 and Limestone Aggregate/Common Sand concrete is shown in Figure 3.15)

3.3.4 Coolant Saturation Line

If a coolant is present, CORCON-MOD2 considers the possibility that it may vaporize. The calculational procedure, described in Section 3.2.9, requires knowledge of the saturation

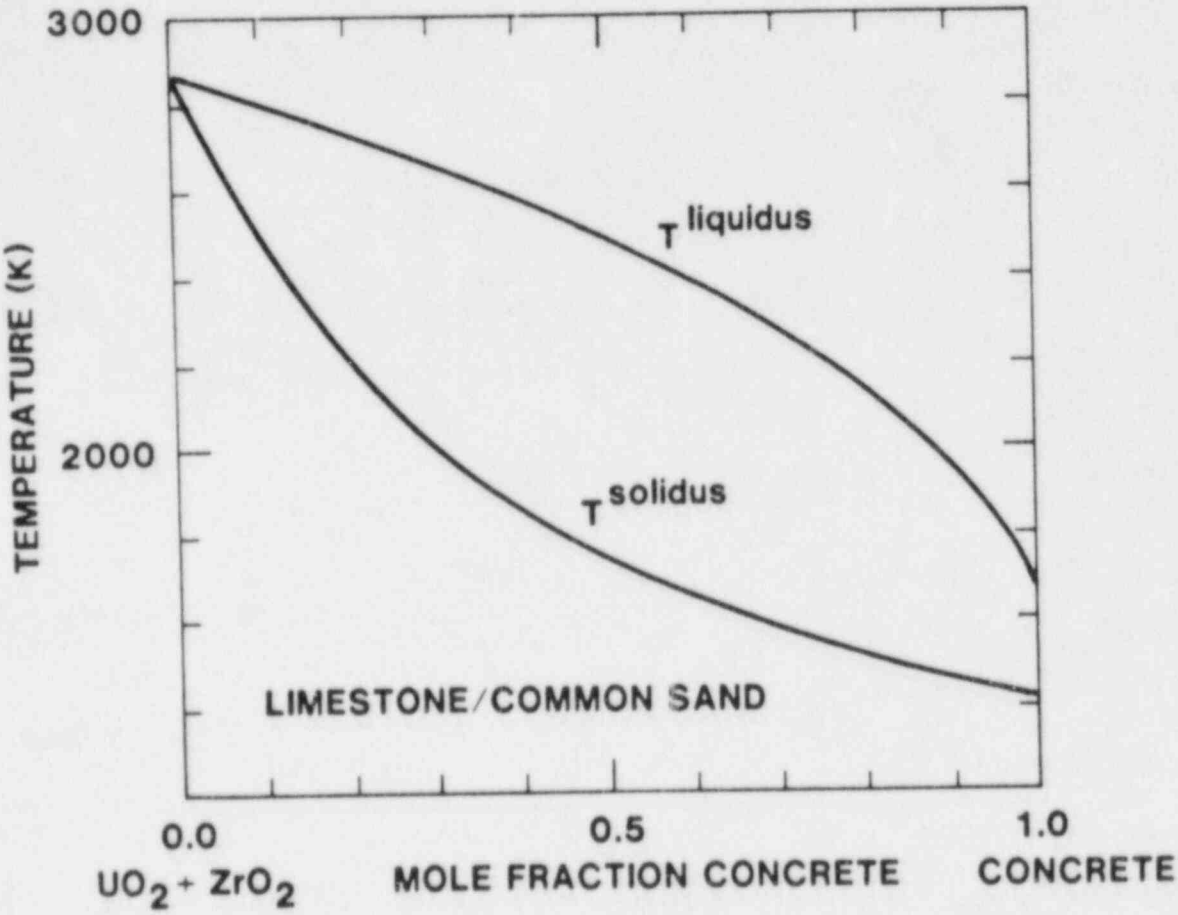

Figure 3.15 Example Liquidus and Solidus Temperatures for Oxidic Mixtures

line for the coolant--that is, the temperature at which it boils at any given pressure. The data in the Steam Tables [Keenan et al, 1978] were fit by a non-linear optimization program as

$$p_{sat}(T) = 1.292 \times 10^{10} \exp[(-3880.4/(T-43.15)] \qquad (3.3.4\text{-}1)$$

in S.I. units (pressure p in Pa, temperature T in K). This simple expression reproduces the original data within 0.5% for $T < 573K$, corresponding to $p_{sat} < 8.5$ MPa (which is far in excess of containment failure pressures), and is in error by only 5% at the critical point. This accuracy seems more than adequate for a code such as CORCON-MOD2. In addition to its extremely compact and efficient form, Equation 3.3.4-1 has the virtue of an exact analytic inverse:

$$T_{sat}(p) = 43.15 - 3800.4/\ell n(p/1.292 \times 10^{10}) \qquad (3.3.4\text{-}2)$$

4. ASSUMPTIONS AND LIMITATIONS

The CORCON-MOD2 code has been designed to be used for the analysis of both reactor accident sequences and melt/concrete interaction experiments. The code input, described in Section 5, is sufficiently flexible to allow a user to describe problems of either type. Accident calculations provide information for assessment of the risks of operation of LWR's. Calculations of experiments are useful both for planning and for interpretation of results. The comparison of experiment and calculation is valuable for guiding further efforts in both areas.

The user, however, should be aware of a number of assumptions, approximations, and simplifications employed in the modelling which may affect the accuracy (or at least the interpretation) of CORCON-MOD2 calculations. Among the more important of these are:

1. The pool is assumed to be composed of well-defined layers, with each containing either oxides or metals but not both. Each liquid layer, or liquid portion of a partially frozen layer, is assumed to be sufficiently well stirred by concrete decomposition gases that it may be treated as isothermal (except for thin boundary layers). A temperature profile may exist in solidified layers or sub-layers. The possible occurrence of heterogeneous mixtures of oxides and metals is allowed for in the code structure but is not operational in CORCON-MOD2. We might sometimes expect such mixtures to exist, at least when density differences are small and gas fluxes large.

2. The atmosphere and surroundings above the pool surface serve only to provide boundary conditions for heat and mass transfer from the pool, as CORCON does not include calculational procedures to update the temperature, pressure, or composition of the atmosphere or the temperature of the surroundings. (However, if these quantities are updated by other code modules coupled to CORCON, the current values will be used.) The calculation of radiative heat loss from the pool surface is based on a one-dimensional model, and the convective loss is calculated using a constant heat transfer coefficient.

3. The calculated concrete response is based on one-dimensional steady-state ablation, with no consideration given to conduction into the concrete or to decomposition in advance of the ablation front. This assumption is probably not a source of serious error in the analysis of reactor accidents, at least for the sequences with long-term interactions between core materials and concrete. The heat fluxes involved are sufficiently large that quasi-steady ablation is approached within the first few minutes

of interaction if the pool is molten; the process continues for a period of hours to days, sustained by decay heat from fission products in the melt. On the other hand, with respect to experimental analysis, many of the experiments performed to date have been driven only by the sensible heat of the melt, without additional heat input. The period of ablative interaction with concrete is these experiments was therefore relatively short, with the melt typically freezing in a manner of minutes. A CORCON calculation will neglect both the initial transient and the continued interaction after freezing, which is clearly inaccurate.

4. The solidification model is preliminary. It assumes that a crust forms on any surface whose temperature falls below the solidification temperature. The mechanical stability of the crusts is not considered. This treatment can result in prediction of freezing "from the bottom up", which has only been observed in simulant experiments. We believe that other regimes may exist, and that both the mechanical strength of a crust and the loads imposed on it by concrete decomposition gases are important in determining the true behavior in any given case.

5. A gas-film model is employed for heat transfer across the melt/concrete interface. It assumes the occurrence of Taylor-instability bubbling on the pool bottom (so long as it is nearly horizontal) and the existence of a flowing gas film along steeper portions of the side of the pool. The evidence in support of (or refuting) the correctness of this model is not compelling. While it gives results which do not differ seriously from those obtained with competing models, there is no convincing proof that they are not all in error.

6. The gas-film model is used even after the melt solidifies, even though the assumptions on which the model is based are no longer valid. In particular, no radial gap develops around a layer of the melt which has completely solidified. Thus, radial ablation continues with the "solid" layer continuing to conform to the changing shape of the cavity rather than behaving as a rigid penetrator. As coded, the model also assumes that the frozen material remains gas-permeable. (This assumption would be easy to modify.) In most cases that have been run, only the metallic layer is predicted to solidify. The oxidic layer remains molten and continues to ablate concrete at a relatively rapid rate. Because the total amount of concrete eroded is largely determined by energy considerations (the available decay energy), the effect of these modelling assumptions is primarily on the calculated shape of the cavity.

7. The possibility of ablation of above-pool surroundings, resulting in the addition of mass to the pool, is not treated. In fact, no mass addition other than that from concrete directly adjacent to the melt is allowed (although most of the necessary coding exists--see Section 6.5).

8. There is no treatment of chemical reactions between the melt and the atmosphere, or of reactions in the atmosphere.

5. USER INFORMATION

5.1 Input Description

Table 5.I describes the data cards needed for input by CORCON-MOD2. Compatibility with CORCON-MOD1 has been retained in the sense that any data deck accepted by CORCON-MOD1 will also be accepted by CORCON-MOD2. Because of this, the numbering of cards and card groups in the Table has not been changed from Reference 3; the new card groups for variable timestep and edit interval are numbered 3A and 3B, while the cards for input of a coolant layer are numbered 18A and 18B. Several input elements which need further discussion are considered in Section 5.1.1 below.

A given problem will not require all the data cards and fields described; in fact, some fields and cards are not yet operational and these are indicated by **[...]**. This has been done to reserve space for later upgrades of the code, and to provide the "adventurous" code modifier with information concerning features which have already been partially implemented.

The data cards are initially read in subroutine DATAIN, echoed to the output file, and written out to a scratch file, TAPE7. They are subsequently read from TAPE7 by routines CONPRP, DATAIN, DCYINT, INCOOL, INGEOM and its subroutines, INPCON, and INPGAS, which interpret the actual data fields.

5.1.1 Discussion of Selected Input Quantities

While most of the input for CORCON is fairly self-explanatory, especially to a user who is familiar with the type of problems it solves, experience has shown that some portions require further discussion.

The parameter TPRIN (card 3) provides the user with detailed printout after time has passed TPRIN. This is of interest primarily in the diagnosis of code problems; the additional information is printed in terms of FORTRAN variables, and requires some detailed knowledge of the internal workings of the code for its interpretation. For routine calculations, TPRIN should be set greater than the problem end time TIMEND.

For both the variable timestep control (card group 3A) and the variable edit control (card group 3B), the last specification is assumed to apply to the end of the problem if TIMEND is greater than the last TEND or TED, respectively. Each group is terminated by a blank card rather than by a specified count. This facilitates insertion of additional control intervals at significant or interesting points in the development of the calculation without belaboring the remainder. The actual timesteps employed may differ from those specified if necessary to produce edits at the requested times.

TABLE 5.I

INPUT INSTRUCTIONS FOR CORCON-MOD2

Card/ Group#	Field	Format	Variable Name	Description
				SECTION 1. PROBLEM IDENTIFICATION, COMPUTATIONAL OPTIONS AND CONTROL PARAMETERS
				PROBLEM TITLE
1	1-80	A80	ITITL	80 Col run identification
				COMPUTATIONAL OPTIONS INDICES
2	1-5	I5	ILYR	Index that specifies initial number of melt layers: 0 - 2 layers - oxidic and metallic 1 - 1 metallic layer 2 - 1 oxidic layer **[3 - 1 heterogeneous mixture]** **[4 - 3 layers - 2 oxidic and 1 metallic]**
	6-10	I5	ICOOL	Coolant index: 0 - no coolant 1 - coolant
	11-15	I5	IGEOM	Cavity geometry index: 1 - Cylinder with hemispherical base 2 - Cylinder with flat base **[3 - Cylinder with spherical-segment base]** 4 - Arbitrary shape
	16-20	I5	ICON	Concrete composition index: 0 - nonstandard concrete 1 - basaltic aggregate concrete 2 - limestone aggregate - common sand concrete 3 - Clinch River Breeder Reactor (CRBR) concrete

Options indicated by **[...]** are not operational.

Table 5.I (cont.)

Card/ Group#	Field	Format	Variable Name	Description
				COMPUTATIONAL OPTIONS INDICES (CONT.)
2 (cont.)	21-25	I5	IGAS	Index that specifies treatment of atmosphere and gas-phase reactions: 0 - atmosphere present **[in chemical equilibrium]** **[1 - no atmosphere considered]**
	26-30	I5	IFP	Decay heat (power) generation index: 0 - decay power computed internally 2 - power deposited into oxidic and metallic layers input versus time
	31-35	I5	ISUR	Surface temperature history of atmosphere surroundings index: **[0 - T_{sur} history computed internally]** 1 - T_{sur} input versus time
	36-40	I5	**[IABL]**	Index that specifies mass addition to pool due to ablation of atmosphere surroundings: **[0 - species mass addition rates computed internally]** **[1 - mass addition rates of metallic and oxidic species input versus time]**
	41-45	I5	ISPLSH	Melt/coolant splashout index: 0 - no splashout from pool **[1 - metallic and oxidic phase splashout mass flow rates input versus time]**
	46-50	I5	IPINC	Print increment: > 0 - program prints output every IPINC time steps ≤ 0 - print controlled by Card Group 3B
	51-55	I5	IFLOR	Index for specifying ray configuration at top of crucible: 0 - no ray along top of crucible **[1 - ray defined along top of crucible]**

Options indicated by **[...]** are not operational.

Table 5.I (cont.)

Card/ Group#	Field	Format	Variable Name	Description
				COMPUTATIONAL OPTIONS INDICES (CONT.)
2 (cont.)	56-60	I5	IRSTRT	Restart option index: 0 - run starts from beginning **[1 - restart calculation based on previously computed results]**
	61-65	I5	IMOV	Cavity shape plot index: 0 - no plots desired 1 - plots desired
	66-70	I5	IPG	Index for specifying plots of prescribed variables versus time: 0 - no plots desired 1 - plots desired
	71-75	I5	ISPABL	Index that specifies ablation of atmosphere surroundings: 0 - no ablation **[1 - surroundings ablate]**
	76-80	I5	IAOPAC	Index that specifies radiative treatment of atmosphere: 0 - treated as transparent 1 - opacity due to aerosols computed and included
				CONTROL PARAMETERS
3	1-10	E10.0	DELTIM	Time-step control: > 0 - Δt, time step (s) ≤ 0 - time step controlled by Card Group 3A
	11-20	E10.0	TIMEO	t_o, initial time at which calculations are to begin (s)
	21-30	E10.0	TIMEND	t_{max}, final time at which calculations are to cease (s)

Options indicated by **[...]** are not operational.

Table 5.I (cont.)

Card/ Group#	Field	Format	Variable Name	Description
				CONTROL PARAMETERS (CONT.)
	31-40	E10.0	**[DPRIN]**	**[Diagnostic print interval - print (diagnostic messages) every DPRIN seconds starting at TIME = TPRIN (s)]**
	41-50	E10-0	TPRIN	Time at which diagnostic printing every **[DPRIN seconds]** timestep is to begin (s)
Variable time step control. Include Card Group 3A only if DELTIM $\leq$ 0.0.				
3A	1-10	F10.0	DTMN	Minimum time step for interval (s)
	11-20	F10.0	DTMX	Maximum time step for interval (s)
	21-30	F10.0	TEND	End time for interval (s)
		Repeat for a maximum of 10 intervals, terminate with DIMN $\leq$ 0.0.		
Variable edit control. Include Card Group 3B only if IPINC $\leq$ 0.				
3B	1-10	F10.0	DED	Time between edits for interval (s)
	11-20	F10.0	TED	End time for interval (s)
		Repeat for a maximum of 10 intervals, terminate with DED $\leq$ 0.0.		

Table 5.I (cont.)

Card/ Group#	Field	Formal	Variable Name	Description
				SECTION 2. PROBLEM INITIAL CONDITIONS
				CONCRETE CRUCIBLE INITIAL GEOMETRY
4	1-5	I5	NRAYS	Number of rays (maximum of 100)
	6-15	F10.0	RO*	R-coordinate of center of ray system (m)
	16-25	F10.0	ZO	Z-coordinate of center of ray system (m). Measured positive downward, reference is arbitrary.
Cylinder with hemispherical base - see Section 5.1.1 (Figure 5.1). Include card 5 only if IGEOM = 1.				
5	1-10	F10.0	RS	Radius of hemispherical base (m)
	11-20	F10.0	HC	Height of cylindrical top section (m)
	21-30	F10.0	RW	External radius of concrete crucible (m)
	31-40	F10.0	HBC	Height from external base of crucible to base of cylindrical section (m)
Cylinder with flat base - see Section 5.1.1 (Figure 5.2). Include card 6 only in IGEOM = 2.				
6	1-10	F10.0	ZT	Z-coordinate of cylinder top edge (m)
	11-20	F10.0	RAD	Radius of cylinder (m)
	21-30	F10.0	HIT	Height of cylinder (m)
	31-40	F10.0	RADC	Radius of corner (m)
	41-50	F10.0	RW	External radius of concrete crucible (m)
	51-60	F10.0	HBB	Height from external base of crucible to base of cavity (flat bottom) (m)

*only permitted value is 0.0

Table 5.I (cont.)

Card/ Group#	Field	Format	Variable Name	Description
				INITIAL GEOMETRY (CONT.)
6 (cont.)	61-65	I5	NBOT	Number of ray points equally spaced along flat bottom of cavity
	66-70	I5	NCORN	Number of ray points equally spaced around corner (not including tangent points)

[Cylinder with spherical-segment base - not operational. No input for IGEOM = .3]

Arbitrary shape - see Section 5.1.1 (Figure 5.3). Include card 7 and groups 8 and 9 only if IGEOM = 4.

7	1-5	I5	NBOT	Number of ray points equally spaced along flat bottom
	6-15	F10.0	RTANG	R-coordinate of tangent point (m)
	16-25	F10.0	RW	External radius of concrete crucible (m)
	26-35	F10.0	HTOTL	Height from external base to top of crucible (m)
8	1-10	F10.0	R(1)	R-coordinate of body point 1 (m)
	11-20	F10.0	Z(1)	Z-coordinate of body point 1 (m)
9	1-10	F10.0	R(I)	R-coordinate of body point I, I = NBOT + 2, NRAYS (m)
	11-20	F10.0	Z(I)	Z-coordinate of body point I, I = NBOT + 2, NRAYS (m)

(There will be (NRAYS - NBOT -1) cards in Group 9)

CONCRETE COMPOSITION AND PROPERTIES

10	1-10	E10.0	TIC	Initial temperature of concrete (K)

Options indicated by **]...]** are not operational.

Table 5.I (cont.)

Card/ Group#	Field	Format	Variable Name	Description
				CONCRETE COMPOSITION AND PROPERTIES (CONT.)
10 (cont.)	11-20	E10.0	TW	Temperature of concrete surface (ablation temperature) (K)
	21-30	E10.0	EW	Emissivity of concrete surface (-)
	31-40	E10.0	RBR	Amount of reinforcing steel in the concrete (mass fraction: kg_{FE}/kg_{CONC})
				Card 11, group 12, and card 13 should be included only if ICON = 0.
11	1-5	I5	NINP	Number of species in concrete mixture; includes only species available in the Master Species List
12	1-8	A8	NAMSP	Species name of concrete species (left justified)
	11-20	E10.0	SM	Mass fraction of concrete species (kg/kg_{CONC})
				(There will be NINP cards in group 12.)
13	1-10	E10.0	RHOC	ρ_C, density of concrete (kg/m^3)
	11-20	E10.0	TSOLCT	Concrete solidus temperature (K)
	21-30	E10.0	TLIQCT	Concrete liquidus temperature (K)
				CORE MELT CONSTITUENTS
				INITIAL MASSES, COMPOSITIONS, AND TEMPERATURES
14	1-5	I5	NOSI	Number of melt oxidic species to be read in; this number includes only species available in the Master Species List (NOSI $\leq$ 19).

Table 5.I (cont.)

Card/ Group#	Field	Format	Variable Name	Description
			INITIAL MASSES, COMPOSITIONS, AND TEMPERATURES (CONT.)	
14 (cont.)	6-10	I5	NMSI	Number of melt metallic species to be read in; this number includes only species available in the Master Species List (NMSI $\leq$ 5).
	11-20	E10.0	TOI	Initial oxidic melt temperature (K)
	21-30	E10.0	TMI	Initial metallic melt temperature (K)
15	1-8	A8	NAMSP	Species name of oxidic species (left justified)
	11-20	E10.0	SM	Mass of oxidic species (kg)
			(There will be NOSI cards in group 15.)	
16	1-8	A8	NAMSP	Species name of metallic species (left justified)
	11-20	E10.0	SM	Mass of metallic species (kg)
			(There will be NMSI cards in group 16.)	
			INTACT CORE SIZE AND POWER, AND NUMBER OF RETENTION FRACTIONS TO BE MODIFIED	
			Card 17 and group 18 should be included only if IFP = 0.	
17	1-10	E10.0	XMTU	Core size (metric tons of uranium)
	11-20	E10.0	XMWTH	Core operating power (MW thermal)
	21-25	I5	NUM	Number of radioactive species in the intact core inventory for which the retention factor will be modified (NUM $\leq$ 27)

Table 5.I (cont.)

Card/ Group#	Field	Format	Variable Name	Description
			INTACT CORE SIZE AND POWER, AND NUMBER OF RETENTION FRACTIONS TO BE MODIFIED (CONT.)	
18	1-4	A4	IFP1	Name of radioactive species whose retention factor is to be modified (left justified)
	11-20	E10.0	RETI	Retention factor of radioactive species IFPI
			(There will be NUM cards in group 18.)	
			COOLANT INITIAL MASS, COMPOSITION, AND TEMPERATURE	
			Include Cards 18A and 18B only if ICOOL = 1	
18A	1-10	E10.0	TCI	Initial coolant temperature (K)
18B	1-8	A8	NAMSP*	Species name of coolant species (left justified)
	21-30	E10.0	FMCI	Mass of coolant species

*Only permitted value is H_2O.

Table 5.I (cont.)

Card/ Group#	Field	Format	Variable Name	Description
				ATMOSPHERE
				INITIAL VOLUME, PRESSURE, TEMPERATURE AND COMPOSITION
19	1-10	E10.0	VA	Initial gas volume (m^3)
	11-20	E10.0	PA	Initial gas pressure (N/m^2) > 0 - constant for problem ≤ 0 - pressure specified by card 20A and group 20B
	21-30	E10.0	TA	Initial gas temperature (K)
	31-35	I5	NGSINP	Number of gaseous species in the atmosphere; includes only species available in the Master Species List (NGSINP ≤ 18).
20	1-8	A8	NAMSP	Species name of gaseous species (left justified)
	11-20	E10.0	SM	Mole fraction of gaseous species (-)
				(There will be NGSINP cards in group 20.)
				Card 20A and group 20B should be included only if PA ≤ 0
20A	1-5	I5	NATMPR	Number of points in table of pressure of gas atmosphere versus time 1 ≤ NATMPR ≤ 10
20B	1-10	E10.0	TPA(1)	Table of PAT versus TPA; alternate values of time, TPA(J) (s), and gas pressure PAT(J) (PA), J = 1, NATMPR. May need up to 2 cards to complete the table.
	11-20	E10.0	PAT(1)	
	21-30	E10.0	TPA(2)	
	31-40	E10.0	PAT(2)	
	.	.		
	.	.		
	.	.		
		E10.0	TPA(NATMPR)	If NATMPR = 1, pressure is constant at PAT(1)
		E10.0	PAT(NATMPR)	

Table 5.I (cont.)

Card/ Group#	Field	Format	Variable Name	Description
				SECTION 3. MELT INTERNAL HEAT GENERATION
				DECAY POWER FOR OXIDIC AND METALLIC PHASES INPUT SEPARATELY VERSUS TIME
				Card 21 and groups 22 and 23 should be included only if IFP = 2.
21	1-5	I5	NDECO	Number of points in table of oxidic phase power versus time 0 ≤ NDECO ≤ 30
	6-10	I5	NDECM	Number of points in table of metallic phase power versus time 0 ≤ NDECM ≤ 30)
				Group 22 should be included only if NDECO > 0
22	1-10	E10.0	TIO(1)	Table of PIO versus TIO; alternate values of time, TIO(J) (s), and oxidic phase power, PIO(J) (W), J = 1, NDECO. May need up to 8 cards to complete the table.
	11-20	E10.0	PIO(1)	
	21-30	E10.0	TIO(2)	
	31-40	E10.0	PIO(2)	If NDECO = 1, power is constant at PIO(1).
	.	.	.	
	.	.	.	
		E10.0	TIO(NDECO)	
		E10.0	PIO(NDECO)	
				Group 23 should be included only if NDECM > 0
23	1-10	E10.0	TIM(1)	Table of PIM versus TIM; alternate values of time, TIM(J) (s), and metallic phase power, PIM(J) (W), J = 1, NDECM. May need up to 8 cards to complete the table.
	11-20	E10.0	PIM(1)	
	21-30	E10.0	TIM(2)	
	31-40	E10.0	PIM(2)	If NDECM = 1, power is constant at TIO(1).
	.	.	.	
	.	.	.	
		E10.0	TIM(NDECM)	
		E10.0	PIM(NDECM)	

Table 5.I (cont.)

Card/ Group#	Field	Format	Variable Name	Description
				SECTION 4. BOUNDARY CONDITIONS OF PROBLEM ATMOSPHERE SURROUNDINGS
				SURROUNDINGS TEMPERATURE HISTORY
				Card 24 and group 25 should be included only if ISUR ≠ 0.
24	1-5	I5	NTP	Number of points in table of surroundings temperature versus time (NTP ≤ 10)
25	1-10	E10.0	TTS(1)	Table of TMPS versus TTS; alternate values of time, TTS(J) (s), and surroundings temperature, TMPS(J) (K), J = 1, NTP. May need up to 3 cards to complete table.
	11-20	E10.0	TMPS(1)	
	21-30	E10.0	TTS(2)	
	31-40	E10.0	TMPS(2)	
	.	.	.	
	.	.	.	
		E10.0	TTS(NTP)	
		E10.0	TMPS(NTP)	
				ABLATION OF SURROUNDINGS
				RATES OF SPECIES MASS ADDITION TO POOL INPUT SEPARATELY VERSUS TIME
				Card 26 and groups 27, 28, and 29 should be included only if IABL ≠ 0 and ISRABL ≠ 0.
** 26	1-5	I5	NSPG	Number of species that make up material of gas phase container; includes only species available in the Master Species List (NSPG ≤ 10)
27	1-	A8	NAMSP	Species names of species in material of gas phase container (left justified) **
				(There will be NSPG cards in group 27.)

Options indicated by **[ ]** are not operational.

Table 5.I (cont.)

Card/ Group#	Field	Format	Variable Name	Description
			RATES OF SPECIES MASS ADDITION TO POOL INPUT SEPARATELY VERSUS TIME (CONT.)	
28	1-5	I5	NMP(1)	Number of points in table of mass flow rate versus time for first species as defined in card group 27
	6-10	I5	NMP(2)	Same as above except for second species as defined in card group 27
	.	.	.	
	.	.	.	
		I5	NMP(NSPG)	Same as above except for species NSPG as defined in card group 27
				NMP(I) $\leq$ 10, I = 1, NSPG
29	1-10	E10.0	TMS(1,1)	Tables of mass flow rate of species I, FMS(J,I) (kg/s), versus time, TMS(J,I)(s), for each species I (I = 1, NSPG) named in group 27; the number of table entries for each species is NMP(I).
	11-20	E10.0	FMS(1,1)	
	21-30	E10.0	TMS(2,1)	
	31-40	E10.0	FMS(2,1)	
	.	.	.	
	.	.	.	
		E10.0	TMS(NMP(1),1)	
		E10.0	FMS(NMP(1),1)	
	1-10	E10.0	TMS(1,2)	Start a new card for each species I, first inputting a time, TMS(J,I), then a mass flow rate, FMS(J,I), and alternate accordingly. May need up to 13 cards in this group to complete the tables.
	11-20	E10.0	FMS(1,2)	
	21-30	E10.0	TMS(2,2)	
	31-40	E10.0	FMS(2,2)	
	.	.	.	
	.	.	.	
		E10.0	TMS(NMP(2),1)	
		E10.0	FMS(NMP(2),1)	
	1-10	E10.0	TMS(1,NSPG)	
	11-20	E10.0	FMS(1,NSPG)	

Options indicated by **[...]** are not operational.

Table 5.I (cont.)

Card/ Group#	Field	Format	Variable Name	Description
			RATES OF SPECIES MASS ADDITION TO POOL INPUT SEPARATELY VERSUS TIME (CONT.)	
** 29 (cont.)	21-30	E10.0	TMS(2,NSPG)	**
	31-40	E10.0	FMS(2,NSPG)	
	.	.	.	
	.	.	.	
		E10.0	TMS(NMP(NSPG),NSPG)	
		E10.0	FMS(NMP(NSPG),NSPG)	
			EMISSIVITIES FOR RADIATION HEAT TRANSFER COMPUTATIONS	
30	1-4	A4	IREO	Variable name (TIME or TEMP) for table of oxidic phase emissivity, ε_o, versus IREO
	5-8	A4	IREM	Variable name (TIME or TEMP) for table of metallic phase emissivity, ε_m, versus IREM
	9-12	A4	IRES	Variable name (TIME or TEMP) for table of surroundings emissivity, ε_{sur}, versus IRES
31	1-5	I5	NEO	Number of values in ε_o versus IREO table ($1 \leq NEO \leq 5$)
	6-10	I5	NEM	Number of values in ε_m versus IREM table ($1 \leq NEM \leq 5$)
	11-15	I5	NS	Number of values in ε_{sur} versus IRES table ($1 \leq NS \leq 5$)
32	1-10	E10.0	TORT1(1)	Table of oxidic phase emissivity, EO(I) (-), versus time (s) or temperature (K), TORT1(I); alternate values of TORT1(I) and EO(I), I = 1, NEO. May need up to 2 cards in this group to complete table.
	11-20	E10.0	EO(1)	
	21-30	E10.0	TORT1(2)	
	31-40	E10.0	EO(2)	
	.	.	.	
	.	.	.	If NEO = 1, emissivity is constant at EO(1).
	.	.	.	
		E10.0	TORT1(NEO)	
		E10.0	EO(NEO)	

Options indicated by **[...]** are not operational.

Table 5.I (cont.)

Card/ Group#	Field	Format	Variable Name	Description
			EMISSIVITIES FOR RADIATION HEAT TRANSFER COMPUTATIONS (CONT.)	
33	1-10	E10.0	TORT2(1)	Table of metallic phase emissivity, EMM(I) (-), versus time (s) or temperature (K), TORT2(I); alternate values of TORT2(I) and EMM(I), I = 1, NEM. May need up to 2 cards in this group to complete table.
	11-20	E10.0	EMM(1)	
	21-30	E10.0	TORT2(2)	
	31-40	E10.0	EMM(2)	
	.	.	.	If NEM = 1, emissivity is constant at EMM(1).
	.	.	.	
	.	.	.	
	.	E10.0	TORT2(NEM)	
		E10.0	EMM(NEM)	
34	1-10	E10.0	TORT6(1)	Table of surroundings emissivity, ES(I) (-), versus time (s) or temperature (K), TORT6(I); alternate values of TORT6(I) and ES(I), I = 1, NS. May need up to 2 cards in this group to complete table.
	11-20	E10.0	ES(1)	
	21-30	E10.0	TORT6(2)	
	31-40	E10.0	ES(2)	
	.	.	.	If NS = 1, emissivity is constant at ES(1)
	.	.	.	
	.	.	.	
		E10.0	TORT6(NS)	
		E10.0	ES(NS)	
			Card 34A should be included only if IAOPAC = 0	
34A	1-10	E10.0	PADLEN	Characteristic path length (m) for atmospheric opacity calculation
			SPLASHOUT OF POOL CONSTITUENTS	
			Card 35 and groups 36 and 37 should be included only if ISPLSH ≠ 0.	
** 35	1-5	I5	NSP1	Number of points in table of metallic phase splashout rate versus time (NSPI ≤ 10)
	6-10	I5	NSP2	Number of points in table of oxidic phase splashout rate versus time (NSP2 ≤ 10) **]

Options indicated by **[...]** are not operational.

Table 5.I (cont.)

Card/ Group#	Field	Format	Variable Name	Description
			SPLASHOUT OF POOL CONSTITUENTS (CONT.)	
36	1-10	E10.0	TMM(1)	Table of metallic phase splashout rate, FMM(I) (kg/s), versus time, TMM(I) (s); alternate values of TMM(I) and FMM(I), I = 1, NSP1. May need up to 3 cards in this group to complete table.
	11-20	E10.0	FMM(1)	
	21-30	E10.0	TMM(2)	
	31-40	E10.0	FMM(2)	
	.	.	.	
	.	.	.	
		E10.0	TMM(NSP1)	
		E10.0	FMM(NSP1)	
37	1-10	E10.0	TMO(1)	Table of oxidic phase splashout rate, FMO(I) (kg/s), versus time, TMO(I) (s); alternate values of TMO(I) and FMO(I), I = 1, NSP2. May need up to 3 cards in this group to complete table.
	11-20	E10.0	FMO(1)	
	21-30	E10.0	TMO(2)	
	31-40	E10.0	FMO(2)	
	.	.	.	
	.	.	.	
		E10.0	TMO(NSP2)	
		E10.0	FMO(NSP2)	

Options indicated by **[...]** are not operational.

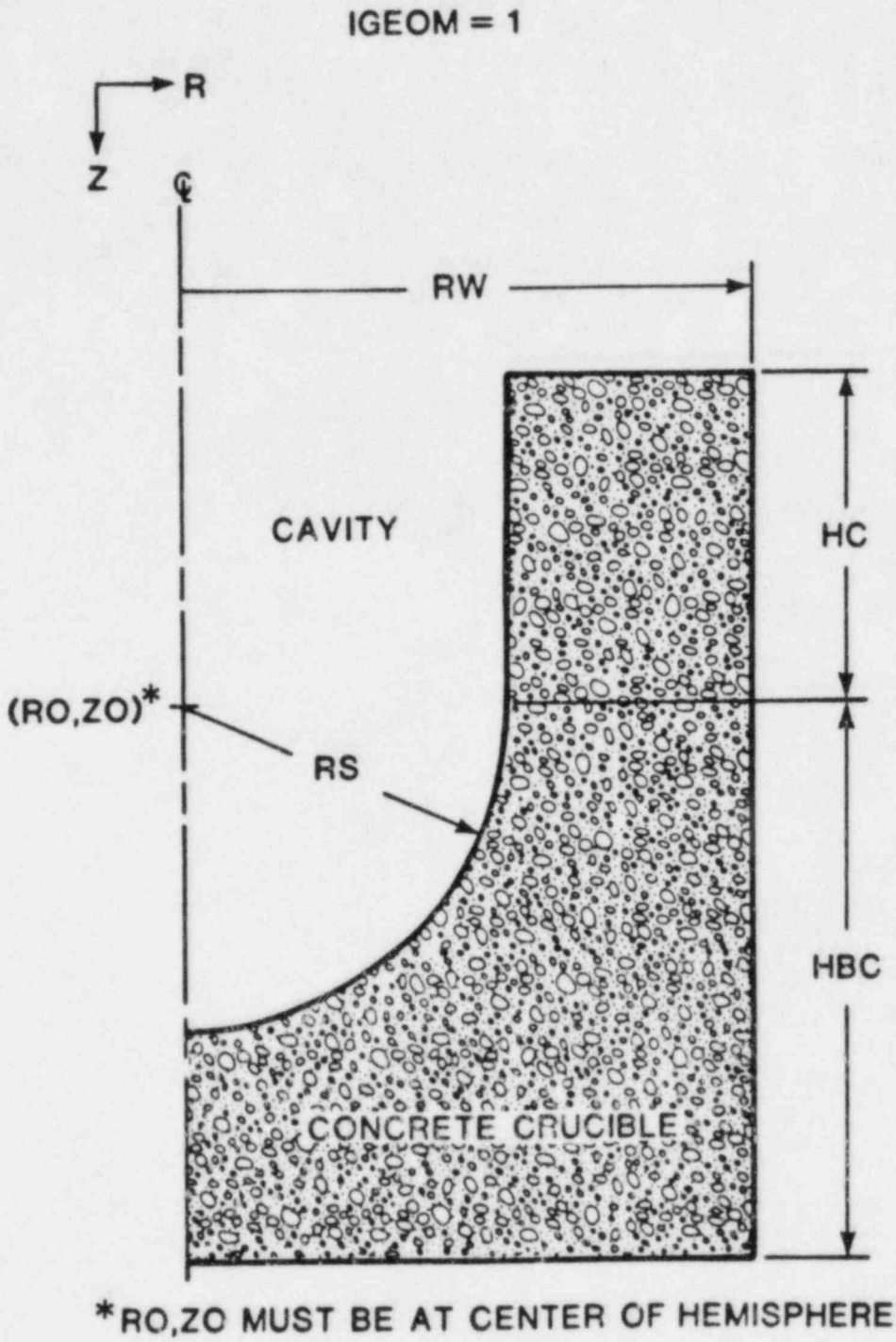

Figure 5.1 Initial Cavity Geometry - Cylinder with Hemispherical Base

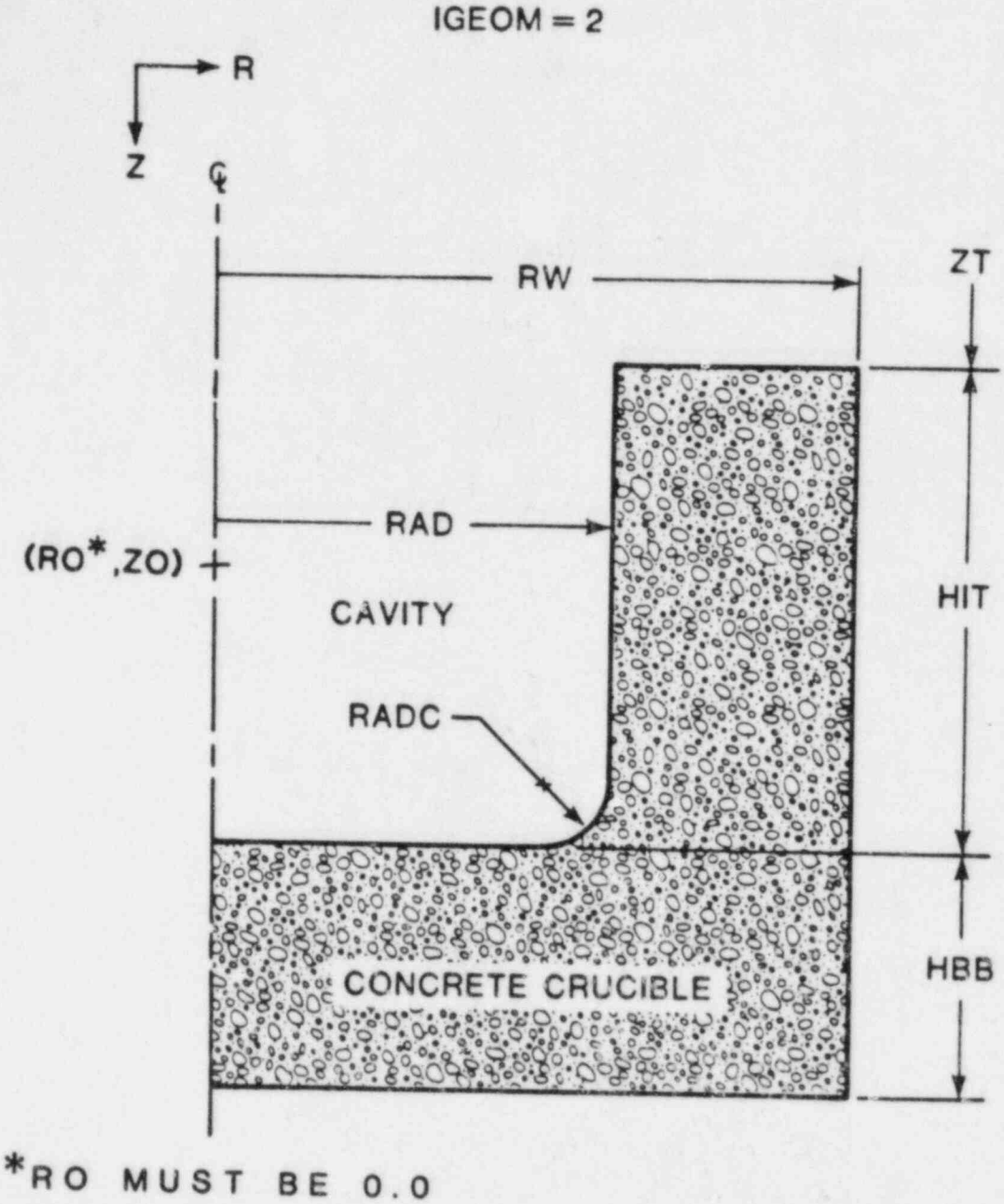

Figure 5.2 Initial Cavity Geometry - Cylinder with Flat Base

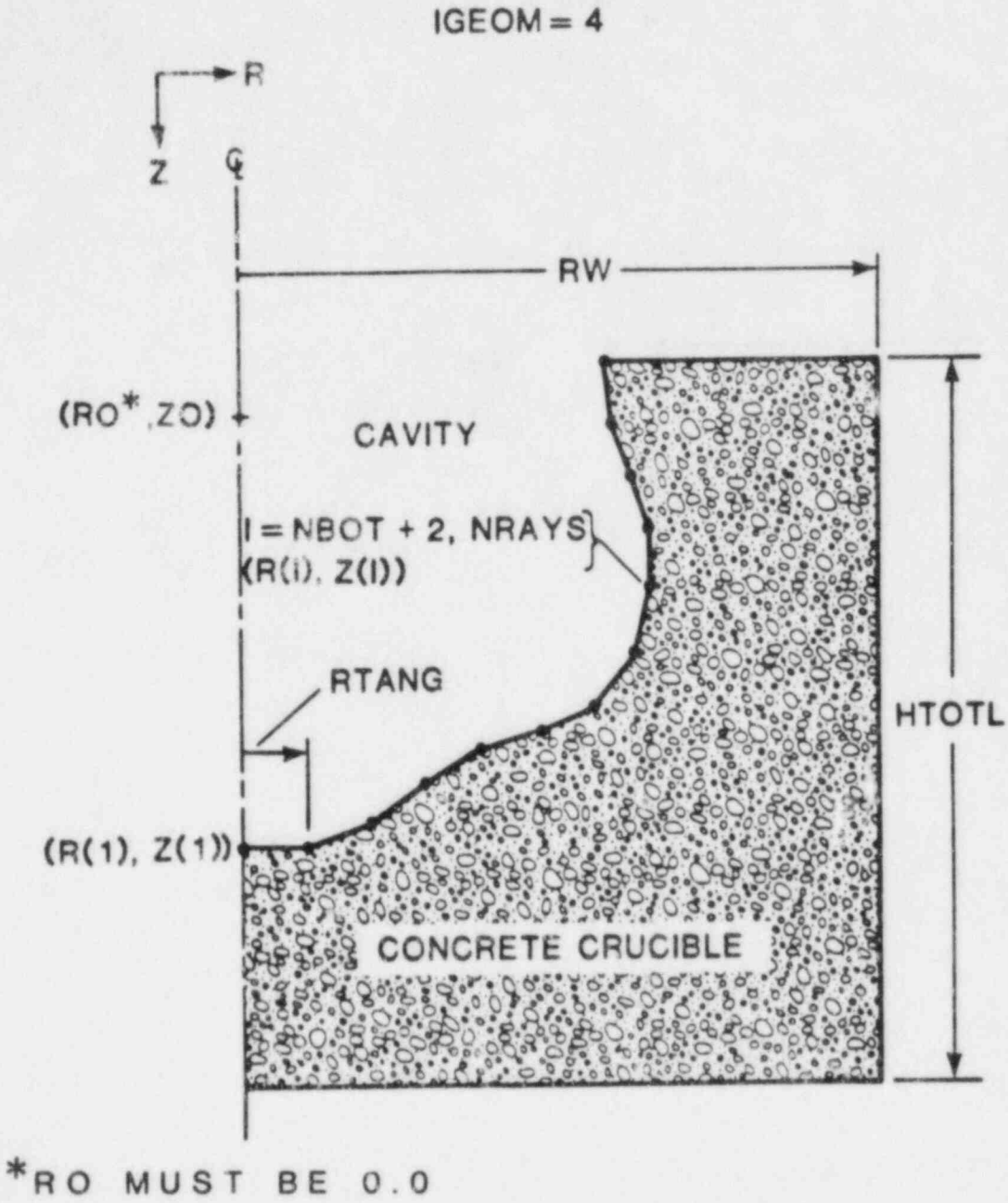

Figure 5.3 Initial Cavity Geometry - Arbitrary Shape

Edits are produced at times which are integral multiples of the edit interval DEDIT(I) (rather than at DEDIT(I) from the previous edit). This minimizes the effect of insertion of additional edits, which is valuable if one must compare the outputs from several calculations. To clarify this, consider as an example a calculation performed with edit controlled by an input card such as

```
1200.0    21600.0
```

This will produce printed output every 1200.0s (20 min), at times of 1200.0s, 2400.0s, 3600.0s, 4800.0s, etc. Suppose that some "interesting" phenomenon is observed at about 3000s, and that more frequent output is desirable to study it: the set of input cards

```
1200.0     3000.00
  60.0     3300.0
1200.0    21600.0
```

will produce additional printed output at 3000.0s, 3060.0s, ..., 3300.0s. However, the later edits will still be written at times of 3600.0s, 4800.0s, etc., rather than being shifted to 4500.0s, 5700.0s, etc.

If variable timestep control is specified (DELTIM < 0.0) but no intervals specified, the calculation will be terminated following input. If variable edit control is specified (IPINC < 0) but no intervals specified, the calculation will be run but no (printed) output generated. This might be desired by a user who is interested only in plots.

The definitions of most of the variables used to describe the initial cavity geometry (cards 5-9) should be apparent from Figures 5.1-5.3 or Section 6.4. However, NBOT and ITANG warrant further discussion. The cavity shape description introduces a "tangent ray" parallel to the cavity axis through the tangent point between the flat bottom of the cavity and the curved sides. This ray is used in the shape-change calculation to maintain the flat bottom as required by the models. For the flat-bottomed cylinder, IGEOM = 2, or the arbitrary cavity shape, IGEOM = 4, there is already a normal ray through this tangent point, numbered NBOT. The tangent ray, numbered ITANG = NBOT + 1, defines an additional body point which initially coincides with that defined by ray NBOT, but diverges from it as the surface recedes. The numbering of the rays is changed as the calculation proceeds, to reflect their actual ordering along the cavity surface (note that "normal" points can cross over the tangent ray). In the case of a hemispherically-based cavity, IGEOM = 1, a flat bottom is assumed to exist with a radius which is 1 percent of the sphere radius RS, and only a single point is defined with the number ITANG = NBOT = 2.

The size and power of the intact core (card 17) is used to determine the concentration of fission products in the fuel if IFP = 0. This concentration as modified by retention factors for each element included, together with the initial UO2 mass in the pool, is used to evaluate the initial fission-product inventory of the melt. If the initial mass exceeds the size of the intact core, a warning is issued.

5.1.2 Recommendations on Selected Input Quantities

The timestep for CORCON is controlled by user input (card 3 and, optionally, Group 3A). In selecting values for the timestep, the user should remember that the CORCON model is explicit in time for the calculation of ablation rates and convective mass and energy flows. Therefore, if too-large timesteps are employed, unphysical results may be generated or the calculation may fail completely. Based on experience with CORCON-MOD1, we recommend timestep values in the range of 15-60s (at least at early times). At later times, the timestep could be increased using the variable control optionally provided through Group 3A. This should be used with care, however, since discontinuities in the physical phenomena (such as those following layer flip or coolant depletion) could lead to numerical problems for very long timesteps.

The ablation temperature for concrete, TW, is not clearly defined, and must be specified by the user. Powers[69] recommends that TW be chosen one third of the way from the solidus, TSOLCT, to the liquidus, TLIQCT. For the default concretes, these temperatures may be found in Table 3.III.

When using the internally-calculated decay-heat generation, the initial time, TIMEO, corresponds to the time following reactor shutdown (SCRAM) that the melt is deposited into the reactor cavity. If a specific time is not known, a value of TIMEO in the range of 2-5 hours would be reasonable.

In specification of the ray system (card 4), the origin must be on the axis of symmetry (RO = 0.0). Based on sensitivity calculations, we recommend that ZO be chosen to maximize the number of rays whose intersection with the cavity surface is close to perpendicular, while avoiding small-angle intersections. In any case, the origin must lie above the bottom of the cavity. The ray spacing should be chosen so that the separation between body points (intersections of rays with the cavity surface) is initially in the range of 3-30cm.

5.2 Output Description

The printed output from CORCON-MOD2 contains several major sections. The first section is an "echo" of the input data; it is an uninterpreted reproduction of the records encountered in

the input stream. This serves as a compact, permanent record of the data used in any particular calculation, and is also useful in finding errors in data input. The second output element is an expansion of the data, identifying input variables. Quantities implied by them, such as the composition of a default concrete or the initial decay power, are also printed. Printed messages will be generated if errors are encountered in the input. In this case, the program will continue with input processing (if possible) but execution will be terminated at the end of input. This can reduce the number of passes needed to find all the errors in an input deck.

The third output section is a "snapshot" edit of the state of the problem. This is generated at the initial time, TIMEO, and as often as requested thereafter. The information is printed under several major headings, each starting a new page of output, with a running header to identify the version of the code in use (for purposes of configuration control), the problem title, the problem time, and the timestep number. The major headings, and information contained under each, are:

GENERAL SUMMARY

Pool configuration, maximum depth and radius of the cavity, an approximate energy budget, and quantities needed to check the accuracy of code numerics.

The energy budget is a summary of the pool's rates of gain or loss of energy (in Watts) through various mechanisms. It must be emphasized that the budget is not exact; some entries are current rates and others are averages over the preceding timestep. In some cases, approximations have been made in the calculation of terms which are not otherwise used in CORCON-MOD2. Therefore, the printed energy budget does not balance exactly, although the error is usually small (a few percent). However, large discrepancies may appear following a major discontinuity in the physical phenomena such as start-of-problem, coolant depletion, or layer flip. Also, the budget is for debris-containing layers only (does not include water or concrete). Detailed checks on conservation of mass and energy in the entire pool (including coolant, if present) are also made, and the results presented in the Summary. The printed quantities are the discrepancies between sums of layer contents and the values required by conservation within the pool boundaries, expressed as relative errors. Under normal conditions, each value should be near machine roundoff (1E-14 for CDC, 1E-7 for IBM machines running in single precision).

GAS GENERATION

Generation rates and cumulative releases of all condensible and noncondensible gas species. These are presented both as masses and as moles, and include bubbles, gas film, and vaporized coolant.

GEOMETRY

Locations of body points defining the cavity shape, the distance of each from bottom center (along the concrete surface), the local slope of the wall, and the angle of the ray which defines the point. Also, the cumulative volume and surface area below each point, the average void fraction at its elevation, and the locations of interfaces between pool layers.

HEAT TRANSFER

For each body point, the local normal ablation rate and gas film conditions including film thickness, filmwise mass flow and average velocity, Reynolds number, film regime, and resulting film heat-transfer coefficient. Also, the temperature of the pool/film interface and the contributions of convection and radiation to the heat flux.

REACTIONS DURING TIMESTEP

A summary of reactants and products for each chemical reaction occurring during the preceding timestep. Also shown is the number of iterations required for convergence of the numerical algorithm.

POOL COMPOSITION

The mass of each species contained in each (occupied) layer, together with total layer masses.

LAYER PROPERTIES

Values of thermophysical and transport properties, for each layer. Also, gas-bubble-related quantities, heat transfer coefficients, crust-model quantities, and (axial) interface temperatures. Finally, important terms in the layer energy equation.

In CORCON, enthalpies are referred to the standard thermochemical reference point of separated elements in their standard states at 298K and 1 atmosphere. The enthalpy of a compound therefore includes its heat of formation, and is negative under most, if not all, conditions encountered.

The heat-transfer coefficients to the top, bottom, and side surfaces of a layer are for the liquid only. If a crust is present, they are for heat transfer from the bulk liquid, at the given average temperature, to the crust. If the layer is completely solid, so that no liquid is present, these coefficients and the average liquid temperature are all printed as 0. In this case, no attempt is made to define a top or bottom crust and for edit purposes, each is given a thickness equal to that of the layer. Also, the printed values of the viscosity (and Prandtl number) printed correspond to the liquid at the solidus temperature, even though no liquid is present.

All quantities are evaluated at the current time (unlike CORCON-MOD1) with the exception of the "heat of reaction" which is an average over the preceding timestep.

A fourth element of output, which contains extensive diagnostic information, may be generated, controlled by the variable TPRIN on Card 3. This printed output is intended primarily for code debugging; it is labelled in terms of FORTRAN variable names and assumes that the user has some detailed knowledge of the code. Under ordinary circumstances, this output should be suppressed by specifying TPRIN greater than the problem end time, TIMEND.

5 3 CORCON-Generated Error Messages

A number of error checks are performed by CORCON-MOD2. First, the input data are examined for obvious errors or inconsistencies. Then, various intermediate results of the transient calculation are tested to determine if they are physically realistic, within the limits of CORCON-MOD2 models, and numerically converged. When an error condition is detected, an appropriate message is issued. Subsequent action depends on the severity of the error and may take the form of immediate termination, termination at the end of the current time-step, or continuation of the calculation with a warning. The messages which a user might encounter are listed below, together with the code action. While most are self-explanatory, a few comments are included in the list which follows:

"* * * ABLATE * * *, INTERPOLATION FOR MASS ADDITION () AT () OFF LOW END OF TABLE ()" (Warning only).

"* * * ABLATE * * *, INTERPOLATION FOR MASS ADDITION () AT () OFF HIGH END OF TABLE ()" (Warning only).

"* * * ATMPRO * * *, INTERPOLATION FOR ATMOSPHERIC PRESSURE AT () OFF LOW END OF TABLE ()" (Warning only).

"* * * ATMPRO * * *, INTERPOLATION FOR ATMOSPHERIC PRESSURE AT () OFF HIGH END OF TABLE ()" (Warning only).

"* * * ATMSUR * * *, INTERPOLATION FOR SURROUNDINGS TEMPERATURE AT () OFF LOW END OF TABLE ()" (Warning only).

"* * * ATMSUR * * *, INTERPOLATION FOR SURROUNDINGS TEMPERATURE AT () OFF HIGH END OF TABLE ()" (Warning only).

"* * * ATMSUR * * *, CONVERGENCE FAILURE" (Immediate Termination). Failure to match above-pool heat transfer to pool surface.

"* * * BUBBLE * * *, NEGATIVE BUBBLE VELOCITY" (Immediate Termination).

"* * * CONPRP * * *, CONCRETE INPUT SPECIES () NOT IN MASTER LIST" (Deferred termination).

"* * * CYLIND * * *, NRAYS = () LESS THAN NBOT+NCORN+3" (Deferred termination). Too few rays or too many bottom and corner points in cavity definition.

"* * * DATAIN * * *, NO DATA ON UNIT 5" (Immediate termination).

"* * * DATAIN * * *, TOO MANY TIMESTEP INTERVALS" (Deferred termination).

"* * * DATAIN * * *, NO TIMESTEP INPUT" (Deferred termination).

"* * * DATAIN * * *, TOO MANY EDIT INTERVALS" (Deferred termination).

"* * * DATAIN * * *, INVALID IFP = ()" (Immediate termination).

"* * * DATAIN * * *, IREO = () IREM = () IRES = ()" (Immediate termination). Improper type for emissivity tables. Should be "TIME" or "TEMP".

"* * * DCYINT * * *, PROBABLE ERROR. POOL CONTAINS () PERCENT OF CORE" (Warning only). Input has specified a mass of UO2 greater than the entire core.

"* * * DHGEN * * *, INTERPOLATION FOR SOURCE POWER IN OXIDE AT () OFF LOW END OF TABLE ()" (Warning only).

"* * * DHGEN * * *, INTERPOLATION FOR SOURCE POWER IN OXIDE AT () OFF HIGH END OF TABLE ()" (Warning only).

"* * * DHGEN * * *, INTERPOLATION FOR SOURCE POWER IN METAL AT () OFF LOW END OF TABLE ()" (Warning only).

"* * * DHGEN * * *, INTERPOLATION FOR SOURCE POWER IN METAL AT () OFF HIGH END OF TABLE ()" (Warning only).

"* * * EMISIV * * *, INTERPOLATION FOR SURROUNDINGS EMISIVITY AT ()OFF LOW END OF TABLE ()" (Warning only).

"* * * EMISIV * * *, INTERPOLATION FOR SURROUNDINGS EMISIVITY AT ()OFF HIGH END OF TABLE ()" (Warning only).

"* * * EMISIV * * *, INTERPOLATION FOR OXIDE EMISIVITY AT ()OFF LOW END OF TABLE ()" (Warning only).

"* * * EMISIV * * *, INTERPOLATION FOR OXIDE EMISIVITY AT ()OFF HIGH END OF TABLE ()" (Warning only).

"* * * EMISIV * * *, INTERPOLATION FOR METAL EMISIVITY AT ()OFF LOW END OF TABLE ()" (Warning only).

"* * * EMISIV * * *, INTERPOLATION FOR METAL EMISIVITY AT ()OFF HIGH END OF TABLE ()" (Warning only).

"* * * ENRCN1 * * *, BAD DQDT, LLO,DQTDTT(LLO), LUP,DQBDTB(LUP)= () () () ()" (Immediate termination). Some heat flux vs temperature relation has a negative slope.

"* * * ENRCN1 * * *, MATRIX AMTRX IS SINGULAR AS DEDECTED BY SAXB" (Immediate termination). The equations for the solution of the implicit energy equation are singular.

"* * * ENRCN2 * * *, CONVERGENCE FAILURE. L,HTOT(L),TLAY(L) = () () ()" (Immediate termination). Failure to determine new layer temperature after energy update.

"* * * FILM * * *, CONVERGENCE FAILURE. JBODY,LYR,EMDO,EMD = () () ()()" (Immediate termination). Failure to determine consistent film properties (heat transfer coefficient and gas generation).

"* * * HTRCLN * * *, CONVERGENCE FAILURE" (Immediate termination). Failure to determine radiative contribution to boiling heat transfer.

"* * * HTRLAY * * *, MATRIX AMTRX IS SINGULAR AS DETECTED BY SAXB" (Immediate termination). The equations for determination of crust thicknesses are singular.

"* * * HTRLAY * * *, AXIAL CONVERGENCE FAILURE. L,KOUNT,LOOPL,LOOPT = () () () ()" (Warning only). Failure to determine state of layer consistent with boundary conditions. Has only been observed for vanishingly thin liquid sublayers, and usually in early iterations of INTEMP (so that result does not affect end-of-timestep results). Code continues, using conductive heat transfer for layer.

"* * * HTRLAY * * *, AXIAL SOLID CORE/LIQUID SURFACE WITH L,TS,TB,TL,TT = () () () () ()" (Warning only). Solid layer is being melted from the top and bottom. Has only been observed in early iterations of INTEMP (so that result does not effect end-of-timestep results). Code continues using convective heat transfer to the solidus temperature.

"* * * HTRLAY * * *, RADIAL CONVERGENCE FAILURE. L,KOUNT,LOOPL,LOOPT = () () () ()" (Immediate termination). Failure to determine state of layer consistent with boundary conditions.

"* * * HTRLAY * * *, RADIAL SOLID CORE/LIQUID SURFACE WITH L,TS,TL,TR = () () () ()" (Immediate termination). Solid layer being melted from the outside.

"* * * INCOOL * * *, COOLANT () NOT IN MASTER LIST" (Deferred termination).

"* * * INGEOM * * *, NRAYS = (), GREATER THAN LIMIT OF 100" (Immediate termination).

"* * * INGEOM * * *, RO = (). MUST BE 0.0" (Immediate termination).

"* * * INITL * * *, INVALID ILYR =,I2" (Deferred termination).

"* * * INPCON * * *, OXIDE () NOT IN MASTER LIST" (Deferred termination).

"* * * INPCON * * *, METAL () NOT IN MASTER LIST" (Deferred termination).

"* * * INPGAS * * *, GAS () NOT IN MASTER LIST" (Deferred termination).

"* * * INTEMP * * *, MATRX AMTRX IS SINGULAR AS DETECTED BY SAXB" (Immediate termination). The equations for determining interface temperatures are singular.

"* * * INTEMP * * *, CONVERGENCE FAILURE" (Warning only). Failure to determine temperatures of interfaces between layers such that heat fluxes are continuous. Code continues, using a weighted average of heat fluxes calculated from each side.

"* * * LEVSWL * * *, CAVITY TOO SMALL FOR MELT" (Immediate termination). Need to specify a larger cavity (remember level swell).

"* * * MASRAT * * *, CONVERGENCE FAILURE" (Immediate termination). Failure to match film heat transfer results to pool heat transfer at bottom of pool.

"* * * MLTREA * * *, REDOING SOLUTION FROM NEW STARTING GUESS" (Warning only). The equations for determining the next correction to equilibrium composition are singular. A new starting guess will usually avoid the problem region.

"* * MLTREA * * *, MATRIX AK IS SINGULAR IN FIRST CALL TO SAXB" (Immediate termination). The equations for determining the next correction to equilibrium composition are singular despite a new starting guess.

"* * * MLTREA * * *, APPARENT CONVERGENCE FAILURE RELATIVE ERROR IN TOTAL MASS = ()" (Warning only). Failure of chemical equilibrium routine. "Apparent" because error is often insignificant although code fails to recognize this. Check to verify that no serious violation of mass conservation has occurred.

"* * * PLLAYR * * *, CONVERGENCE FAILURE. L,HTOT(L),TLAY(L) = () () ()" (Immediate termination). Failure to determine new temperature of combined oxides in layer L following layer flip.

"* SOLLIQ * * *, METAL CONTAINS () NON CR-FE-NI MELT RANGE MAY BE INACCURATE" (Warning only). Metal contains more than 10% non-steel. Code continues, using liquidus and solidus for steel component.

"* * * SPHCYL * * *, IGEOM = 3 NOT OPERATIONAL" (Immediate termination).

"* * * SURFEB * * *, CONVERGENCE FAILURE. ICOUNT,TTA,QP,DQPDTA,QW,DQWDTA = () () () () () ()" (Immediate termination). Failure to match film heat transfer results to pool heat transfer.

"* * * SVLAAR * * *, CONVERGENCE FAILURE" (Immediate termination). Failure to determine liquidus and solidus temperatures for oxidic mixture.

A close inspection of the code listing will reveal several other places where a message could be printed and execution terminated by a call to FAIL. They correspond to conditions which, short of a machine error, cannot exist in CORCON-MOD2. These messages might appear if modifications were made to the code, and are included for that reason, but will not be described here.

6. CODING INFORMATION

6.1 List of Subroutines

Subroutines developed specifically for CORCON (excluding SAXB) are listed below along with brief descriptions of the functions they perform.

CORCON - controls program flow

ABLATE* - computes mass flow rate of each species in surroundings material as it ablates and falls into pool

ANGAVL - finds body angle at each ray (body) point

ARBINP - initializes an arbitrary shape cavity

ATMPRO* - determines bulk properties of the gas mixture (atmosphere) above the molten pool

ATMSUR - updates atmosphere and surroundings, or serves as an interface to a containment response code

BLKDAT - contains data tables including master species list, master molecular weight list, stoicheometric coefficients and phase table for MLTREA, and various pointers and global constants

BUBBLE - determines bubble sizes and velocities where the gas enters the pool and within pool layers

CHEMPO - computes enthalpy, entropy, and Gibbs free-energy of each species required for the melt-gas chemical reaction calculation in MLTREA

COMBIN - adds one mixture to another to produce a single mixture mass, composition, and enthalpy

CONFND - initializes data tables and finds coefficients for specific heat, enthalpy and entropy for a species as necessary for calculations in CHEMPO or CPENTH

CONPRP - initializes concrete composition and properties

---

*Not operational

CPENTH - computes specific heat and enthalpy of condensed melt phases for both single- and two-phase (liquid-solid) mixtures

CYLIND - initializes a flat-based cylindrical cavity shape

DATAIN - handles the input of data for the program

DCYINT - sets up initial intact core inventory of radioactive species and associated retention fractions, and initializes decay product pseudo-species

DCYPOW - evaluates the decay power of each radioactive element as a function of time

DENSTY - computes density of the condensed phases in melt

DHGEN - computes the decay heat generated within each pool layer

EDIT - manages the printed output of the code

EMISIV - determines the emissivities of the condensed phases of the pool from input tables of emissivity versus time or temperature

ENRCN1 - performs explicit update of layer energy equations, including boiling of coolant, and sets up implicit terms

ENRCN2 - finishes update of layer energy equations by adding implicit terms, and calculates new temperatures

EXPRNT - controls generation of extra debug print

FAIL - performs error handling when called by a subroutine which detects abnormal data or an invalid computation

FILM - advances state of gas film from one point to another and integrates results

GEOM - determines volume, surface area and stream length of the concrete cavity geometry as a function of body point

GFLMPR - computes average gas mixture properties in the gas film at each body point

HCBBOT - calculates bubble-enhanced liquid-liquid heat transfer coefficient at bottom of layer

HCBINJ - calculates heat transfer coefficient for bubble injection at bottom of pool

HCBSID - calculates bubble-enhanced heat transfer coefficient at side of pool

HCBTOP - calculates bubble-enhanced liquid-liquid heat transfer coefficient at top of layer

HSPCYL - initializes a hemispherically-based cylindrical cavity shape

HTRCLN - evaluates heat transfer in coolant layer, including boiling

HTRLAY - evaluates heat transfer in a layer, including conduction in solid regions

HTRLIQ - computes heat transfer coefficients in liquid layer or sub-layer, including bubble-enhanced convection, natural convection, and conduction

HTRN - computes gas film heat transfer coefficients in all regimes

INCOOL - inputs initial mass, temperature, and identity of coolant

INGEOM - inputs and defines the initial geometry of the concrete crucible

INITL - initializes necessary variables before entering main calculational loop

INPCON - inputs initial masses of core constituents and their temperatures

INPGAS - inputs and defines initial composition and state of atmosphere

INTEMP - computes temperatures and heat flows at layer interfaces

LEVSWL - calculates pool level swell, layer interface locations and layer average void fractions

LININT - performs linear interpolation or extrapolation from tables

MASLOS - computes mass loss from melt due to volatilization of fission products

MASRAT - determines concrete ablation rates (mass loss rates) at body points

MASSEX - serves as interface for mass exchange with atmosphere and surroundings

MHTRAN - updates layer species masses and evaluates effects of mass transport and chemical reactions on layer enthalpies

MLTPRP - determines transport properties of metallic and oxidic phases of melt

MLTREA - solves problem of chemical equilibrium iteratively by a constrained first-order steepest descent technique to minimize free energy

PAGEHD - prints page header with version identification and problem title

PLLAYR - calculates layer densities and determines layer flips

PLOTS - writes data file for post-processor plot program

PRTGAS - prints results from the metal/gas and/or oxide/gas reactions

QMELT - evaluates local heat flux on pool side of gas film

REACT - sets up necessary reactants for call to MLTREA and distributes the products returned

RECEDE - computes concrete normal recession and relocation of body points during a time step

RFBS - module of the equation solver SAXB

RLUD - module of the equation solver SAXB

SATP - evaluates saturation pressure as a function of temperature

SATT - evaluates saturation temperature as a function of pressure (an ENTRY in SATP)

SAXB - solves a system of real linear algebraic equations, AX = B. A Sandia Mathematical Library routine.

SETUP - performs code setup requiring execution (as opposed to data statements) including evaluation of machine roundoff

SIGMY - computes surface tensions of the condensed phases of the pool

SOLLIQ - sets up the components of pseudo-mixtures of oxides or metals and calls either SSMELT or SVLAAR to calculate mixture solidus and liquidus temperatures

SOURCE - evaluates decay heat source in pool

SPHCYL* - initializes a cylindrical cavity with a spherical segment bottom

SSMELT - calculates the liquidus and solidus temperatures of a metallic phase based on stainless steel (CR-FE-NI ternary)

SURFEB - performs a surface energy balance at a point on the cavity surface to determine mass flux of ablating concrete at a point

SVLAAR - does a Schroeder-von Laar pseudo-binary construction of T-solidus and T-liquidus for the oxidic phase

THKCND - determines the thermal conductivity of the condensed phases in the pool

TIMSTP - determines new time step

TMPFND - determines mixture temperature, given composition and enthalpy

UDU - module of equation solver SAXB

VISCTY - computes viscosity of the metallic and nonsiliceous oxidic phases of the melt

VIS2PH - computes Kunitz two-phase viscosity multiplier for suspended solids in the melt

VSCRIT - computes the critical superficial gas velocities into the pool for use in determining bubble sizes

6.2 Program Flow

The basic logic of CORCON-MOD2 is given in Figure 6.1 which is a flow chart of the main program. This corresponds to the verbal description given in Section 2.2. A list of subroutines called by each subroutine is presented in Table 6.I. Locations of subroutine calls are given in Table 6.II.

---

*Not operational

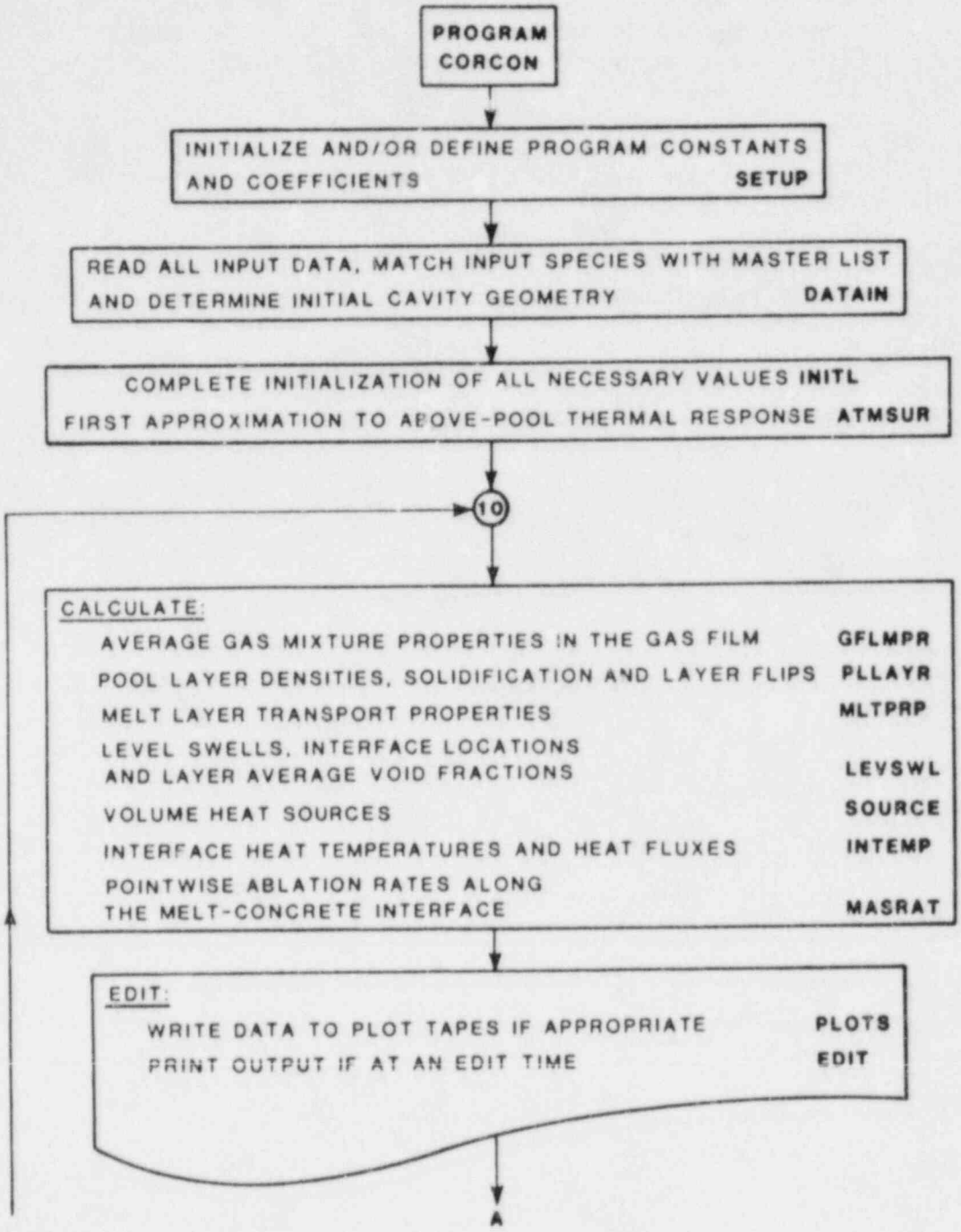

Figure 6.1 CORCON-MOD2 Flow Chart

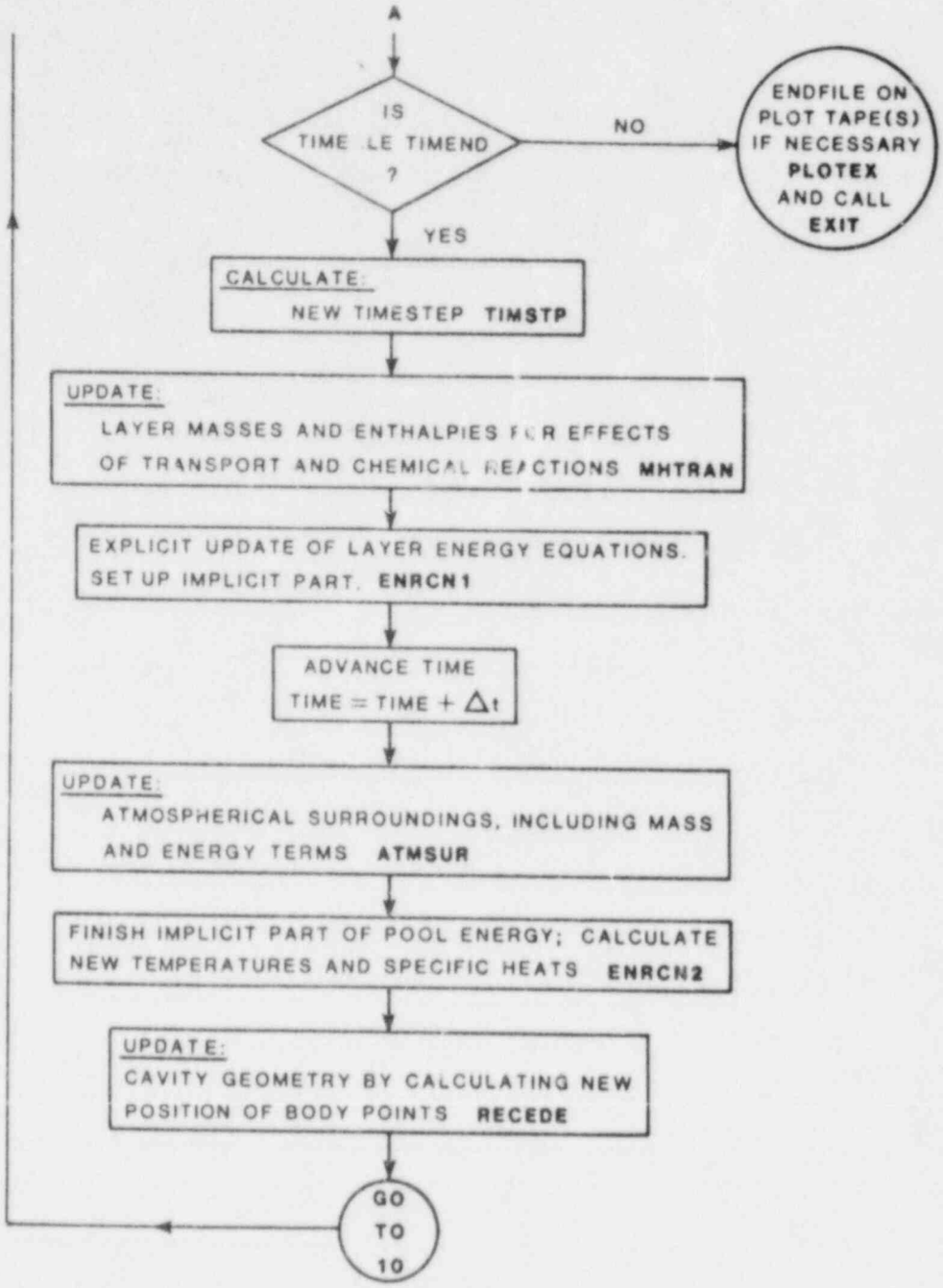

Figure 6.1 CORCON-MOD2 Flow Chart (continued)

Table 6.I
CORCON subroutines called by each program segment

ABLATE	calls	FAIL	LININT				
ANGAVL	calls						
ARBINP	calls						
ATMPRO	calls	FAIL	LININT				
ATMSUR	calls	ATMPRO	EMISIV	EXPRNT	FAIL	LININT	
BUBBLE	calls	FAIL	VIS2PH	VSCRIT			
CHEMPO	calls	CONFND					
COMBIN	calls						
CONFND	calls	FAIL					
CONPRP	calls	CPENTH	DENSTY	FAIL	SOLLIQ		
CORCON	calls	ATMSUR	DATAIN	EDIT	ENRCN1	ENRCN2	GFLMPR
		INITL	INTEMP	LEVSWL	MASRAT	MHTRAN	MLTPRP
		PLLAYR	PLOTEX	PLOTIN	PLOTS	RECEDE	SETUP
		SOURCE	TMSTP				
CPENTH	calls	CONFND	FAIL				
CYLIND	calls	FAIL					
DATAIN	calls	CONPRP	FAIL	INCOOL	INGEOM	INPCON	INPGAS
DCYINT	calls	DCYPOW	FAIL				
DCYPOW	calls						
DENSTY	calls						
DHGEN	calls	DCYPOW	FAIL	LININT			
EDIT	calls	PAGEHD	PRTGAS				
EMISIV	calls	FAIL	LININT				
ENRCN1	calls	CPENTH	EXPRNT	FAIL	MASSEX	SAXB	SOLLIQ
ENRCN2	calls	EXPRNT	FAIL	TMPFND			
EXPRNT	calls						
FAIL	calls						
FILM	calls	FAIL	HTRN	SURFEB			
GEOM	calls	ANGAVL					
GFLMPR	calls						
HCBBOT	calls	VIS2PH					
HCBINJ	calls	VIS2PH					
HCBSID	calls	VIS2PH					
HCBTOP	calls	VIS2PH					
HSPCYL	calls						
HTRCLN	calls	EXPRNT	FAIL	HTRLIQ			
HTRLAY	calls	EXPRNT	FAIL	HTRLIQ	SAXB		
HTRLIQ	calls	HCBBOT	HCBINJ	HCBSID	HCBTOP	VIS2PH	
HTRN	calls						
INCOOL	calls	FAIL					
INGEOM	calls	ARBINP	CYLIND	FAIL	GEOM	HSPCYL	SPHCYL
INITL	calls	ATMSUR	CPENTH	FAIL	SOLLIQ	TMPFND	
INPCON	calls	DCYINT	FAIL				
INPGAS	calls	FAIL	LININT				
INTEMP	calls	EXPRNT	FAIL	FILM	HTRCLN	HTRLAY	SAXB
LEVSWL	calls	BUBBLE	EXPRNT	FAIL			
LININT	calls						
MASLOS	calls	CPENTH					
MASRAT	calls	CPENTH	EXPRNT	FAIL	FILM	HCBINJ	

MASSEX	calls	FAIL					
MHTRAN	calls	COMBIN	CPENTH	EXPRNT	FAIL	MASLOS	MASSEX
		REACT	SOLLIQ				
MLTPRP	calls	CPENTH	EMISIV	EXPRNT	FAIL	SATT	SIGMY
		THKOND	VISCTY				
MLTREA	calls	CHEMPO	FAIL	PRTGAS	SAXB		
PAGEHD	calls						
PLLAYR	calls	COMBIN	DENSTY	EXPRNT	FAIL	SOLLIQ	TMPFND
PLOTEX	calls						
PLOTIN	calls						
PLOTS	calls						
PRTGAS	calls	FAIL	PAGEHD				
QMELT							
REACT	calls	CPENTH	EXPRNT	FAIL	MLTREA	SOLLIQ	
RECEDE	calls	GEOM					
RFBS	calls	FAIL					
RLUD	calls	FAIL					
SATP	calls						
SATT	calls						
SAXB	calls	FAIL	RFBS	RLUD	UDU		
SETUP	calls	CONFND					
SIGMY	calls						
SOLLIQ	calls	FAIL	SSMELT	SVLAAR			
SOURCE	calls	DHGEN					
SPHCYL	calls	FAIL					
SSMELT	calls						
SURFEB	calls	FAIL	QMELT				
SVLAAR	calls	FAIL					
THKOND	calls						
TIMSTP	calls	EXPRNT					
TMPFND	calls	CPENTH	FAIL				
UDU	calls						
VIS2PH	calls						
VISCTY	calls	FAIL					
VSCRIT	calls						

Table 6.II
CORCON program segments calling each subprogram

ABLATE	called by						
ANGAVL	called by	GEOM					
ARBINP	called by	INGEOM					
ATMPRO	called by	ATMSUR					
ATMSUR	called by	CORCON	INITL				
BUBBLE	called by	LEVSWL					
CHEMPO	called by	MLTREA					
COMBIN	called by	MHTRAN	PLLAYR				
CONFND	called by	CHEMPO	CPENTH	SETUP			
CONPRP	called by	DATAIN					
CORCON	called by						
CPENTH	called by	CONPRP	ENRCNI	INITL	MASLOS	MASRAT	MHTRAN
		MLTPRP	REACT	TMPFND			

CYLIND	called by	INGEOM					
DATAIN	called by	CORCON					
DCYINT	called by	INPCON					
DCYPOW	called by	DCYINT	DHGEN				
DENSTY	called by	CONPRP	PLLAYR				
DHGEN	called by	SOURCE					
EDIT	called by	CORCON					
EMISIV	called by	ATMSUR	MLTPRP				
ENRCN1	called by	CORCON					
ENRCN2	called by	CORCON					
EXPRNT	called by	ATMSUR	ENRCN1	ENRCN2	HTRCLN	HTRLAY	INTEMP
		LEVSWL	MASRAT	MHTRAN	MLTPRP	PLLAYR	REACT
		TIMSTP					
FAIL	called by	ABLATE	ATMPRO	ATMSUR	BUBBLE	CONFND	CONPRP
		CPENTH	CYLIND	DATAIN	DCYINT	DHGEN	EMISIV
		ENRCN1	ENRCN2	FILM	HTRCLN	HTRLAY	INCOOL
		INGEOM	INITL	INPCON	INPGAS	INTEMP	LEVSWL
		MASRAT	MASSEX	MHTRAN	MLTPRP	MLTREA	PLLAYR
		PRTGAS	REACT	RFBS	RLUD	SAXB	SOLLIQ
		SPHCYL	SURFEB	SVLAAR	TMPFND	VISCTY	
FILM	called by	INTEMP	MASRAT				
GEOM	called by	INGEOM	RECEDE				
GFLMPR	called by	CORCON					
HCBBOT	called by	HTRLIQ					
HCBINJ	called by	HTRLIQ	MASRAT				
HCBSID	called by	HTRLIQ					
HCBTOP	called by	HTRLIQ					
HSPCYL	called by	INGEOM					
HTRCLN	called by	INTEMP					
HTRLAY	called by	INTEMP					
HTRLIQ	called by	HTRCLN	HTRLAY				
HTRN	called by	FILM					
INCOOL	called by	DATAIN					
INGEOM	called by	DATAIN					
INITL	called by	CORCON					
INPCON	called by	DATAIN					
INPGAS	called by	DATAIN					
INTEMP	called by	CORCON					
LEVSWL	called by	CORCON					
LININT	called by	ABLATE	ATMPRO	ATMSUR	DHGEN	EMISIV	INPGAS
MASLOS	called by	MHTRAN					
MASRAT	called by	CORCON					
MASSEX	called by	ENRCN1	MHTRAN				
MHTRAN	called by	CORCON					
MLTPRP	called by	CORCON					
MLTREA	called by	REACT					
PAGEHD	called by	EDIT	PRTGAS				
PLLAYR	called by	CORCON					
PLOTEX	called by	CORCON					
PLOTIN	called by	CORCON					
PLOTS	called by	CORCON					
PRTGAS	called by	EDIT	MLTREA				

QMELT	called by	SURFEB					
REACT	called by	MHTRAN					
RECEDE	called by	CORCON					
RFBS	called by	SAXB					
RLUD	called by	SAXB					
SATP	called by						
SATT	called by	MLTPRP					
SAXB	called by	ENRCN1	HTRLAY	INTEMP	MLTREA		
SETUP	called by	CORCON					
SIGMY	called by	MLTPRP					
SOLLIQ	called by	CONPRP	ENRCN1	INITL	MHTRAN	PLLAYR	REACT
SOURCE	called by	CORCON					
SPHCYL	called by	INGEOM					
SSMELT	called by	SOLLIQ					
SURFEB	called by	FILM					
SVLAAR	called by	SOLLIQ					
THKOND	called by	MLTPRP					
TIMSTP	called by	CORCON					
TMPFND	called by	ENRCN2	INITL	PLLAYR			
UDU	called by	SAXB					
VIS2PH	called by	BUBBLE	HCBBOT	HCBINJ	HCBSID	HCBTOP	HTRLIQ
VISCTY	called by	MLTPRP					
VSCRIT	called by	BUBBLE					

6.3 Use of COMMON

Most of the internal data in CORCON-MOD2 are contained in and communicated through named COMMON blocks. Tables 6.III below lists the COMMON blocks contained in each program segment while Table 6.IV provides the inverse list of program segments containing each COMMON block.

Table 6.III
CORCON common blocks contained by each program segment

BLKDAT	contains	B0	B4	B6	B9	CNSTNT	MASTER
		PFDAT	SPECNM				
ABLATE	contains	A42	MASTER	TWO			
ANGAVL	contains	A3	CNSTNT	ONE	TWNEIT		
ARBINP	contains	A3	ONE	TWNEIT			
ATMPRO	contains	A21	ATMDAT	TWO			
ATMSUR	contains	A20	A23	A4	ATMDAT	B0	B1
		CNSTNT	HEATEX	TWO			
BUBBLE	contains	A32	B0	B1	B3	CNSTNT	TWNTWO
CHEMPO	contains	PFDAT					
COMBIN	contains						
CONFND	contains	MASTER					
CONPRP	contains	A32	B3	MASTER	SPECNM		
CORCON	contains	B4	ONE	TWO			
CPENTH	contains	MASTER					
CYLIND	contains	A3	CNSTNT	FORTN	ONE	TWNEIT	

DATAIN	contains	A17	A19	A20	A23	A4	A42
		A9	B1	ONE	SPECNM	THREE	TITLE
		TWO					
DCYINT	contains	A31	B6	MASTER	SPECNM	TWO	
DCYPOW	contains	B6					
DENSTY	contains	MASTER					
DHGEN	contains	A17	A4	B0	B1	B2	B6
		MASTER					
EDIT	contains	A3	A32	A39	A4	A44	A45
		B0	B1	B2	B5	B8	B9
		CNSTNT	CONSRV	FOUR	GASEDT	MASTER	ONE
		SPECNM	THREE	TWNTWO	TWO		
EMISIV	contains	A19	A20	B9	MASTER	TWO	
ENRCN1	contains	A4	B0	B1	B2	B5	B7
		B9	CONSRV	HEATEX	IMP	MASTER	TWO
ENRCN2	contains	B0	B1	CONSRV	HEATEX	IMP	
EXPRNT	contains	ONE	TWO				
FAIL	contains	B4	ONE	TWO			
FILM	contains	A32	ARGLST	B1	CNSTNT		
GEOM	contains	A3	CNSTNT	FORTN	FOUR	ONE	TWNEIT
GFLMPR	contains	A32	A39	ONE			
HCBBOT	contains	B1	CNSTNT				
HCBINJ	contains	B1	CNSTNT				
HCBSID	contains	B1	CNSTNT				
HCBTOP	contains	B1	CNSTNT				
HSPCYL	contains	A3	CNSTNT	FORTN	FOUR	ONE	TWNEIT
HTRCLN	contains	B1	B5	B8	B9	CNSTNT	
HTRLAY	contains	B1	B5	B8	CNSTNT	TWO	
HTRLIQ	contains	B0	B1	CNSTNT			
HTRN	contains	A39	B1	CNSTNT			
INCOOL	contains	B9					
INGEOM	contains	CNSTNT	FORTN	ONE			
INITL	contains	A10	A3	A31	A32	A4	A45
		B0	B1	B2	B3	B5	B8
		B9	CNSTNT	CONSRV	GASEDT	HEATEX	MASTER
		ONE	TWNTWO				
INPCON	contains	A10	A31	A4	B6	MASTER	SPECNM
INPGAS	contains	A10	A21	A31	MASTER	SPECNM	TWO
INTEMP	contains	A3	A32	ARGLST	B0	B1	B5
		B8	CNSTNT	HEATEX	TWO		
LEVSWL	contains	A3	A32	A44	B0	B1	B3
		CNSTNT	ONE	TWNEIT	TWNTWO		
LININT	contains						
MASLOS	contains	B0	B1	B2	B6	CONSRV	MASTER
		TWO					
MASRAT	contains	A3	A32	ARGLST	B0	B1	B3
		B5	CNSTNT	MASTER	ONE	TWNEIT	TWNTWO
		TWO					
MASSEX	contains	B0	B1	B2	B7	B9	CONSRV
		MASTER					
MHTRAN	contains	A32	A4	B0	B1	B2	B3
		B7	B8	CONSRV	MASTER	TWO	

MLTPRP	contains	B0	B1	B2	B8	B9	MASTER
MLTREA	contains	PFDAT	RNDOFF				
PAGEHD	contains	ONE	TITLE	TWO			
PLLAYR	contains	A45	B0	B1	B2	B8	B9
		MASTER	TWO				
PLOTEX	contains	A3	A4	B0	B1	B2	CNSTNT
		MASTER	ONE	TWO			
PLOTIN	contains	A3	A4	B0	B1	B2	CNSTNT
		MASTER	ONE	TWO			
PLOTS	contains	A3	A4	B0	B1	B2	CNSTNT
		MASTER	ONE	TWO			
PRTGAS	contains	A45	MASTER	PFDAT	SPECNM		
QMELT	contains	B1	B5	B8			
REACT	contains	A45	B0	B1	B2	B7	CONSRV
		GASEDT	MASTER	ONE	PFDAT	TWO	
RECEDE	contains	A3	FOUR	ONE	TWNEIT	TWO	
RFBS	contains						
RLUD	contains						
SATP	contains						
SATT	contains						
SAXB	contains						
SETUP	contains	CNSTNT	RNDOFF				
SIGMY	contains						
SOLLIQ	contains	A32	B9	MASTER			
SOURCE	contains	B0	B1	TWO			
SPHCYL	contains						
SSMELT	contains						
SURFEB	contains	A32					
SVLAAR	contains						
THKOND	contains						
TIMSTP	contains	A3	FOUR	ONE	THREE	TWNEIT	TWO
TMPFND	contains	B0	B1	B2	B9	MASTER	TWO
UDU	contains	RNDOFF					
VIS2PH	contains						
VISCTY	contains	B9	MASTER				
VSCRIT	contains	CNSTNT					

Table 6.IV

CORCON program segments containing each common block

A10	is in	INITL	INPCON	INPGAS			
A17	is in	DATAIN	DHGEN				
A19	is in	DATAIN	EMISIV				
A20	is in	ATMSUR	DATAIN	EMISIV			
A21	is in	ATMPRO	INPGAS				
A23	is in	ATMSUR	DATAIN				
A3	is in	ANGAVL	ARBINP	CYLIND	EDIT	GEOM	HSPCYL
		INITL	INTEMP	LEVSWL	MASRAT	PLOTEX	PLOTIN
		PLOTS	RECEDE	TIMSTP			
A31	is in	DCYINT	INITL	INPCON	INPGAS		
A32	is in	BUBBLE	CONPRP	EDIT	FILM	GFLMPR	INITL
		INTEMP	LEVSWL	MASRAT	MHTRAN	SOLLIQ	URFEB

A39	is in	EDIT	GFLMPR	HTRN			
A4	is in	ATMSUR	DATAIN	DHGEN	EDIT	ENRCN1	INITL
		INPCON	MHTRAN	PLOTEX	PLOTIN	PLOTS	
A42	is in	ABLATE	DATAIN				
A44	is in	EDIT	LEVSWL				
A45	is in	EDIT	INITL	PLLAYR	PRTGAS	REACT	
A9	is in	DATAIN					
ARGLST	is in	FILM	INTEMP	MASRAT			
ATMDAT	is in	ATMPRO	ATMSUR				
B0	is in	BLKDAT	ATMSUR	BUBBLE	DHGEN	EDIT	ENRCN1
		ENRCN2	HTRLIQ	INITL	INTEMP	LEVSWL	MASLOS
		MASRAT	MASSEX	MHTRAN	MLTPRP	PLLAYR	PLOTEX
		PLOTIN	PLOTS	REACT	SOURCE	TMPFND	
B1	is in	ATMSUR	BUBBLE	DATAIN	DHGEN	EDIT	ENRCN1
		ENRCN2	FILM	HCBBOT	HCBINJ	HCBSID	HCBTOP
		HTRCLN	HTRLAY	HTRLIQ	HTRN	INITL	INTEMP
		LEVSWL	MASLOS	MASRAT	MASSEX	MHTRAN	MLTPRP
		PLLAYR	PLOTEX	PLOTIN	PLOTS	QMELT	REACT
		SOURCE	TMPFND				
B2	is in	DHGEN	EDIT	ENRCN1	INITL	MASLOS	MASSEX
		MHTRAN	MLTPRP	PLLAYR	PLOTEX	PLOTIN	PLOTS
		REACT	TMPFND				
B3	is in	BUBBLE	CONPRP	INITL	LEVSWL	MASRAT	MHTRAN
B4	is in	BLKDAT	CORCON	FAIL			
B5	is in	EDIT	ENRCN1	HTRCLN	HTRLAY	INITL	INTEMP
		MASRAT	QMELT				
B6	is in	BLKDAT	DCYINT	DCYPOW	DHGEN	INPCON	MASLOS
B7	is in	ENRCN1	MASSEX	MHTRAN	REACT		
B8	is in	EDIT	HTRCLN	HTRLAY	INITL	INTEMP	MHTRAN
		MLTPRP	PLLAYR	QMELT			
B9	is in	BLKDAT	EDIT	EMISIV	ENRCN1	HTRCLN	INCOOL
		INITL	MASSEX	MLTPRP	PLLAYR	SOLLIQ	TMPFND
		VISCTY					
CNSTNT	is in	BLKDAT	ANGAVL	ATMSUR	BUBBLE	CYLIND	EDIT
		FILM	GEOM	HCBBOT	HCBINJ	HCBSID	HCBTOP
		HSPCYL	HTRCLN	HTRLAY	HTRLIQ	HTRN	INGEOM
		INITL	INTEMP	LEVSWL	MASRAT	PLOTEX	PLOTIN
		PLOTS	SETUP	VSCRIT			
CONSRV	is in	EDIT	ENRCN1	ENRCN2	INITL	MASLOS	MASSEX
		MHTRAN	REACT				
FORTN	is in	CYLIND	GEOM	HSPCYL	INGEOM		
FOUR	is in	EDIT	GEOM	HSPCYL	RECEDE	TIMSTP	
GASEDT	is in	EDIT	INITL	REACT			
HEATEX	is in	ATMSUR	ENRCN1	ENRCN2	INITL	INTEMP	
IMP	is in	ENRCN1	ENRCN2				
MASTER	is in	BLKDAT	ABLATE	CONFND	CONPRP	CPENTH	DCYINT
		DENSTY	DHGEN	EDIT	EMISIV	ENRCN1	INITL
		INPCON	INPGAS	MASLOS	MASRAT	MASSEX	MHTRAN
		MLTPRP	PLLAYR	PLOTEX	PLOTIN	PLOTS	PRTGAS
		REACT	SOLLIQ	TMPFND	VISCTY		
ONE	is in	ANGAVL	ARBINP	CORCON	CYLIND	DATAIN	EDIT
		EXPRNT	FAIL	GEOM	GFLMPR	HSPCYL	INGEOM

		INITL	LEVSWL	MASRAT	PAGEHD	PLOTEX	PLOTIN
		PLOTS	REACT	RECEDE	TIMSTP		
PFDAT	is in	BLKDAT	CHEMPO	MLTREA	PRTGAS	REACT	
RNDOFF	is in	MLTREA	SETUP	UDU			
SPECNM	is in	BLKTAD	CONPRPDATAIN		DCYINT	EDIT	INPCON
		INPGAS	PRTGAS				
THREE	is in	DATAIN	EDIT	TIMSTP			
TITLE	is in	DATAIN	PAGEHD				
TWNEIT	is in	ANGAVL	ARBINP	CYLIND	GEOM	HSPCYL	LEVSWL
		MASRAT	RECEDE	TIMSTP			
TWNTWO	is in	BUBBLE	EDIT	INITL	LEVSWL	MASRAT	
TWO	is in	ABLATE	ATMPRO	ATMSUR	CORCON	DATAIN	DCYINT
		EDIT	EMISIV	ENRCNI	EXPRNT	FAIL	HTRLAY
		INPGAS	INTEMP	MASLOS	MASRAT	MHTRAN	PAGEHD
		PLLAYR	PLOTEX	PLOTIN	PLOTS	REACT	RECEDE
		SOURCE	TIMSTP	TMPFND			

6.4 Principal Variables

This section is a dictionary of the principal FORTRAN variables in CORCON-MOD2. For arrays, the different elements may correspond to different layers, to different chemical species, etc. This is indicated by the index used as follows:

I - species

J - body point

K - element

L - layer interface

M - Temperature

N - Time

Interface L is between layer L and layer L-1.

Fortran Symbol	Algebraic Symbol	Description	Units
ALPHZB(J)	$\alpha(Z)$	Local axial void fraction at Z(J)	--
ALPLAY(L)	α_L	Average void fraction	--
AM(I)	--	Amount of species	g-mol
AMLAY(L)	m_L	Mass	kg
AMLSRT(L)	m_L^o	Mass at start of timestep	kg

ANE(I,K)	--	Stoichiometric coefficients	--
ARINT(L)	--	Interface area	m^2
BETLAY(L)	β_L	Volumetric coefficient of expansion	K^{-1}
BUBMLI(J)	--	Molar flux of gas entering bubbles	$g\text{-}mol/m^2s$
BUBRAD(L)	r_b	Average bubble radius	m
CHPOT(I)	μ_i^o	Standard-state chemical potential	cal/g-mol
CONINP(I)	m_i	Initial mass of condensed species	kg
	x_i	Initial mole fractions of gaseous species	--
CPLAY(L)	c_{p_L}	Specific heat	J/kg K
CRUSTx(L)	δ_{x_L}	Crust thickness on face x (= B, bottom; = T, top; = R, radial)	m
DDODS	--	Ratio of normal recession to normal distance to adjacent ray	--
DELH	ΔH_{abl}	Heat of ablation of concrete	J/kg
DELL(J)	δ	Gas film thickness	m
DELSMG(I)	--	Mass of gaseous species generated during timestep	kg
DELTIM	Δt	Timestep	s
DHPOW	--	Decay heat power	W
DPRIN	--	Time interval for diagnostic prints	s
DQBDTx(L)	dq_B/dT_x	Rate of change of upward heat flux at bottom surface with respect to temperature x (= B, bottom; = L, layer; = T, top)	W/m^2K
DQRDTA(L)	--	Rate of change of heat flux to radial surface with respect to surface temperature	W/m^2K

DQSDTS	dq_s/dT_s	Rate of change of heat flux to/from pool surface with respect to surface temperature	W/m^2K
DQTDTx(L)	dq_T/dT_x	Rate of change of upward heat flux at top surface with respect to temperature x (= B, bottom; = L, layer; = T, top)	W/m^2K
DQZDTA(L)	--	Rate of change of heat flux to axial surface with respect to surface temperature	W/m^2K
EMLAY(L)	ϵ_L	Emissivity	--
EMM(M or N)	ϵ_m	Emissivity of metallic phase	--
EMSUR	ϵ_{sur}	Emissivity of above-pool surroundings	--
EO(M or N)	ϵ_o	Emissivity of oxidic phase	--
ES(M or N)	ϵ_{sur}	Emissivity of atmosphere surroundings	--
EW	ϵ_w	Emissivity of ablating concrete surface	--
FCTRN	--	Mass of coolant added during timestep	kg
FGFLM	--	Mass of gas transported in film during timestep	kg
FGSAV	--	Mass of gas transformed by oxide/atmosphere reaction during timestep	kg
FGTRN	--	Mass of gas transported as bubbles during timestep	kg
FLMANG(J)	--	Average slope of gas film over Taylor cell radius	kg/m^2s
FMM(N)	--	Metallic phase splashout rate	kg/s
FMO(N)	--	Oxidic phase splashout rate	kg/s

FMOL(I)	--	Amount of species in chemical reaction	g-mol
FMS(N,I)	--	Specified rate of addition to pool	kg/s
FMSAV	-	Mass of reinforcing steel ablated by LOX during timestep	kg
FMTRN	-	Mass of metal rising or sinking in pool during timestep	kg
FOTRN	-	Mass of oxide rising or sinking in pool during timestep	kg
GDPMWT	-	Molecular weight of gaseous products of concrete ablation	g/g-mol
GFCP(J)	-	Gas film specific heat	J/kg K
GFKOND(J)	--	Gas film thermal conductivity	W/m K
GFLINT(L)	--	Mass flow of gas at interface	kg/s
GFLMFL(J)	--	Mass flow of gas in film	kg/s
GFMWT(J)	--	Gas film molecular weight	g/g-mol
GFPR(J)	--	Gas film Prandtl number	--
GFRHO(J)	--	Gas film density	kg/m^3
GFVISC(J)	--	Gas film dynamic viscosity	kg/ms
GMWINT(L)	--	Molecular weight of gas at interface	g/g-mol
GRAV	g	Gravitational acceleration	m/s^2
HANGL(J)	--	Negative of cavity surface inclination angle	rad
HBB	-	Concrete crucible base thickness, Figure 5.2	m
HBC	-	Concrete crucible dimension, top to center of hemisphere, Figure 5.1	m
HC	-	Concrete crucible dimension, top to center of hemisphere, Figure 5.1	m
HCINTB(L)	h_L	Heat transfer coefficient, bulk to bottom	W/m^2K

HCINTT(L)	h_U	Heat transfer coefficient, bulk to top	W/m^2K
HCON(J)	h	Gas film heat transfer coefficient	W/m^2K
HCSIDE(L)	h	Heat transfer coefficient, bubble agitation	W/m^2K
HEATUP	--	Heat to concrete decomposition products during timestep. Converted to rate (W) in EDIT	J
HIT	--	Concrete crucible depth, Figure 5.2	m
HTOT(L)	--	Total enthalpy	J
HTCTRN	-	Total enthalpy of coolant added during timestep	J
HTGFLM	-	Total enthalpy of gas transported in film during timestep	J
HTGSAV	--	Total enthalpy of gas transformed by oxide/atmosphere reaction during timestep	J
HTGTRN	--	Total enthalpy of gas transported as bubbles during timestep	J
HTMSAV	-	Total enthalpy of reinforcing steel ablated by LOX during timestep	J
HTMTRN	--	Total enthalpy of metal rising or sinking in pool during timestep	J
HTOTL	--	Concrete crucible total height, Figure 5.3	m
HTOTRN	-	Total enthalpy of oxide rising or sinking in pool during timestep	J
IABL	--	Surroundings ablation index	--
IAOPAC	--	Aerosol opacity index	--
ICON	--	Concrete composition index	--
ICOOL	--	Coolant layer flag	-
IFLOR	-	Index for cavity top ray	-

IFP	--	Decay heat (power) index	--
IGAS	--	Gas-phase index	--
IGEOM	--	Cavity geometry index	--
ILYR	--	Melt layer configuration index	--
IMAXR	--	Body point at maximum cavity radius	--
IMAXZ	--	Body point at maximum depth	--
IMOD(J)	--	Heat transfer model number	--
IMOV	--	Cavity shape plot index	--
IPG	--	Time-plot index	--
IPINC	--	Print increment, number of time steps	--
IRE	--	Identifying number of chemical reaction	--
IRSTRT	--	Restart option index	--
ISPLSH	--	Melt/coolant splashout index	--
ISPNAM	--	CHARACTER*8 name of master-list species	--
ISRABL	--	Atmosphere surroundings ablation index	--
ISUR	--	Atmosphere surroundings temperature history index	--
IT	--	Iteration (time step) number	--
ITANG	--	Number of the body point constrained to move vertically at the limit of flat bottom	--
ITITL	--	CHARACTER*80 run identification	--
LAYER( )	--	Numbers (1-7) of occupied layers	--
NBOT	--	Number of body points on flat bottom of cavity including center line and tangency point	--

NCL	--	Master-list number of coolant species	--
NCORN	--	Number of body points defining cavity corner, not including tangency points	--
NDECM	--	Number of points in metallic phase power input table	--
NDECO	--	Number of points in oxidic phase power input table	--
NEM	--	Number of points in metallic phase emissivity table	--
NEO	--	Number of points in oxidic phase emissivity table	--
NGSINP	--	Number of gas species input	--
NG1	--	Location of first gas in master species list	--
NG2	--	Location of last gas in master species list	--
NINP	--	Number of concrete species input	--
NLAYER	--	Total number of occupied layers	--
NLYR	--	Maximum possible number of layers in pool	--
NMP(I)	--	Number of points in input mass addition tables	--
NMSI	--	Number of metallic species input	--
NM1	--	Location of first metal in master species list	--
NM2	--	Location of last metal in master species list	--
NOS1	--	Number of oxidic species input	--
NO3	--	Location of last oxide in master species list	--
NRAYS	--	Number of rays	--

NS	--	Number of points in surroundings emissivity table	--
NSIDE	--	Number of body points defining side of cylindrical cavity	--
NSPG	--	Number of species in surroundings	--
NSP1	--	Number of metallic species in splashout tables	--
NSP2	--	Number of oxidic species in splashout tables	--
NTP	--	Number of points in surroundings temperature table	--
NAMSP	--	CHARACTER*8 name of input species	--
PA	P_a	Initial gas pressure	Pa
PAT(N)	--	Gas (atmosphere) pressure	Pa
PI	π	Pi	--
PIM(N)	P_m	Metallic phase input power	W
PINT(L)	--	Interface pressure	Pa
PIO(N)	P	Oxidic phase input power	W
PLAY(L)	P	Average pressure	Pa
QABL(L)	--	Rate of change in enthalpy due to heat loss to concrete	W
QCONV	q_{conv}	Convective heat flux across gas film	W/m^2
QDCY(L)	--	Internal heat source rate	W
QINT(L)	--	Interface heat flow rate (positive up)	W
QPOOL(L)	--	Rate of change in enthalpy due to heat flow from adjacent layers	W
QRAD	$q_{rad_{net}}$	Net radiative heat flux across gas film	W/m^2

QREAC(L)	--	Heat source rate from chemical reactions	W
QZEROR(L)	--	Radial heat flux to gas film, extrapolated to surface temperature equal layer temperature	W
QZEROZ(L)	--	Axial heat flux to gas film, extrapolated to surface temperature equal layer temperature	W
R(J)	r	Radial coordinate	m
RAD	--	Concrete crucible radius, Figure 5.2	m
RADC	--	Concrete crucible corner radius, Figure 5.2	m
RBR	--	Mass fraction of reinforcing steel in concrete	--
RELERH	--	Relative (numerical) error in energy conservation	--
RELERM	--	Relative (numerical) error in mass conservation	--
REYNLD(J)	Re	Gas film Reynolds number	--
RHOC	ρ_C	Concrete density	kg/m^3
RHOPCT	--	Partial density of concrete in reinforced concrete	kg/m^3
RHOLAY(L)	ρ_L	Average density	kg/m^3
RI	--	Interface radius in EDIT. Also used as R(J) elsewhere	m
RMAX	--	Maximum radius of concrete cavity	m
RNOT	R_o	Universal gas constant	J/g-mol K
RO	--	Radial location of ray origin ($\equiv$ 0)	m
RS	--	Concrete crucible radius, Figure 5.1	m

RTANG	--	Radius of flat bottom of concrete crucible	m
RW	--	Outer radius of concrete crucible, Figure 5.1-5.3	m
SAREA	--	Surface area of cavity	m^3
SCALRG	--	Free energy divided by R_oT for chemical system	--
SCALRM	--	Total moles in gas phase of chemical system	g-mol
SDOT	s	Concrete recession rate	m/s
SI	--	Mass fraction of concrete decomposing to gas	--
SIGEFF	$\sigma_B F$	Stefan-Boltzmann constant times shape factor	W/m^2K^4
SIGLAY(L)	σ_L	Surface tension	N/m
SIGMA	σ_B	Stefan-Boltzmann constant	W/m^2K^4
SM	--	Mass fraction of concrete species Mole fraction of gaseous species	--
SMCTRN	--	Mass of coolant species added during timestep	kg
SMGATM(I)	--	Mass of gas in atmosphere	kg
SMGFLM(I)	--	Mass of gas transported in film during time step	kg
SMGGEN(I)	--	Cumulative mass of gaseous species generated	kg
SMGSAV(I)	--	Mass of gas transformed by oxide/atmosphere reaction during time-step	kg
SMGTRN(I)		Mass of gas transported as bubbles during timestep	kg
SMMET(I,L)	--	Mass of metallic species	kg

SMMSAV(I)	--	Mass of metallic products of oxide/atmosphere reaction during timestep	kg
SMMTRN(I)	--	Mass of metal rising or sinking in pool during timestep	kg
SMOTRN(I)	--	Mass of oxide rising or sinking in pool during timestep	kg
SMOXY(I,L)	--	Mass of oxidic species	kg
SPEMW(I)	--	Molecular weight	g/g-mol
SUMMHO	--	Total enthalpy of new pool mass for old temperatures and melting ranges	J
TA	T_a	Initial gas (atmosphere) temperature	K
TCTR	--	Temperature of coolant added	K
TEDIT	--	Time when next edit will be generated	s
TEMPA(J)	--	Temperature of pool/film interface at Z(J)	K
TEMPx	--	Flag for emissivity table for x (= M, metal; = O, oxide; = S, surroundings). True if independent variable is temperature rather than time	--
TGFL	--	Temperature of gas transported through film	K
TGSV	--	Temperature of gas transformed by oxide atmosphere reaction	K
TGTR	--	Temperature of gas transported as bubbles	K
THET(J)	--	Ray angle	rad
THKLAY(L)	k_L	Thermal conductivity	W/m K
TIC	--	Initial concrete temperature	K
TIME	t	Current time	s
TIMEND	--	End time for calculation	s

TIMEO	--	Start time for calculation	s
TINT(L)	T_I	Interface temperature	K
TIM(L)	--	Times in metal input power table	s
TIO(N)	--	Times in oxide phase input power table	s
TLAY(L)	T_L	Average (bulk) temperature	K
TLCNTR(L)	$\overline{T}_{\ell r}$	Average liquid temperature, radial	K
TLCNTZ(L)	$\overline{T}_{\ell z}$	Average liquid temperature, axial	K
TLIQCT	T_c^{ℓ}	Concrete liquidus temperature	K
TLIQLA(L)	T_L^{ℓ}	Liquidus temperature	K
TMI	--	Initial temperature of metallic phase	K
TMM(N)	--	Times for metallic phase splashout table	s
TMO(N)	--	Times for oxidic phase splashout table	s
TMSV	--	Temperature of metallic products of oxide/atmosphere reaction	K
TMTR	--	Temperature of metal rising or sinking in pool	K
TMPS(N)	--	Temperature of surroundings	K
TMS(N,I)	--	Time in mass addition table	s
TOI	--	Initial temperature of oxidic phase	K
TORT1(M or N)	--	Time or temperature for oxidic phase emissivity table	s or K
TORT2(M or N)	--	Time or temperature for metallic phase emissivity table	s or K
TORT6(M or N)	--	Time or temperature for surroundings emissivity table	s or K

TOTALH	--	Total pool enthalpy required by conservation	J
TOTALM	--	Total pool mass required by conservation	kg
TOTR	--	Temperature of oxide rising or sinking in pool	K
TPA(N)	--	Time in gas (atmosphere) pressure table	s
TPRIN	--	Time for start of diagnostic print	s
TSIDE(L)	--	Side (radial) boundary temperature	K
TSOLCT	T_c^s	Concrete solidus temperature	K
TSOLID(L)	--	Solidification temperature	K
TSOLLA(L)	T_L^s	Solidus temperature	K
TSTART(L)	--	Temperature at start of timestep	K
TTS(N)	--	Time in surroundings temperature table	s
TW	T_W	Concrete ablation temperature	K
UBUB(L)	U_g	Bubble rise velocity	m/s
VA	--	Initial gas volume	m^3
VISLAY(L)	--	Dynamic viscosity	kg/m s
VISLIQ(L)	μ_ℓ	Dynamic viscosity of liquid	kg/m s
VOL(J)	--	Cumulative cavity volume	m^3
VSGINT(L)	V_s	Superficial gas velocity	m/s
X(J)	--	Path length in film	m
XMTU	--	Core size, metric tonnes of uranium	Mg
XMWTH	--	Core operating power (thermal)	MW
Z(J)	z	Axial coordinate (positive down)	m

ZB	--	Axial coordinate of bottom of concrete crucible	m
ZINT(L)	--	Interface location	m
ZMAX	--	Axial coordinate of deepest point in cavity	m
ZO	--	Axial coordinate of ray origin	m
ZT	--	Axial coordinate of top of concrete crucible, Figure 5.2	m

6.5 Partially Implemented Features

In addition to the fully-implemented and operational features of CORCON-MOD2 described in this report, there is also partial coding for a number of additional models and user options. Several of these will be briefly summarized here, as an aid to future workers.

1. The detailed diagnostic print remains an all-or-nothing proposition in CORCON-MOD2 as it was in CORCON-MOD1. However, this output is now controlled by the routine EXPRNT (EXtra PRINT) which is called by all routines which could produce additional output. The name of the calling routine is passed as an argument, and EXPRNT determines whether output is desired from that routine at the current time. The simple test currently implemented is for TIME .GT. TPRIN; EXPRNT could easily be modified to provide more flexibility in control of this output.

2. Addition of core material or coolant to the debris pool after the start of the calculation is not allowed in CORCON-MOD2. However, provision has been made for such mass addition through input (card 26 and groups 27-29); the logic for treating the added material is included in the code. (It is, of course, not completely tested.) The addition rate is defined (currently as 0) in subroutine MASSEX (MASS EXchange). The tables of addition rates may be accessed by a call to subroutine ABLATE, which is included but not called in the distributed version of the code. The only additional coding which should be necessary to activate the model is a procedure for defining the initial temperature(s) of the added materials.

3. Provision is made in the structure of CORCON-MOD2, and in its calculational procedures, for the inclusion of pool layers which are heterogeneous mixtures of metals and

oxides. Because no procedure is available for getting material into (or out of) these layers, however, they are not "available" to the user. If procedures were defined to eliminate the restriction, coding would have to be added to routine MLTPRP to define the transport properties for such mixed layers. In addition, provision would have to be made to preserve the results of chemical reactions calculated in REACT for later output from EDIT by way of PRTGAS. The existing code calculates the reactions correctly, including updating of masses and energies, but does not provide space for saving the information for reactions in more than one layer in any timestep. Finally, each phase in the layer has its own freezing range; this has implications for the thermal equation of state and for heat-transfer mechanisms in the layer.

4. The possibility of a reduction reaction between the surface of an oxidic layer and the atmosphere above it is included, but the calculation is bypassed because the state of the atmosphere is not updated. If the bypass were to be removed, the temperature and composition of the atmosphere would have to be redefined in ATMSUR. Because the redefinition should include the effects of communication between the reactor cavity and the rest of the containment, this feature is more appropriate for a code which couples CORCON-MOD2 to a full containment code such as CONTAIN or MARCH than for the stand-alone version.

5. The properties of the gas film between the melt and the concrete are defined at each body point in subroutine GFLMPR. Studies[70] have shown little sensitivity to these properties; therefore, CORCON-MOD2 uses hard-wired constant values for them. Improvement of this model would probably require a point-wise definition of the gas composition. The composition at each interface between layers is available (but is not saved) in subroutine MHTRAN; a determination of the composition at intermediate points would be greatly complicated by the possibility of chemical reactions.

7. SAMPLE PROBLEM

7.1 Problem Definition

As an illustration of the use of CORCON-MOD2, we have defined a sample problem. It is intended to demonstrate some of the capabilities of the code, and does not model any particular plant or accident sequence. By providing an example of a correctly set up data deck, it may also be helpful to a new user. When CORCON-MOD2 is installed at a new site, we suggest that the sample problem be run to verify that the code is performing correctly.

The problem describes deposition of essentially the entire core of a typical large (3400 MWt) PWR into a reactor cavity formed of limestone aggregate/common sand concrete. Deposition takes place 3 hours after reactor SCRAM, at which time the zirconium cladding is assumed to be approximately 50% oxidized. The melt also includes a significant amount of steel, from the upper internals and the breached lower head; the steel is assumed to be 5% oxidized. The initial water inventory of 60 metric tonnes represents the contents of the accumulators of a typical PWR. The cavity radius is taken as 3.0m, and does not include the area of the keyway in a plant such as Zion or Indian Point. Containment pressure is assumed to rise linearly from 1.5 bars at deposition time to 3.0 bars 3 hours later. The effects of aerosol opacity are included with the characteristic path length taken as a nominal 1.0m.

7.2 Input Data

The data cards used for this problem are shown in Table 7.I, keyed to the input description of Section 5.1.

7.3 Output Listing

A partial listing of the sample problem output is given in the following pages. This includes the echo of input data records, the expansion and interpretation of input data during initialization, the cycle-zero (initial time) edit, messages generated when the oxidic and metallic layers invert and when the coolant is depleted, and the final (end time) edit. Two warning messages may be observed after the initial-time edit of layer properties: for the first two timesteps, the metallic layer contained more than 10% Zr.

The temporal variation of several parameters of interest is shown in Figures 7.1-7.7. One may see that the pool contains four layers (heavy oxide, metal, light oxide, and coolant) until 11850s, when the density of the heavy oxide becomes equal to that of the metal (Figure 7.3). The two oxide layers then combine to

form one, which is less dense than the metal. The resulting three-layer pool persists until the coolant is depleted at 15660s, leaving only two layers (metal and light oxide). The coolant is initially subcooled, but is heated to saturation at about 11100s (Figure 7.1). While the coolant is boiling, the resulting steam dominates the gas generation. Most of the gas from concrete decomposition is reduced by the molten metal to hydrogen and carbon monoxide (Figure 7.5). Initially, the metallic layer contains zirconium and much of the carbon monoxide is further reduced to elemental carbon, which is retained in the pool. When the zirconium is depleted at about 11600s, this carbon is rapidly re-oxidized. This may be seen in Figure 7.5 as a relative suppression of carbon monoxide production before 11600s followed by enhanced production until the elemental carbon is depleted at about 12300s. The average temperatures of the oxidic and metallic layers are almost equal, even after 18000s when a 0.07m solid crust forms on the bottom of the metallic layer. The crusting results in decreased axial erosion as may be seen in Figures 7.6 and 7.7.

TABLE 7.I Input Data for CORCON-MOD2 Standard Problem

```
     ....-....1....-....2....-....3....-....4....-....5....-....6....-....7....-....8
 1.  CORCON-MOD2 STANDARD PROBLEM (23 FEB 84)
 2.      0    1    2    2    0    0    1    0    0  360    0    0    1    1    0    1
 3.         30.0    10800.    21600.                21601.
 4.     95        0.0       0.5
 6.          0.0       3.0       5.00       0.1       4.0       2.0   10   10
10.        350.0     1550.        .6      .135
14.       3    4     2500.     2500.
15.  UO2            1.0E5
     ZRO2           1.4E4
     FEO            6.0E3
     ZR             1.0E4
16.  FE             7.0E4
     CR             1.0E4
     NI             6.0E3
17.          90.    3400.    0
18A.        322.
18B. H2O            6.0E4
19.       5.0E4       0.0      380.    2
20.  H2O              0.5
     H2               0.5
20A.      2
20B.    10800.0     1.5E5   21600.0     3.0E5
24.       2
25.     10800.0     400.0   21600.0     800.0
30.  TIMETIMETIME
31.       1    1    1
32.          0.0       0.8
33.          0.0       0.8
34.          0.0       0.8
34A.         1.0
     ....-....1....-....2....-....3....-....4....-....5....-....6....-... 7....-....8
```

```
CARD IMAGES IN INPUT FILE (TAPE5)
 1.   CORCON-MOD2 STANDARD PROBLEM
 2.       0    1    2    2    0    0    1    0    0   30    0    0    1    1    0    1
 3.         30.0    10800.    21600.              21601.
 4.      95        0.0       0.5
 5.          0.0       3.0       5.00       0.1       4.0       2.0   10   10
 6.        350.0     1550.        .6      .135
 7.       3    4     2500.     2500.
 8.   UO2            1.0E5
 9.   ZRO2           1.4E4
10.   FEO            6.0E3
11.   ZR             1.0E4
12.   FE             7.0E4
13.   CR             1.0E4
14.   NI             6.0E3
15.          90.     3400.     0
16.         322.
17.   H2O            6.0E4
18.        5.0E4       0.0       380.    2
19.   H2O               0.5
20.   H2                0.5
21.       2
22.      10800.0     1.5E5   21600.0     3.0E5
23.       2
24.      10800.0     400.0   21600.0     800.0
25.   TIMETIMETIME
26.       1    1    1
27.          0.0       0.8
28.          0.0       0.8
29.          0.0       0.8
30.          1.0
```

CONCON-MOD2 STANDARD PROBLEM

* * * I N P U T * * *

```
                    ***  FLAGS  ***                                        ***  CONTROL PARAMETERS  ***
   ILYR  = 0    ICOCL  = 1    IGEOM  = 2    ICON   = 2          TIMEO  = 10800.00 (SEC)    DELTIM =  30.0000 (SEC)
   IGAS  = 0    IFP    = 0    ISUR   = 1    IABL   = 0          TIMEND = 21600.00 (SEC)
   ISPLSH= 0    IPINC  =30    IFLOR  = 0    IRSTRT = 0          DPRIN  =     0.00 (SEC)    TPRIN  = 21601.00 (SEC)
   IMCV  = 1    IPG    = 1    ISHABL = 0    IADPAC = 1

TIMESTEP CONTROL,  DTMIN(I)  DTMAX(I)      TIMDT(I)
                    30.000    30.000     1.000E+10

EDIT CONTROL,  DEDIT(I)      TEDIT(I)
               900.000     1.000E+10
                                  RAY CENTER COORDINATES

                         R0 =  0.                    Z0 =   .500000

                                CONCRETE CAVITY GEOMETRY

                                     RIGHT CYLINDER

                              NRAYS - NUMBER OF RAYS =   95

                              ZT - Z-COORDINATE OF TOP =   0.

                              RAD - CYLINDER RADIUS (M) =    3.00000

                              HIT - CYLINDER HEIGHT (M) =    5.00000

                              RADC - CORNER RADIUS (M) =    .100000

                              NBOT - NUMBER OF BOTTOM POINTS =   10

                              NCORN = NUMBER OF CORNER POINTS =   10
```

* * * CONCRETE SPECIFICATIONS * * *

LIMESTONE AGGREGATE - COMMON SAND CONCRETE

RHOC (KG/M3)	RER (KG/KG C)	SI (-)	TSCL (K)	TLIQ (K)	TIC (K)	TM (K)	DELH (J/KG)	EM (-)
2.340000E+03	1.350000E-01	2.585400E-01	1.420000E+03	1.670000E+03	3.500000E+02	1.550000E+03	2.734253E+06	6.000000E-01

SPECIES NAME	MASS FR.(KG/KG C)	MOLECULAR WT.
SIO2	.3580	60.0843
TIO2	.0018	79.8988
MNO	.0003	70.9374
MGO	.0048	40.3044
CAO	.3130	56.0794
NA2O	.0008	61.9790
K2O	.0122	94.1960
FE2O3	.0144	159.6922
AL2O3	.0360	101.9613
CR2O3	.0001	151.9902
CO2	.2115	44.0098
H2OEVAP	.0270	18.0152
H2OCHEM	.0200	18.0152

MELT FISSION PRODUCT INVENTORY
BASED ON 9.00000E+01 METRIC TON URANIUM CORE OPERATED AT 3.40000E+03 MW(THERMAL)
MELT CONTAINS 8.81390E+01 METRIC TONS URANIUM, CORRESPONDING TO 97.93 PERCENT OF CORE

ELEMENTS, RETAINED FRACTIONS (**DENOTES USER INPUT, OTHERS FROM WASH 1400), AND GRAM-ATOMS IN MELT

MO	(.970)	1.9550E+03	TC	(.970)	4.9900E+02	RU	(.970)	1.2548E+03	RH	(.970)	2.2286E+02
SB	(.850)	6.9058E+00	TE	(.850)	1.7746E+02	SR	(.900)	6.4579E+02	BA	(.900)	5.7387E+02
ZR	(.990)	2.4235E+03	CE	(.990)	1.2757E+03	NP	(.990)	1.3911E+02	CM	(.990)	6.7247E+00
NB	(.990)	3.7546E+01	PU	(.990)	2.6111E+03	AM	(.990)	1.9548E+01	Y	(.990)	3.6227E+02
LA	(.990)	5.4766E+02	PR	(.990)	4.7666E+02	ND	(.990)	1.5289E+03	SM	(.990)	1.7768E+02
EU	(.990)	5.6204E+01	RB	(.190)	5.1813E+01	CS	(.190)	2.3889E+02	BR	(.100)	1.7647E+00
I	(.100)	1.0655E+01									

FISSION PRODUCTS GROUPED AS 4 PSEUDO-SPECIES

4.11600E+03 GRAM-ATOMS OF FPM WITH ATOMIC FRACTIONS

MO	4.74976E-01	TC	1.21235E-01	RU	3.04054E-01	RH	5.41439E-02	SB	1.67779E-03
TE	4.31137E-02								

1.08824E+04 GRAM-ATOMS OF FPOX WITH ATOMIC FRACTIONS

SR	5.9342EE-02	BA	5.27339E-02	ZR	2.22699E-01	CE	1.17226E-01	NP	1.27828E-02
CM	6.17937E-04	NB	3.45015E-03	PU	2.39535E-01	AM	1.79625E-03	Y	3.32898E-02
LA	5.03437E-02	PR	4.38006E-02	ND	1.40490E-01	SM	1.63265E-02	EU	5.16462E-03

2.90699E+02 GRAM-ATOMS OF FPALKMET WITH ATOMIC FRACTIONS

RB	1.78237E-01	CS	8.21763E-01

1.24198E+01 GRAM-ATOMS OF FPHALOGN WITH ATOMIC FRACTIONS

BR	1.42091E-01	I	8.57909E-01

INITIAL POWER AT START OF CORCON, 1.08000E+04 SEC AFTER SCRAM IS 2.16421E+07 WATTS
REPRESENTING .65 PERCENT OF OPERATING POWER OF FRACTION OF CORE IN MELT

INITIAL CORE MASSES (KG) OF CONSTITUENTS AND TEMPERATURES

OXIDES	SPEMW	CONINP	METALS	SPEMW	CONINP
FEO	7.1646400E+01	6.0000000E+03	FE	5.5847000E+01	7.0000000E+04
UO2	2.7002760E+02	1.0000000E+05	CR	5.1996000E+01	1.0000000E+04
ZRO2	1.2321880E+02	1.4000000E+04	NI	5.8710000E+01	6.0000000E+03
FEOX	1.3716610E+02	1.4927010E+03	ZR	9.1220000E+01	1.0000000E+04
FEALMET	1.3300000E+02	3.8662976E+01	FEM	9.8336300E+01	4.0476075E+02
FEALOGN	1.2700000E+02	1.5773101E+00			

INITIAL TEMPERATURE (TO) IN DEGREES K = 2.5000000E+03

INITIAL TEMPERATURE (TM) IN DEGREES K = 2.5000000E+03

INITIAL MASS OF OXIDES = 1.2153294E+05

INITIAL MASS OF METALS = 9.6404761E+04

COOLANT IS H2O

INITIAL MASS OF COOLANT = 6.0000000E+04

INITIAL TEMPERATURE OF COOLANT = 3.2200000E+02

* * * REACTING GAS MIXTURE * * *

*** ATMOSPHERIC PRESSURE SPECIFIED AS OF TIME ***

TIME	1.0800E+04	2.1600E+04
PRESSURE	1.5000E+05	3.0000E+05

VA (M3)	PA (N/M2)	TA (DEG K)
5.0000000E+04	1.5000000E+05	3.8000000E+02

GAS INPUT

SPECIES NAME	MOLE FR. (-)	MOLECULAR WT.
H2	.5000	2.0158
H2O	.5000	18.0152

*** MELT INTERNAL CONDITIONS ***

*** BOUNDARY CONDITIONS - SURROUNDINGS ABOVE MELT ***

*** SURFACE TEMPERATURE VARIATION WITH TIME ***

*** TS(DEG K) INPUT AS TABLES .VS. TIME ***

TIME(SEC)	TS(DEG K)
1.0800E+04	4.0000E+02
2.1600E+04	8.0000E+02

*** SURROUNDINGS MATERIAL MELTING OR ABLATION DURING INTERACTION ***

```
*** BOUNDARY CONDITIONS - RADIATIVE HEAT TRANSFER ***

                                    *** SURFACE EMISSIVITIES ,VS. TIME OR TEMP. ***

     TIME  0.
       EO  8.0000E-01

     TIME  0.
       EM  8.0000E-01

     TIME  0.
       ES  8.0000E-01

      *** AEROSOL OPACITY INCLUDED IN ATMOSPHERE ***
            CHARACTERISTIC PATH LENGTH (M) =  1.0000E+00

      *** NO MELT/COOLANT SPLASHOUT ***

                                                  * * *  END OF INPUT  * * *

* * * SOLLIQ * * *, METAL CONTAINS  10.8 PERCENT NON CR-FE-NI,  MELT RANGE MAY BE INACCURATE
********** POSSIBLE ERROR, EXECUTION CONTINUES AT CYCLE NUMBER   0, TIME =  1.08000E+04 **********
```

```
                                        CORCON VERSION 2.00.00
  TIME =  10800.00        CORCON-MOD2 STANDARD PROBLEM                                          IT. NO. =   0
                                   * * * * G E N E R A L   S U M M A R Y * * * *

MELT AND COOLANT LAYERS

  NUMBER OF LAYERS,   NLYR  = 3
  CONFIGURATION,      ILYR  = 0
  COOLANT PRESENT,    ICOOL = 1

EXTREME CAVITY DIMENSIONS, WITH LOCATIONS

      RADIAL                                                    AXIAL
  MAXIMUM CAVITY RADIUS        (M) =   3.00000          DEEPEST POINT IN CAVITY      (M) =   5.00000
  OUTSIDE RADIUS OF CONCRETE   (M) =   4.00000          MAXIMUM DEPTH OF CONCRETE    (M) =   7.00000
  REMAINING THICKNESS          (M) =   1.00000          REMAINING THICKNESS          (M) =   2.00000
  CORRESPONDING BODY POINT         =       22           CORRESPONDING BODY POINT         =       1

APPROXIMATE OVERALL ENERGY BUDGET FOR DEBRIS
(SEE MANUAL FOR EXPLANATION AND CAVEATS)

  INTERNAL (DECAY) SOURCE      (W) =  2.155E+07
  CHEMICAL REACTION SOURCE     (W) =  0.

  HEAT LOSS TO CONCRETE        (W) =  6.731E+07
  HEATUP OF ABLATION PRODUCTS  (W) =   .
  HEAT LOSS FROM SURFACE       (W) =   .415E+07
    (TO COOLANT)

  CHANGE IN POOL ENTHALPY      (W) =  0.
   (SUMMATION OF M*DH/DT)

NUMERICAL CHECKS ON MASS AND ENERGY CONSERVATION

  RELATIVE ERROR IN MASS     =    0.                    RELATIVE ERROR IN ENTHALPY =    0.

CHECK ON RECESSION CALCULATION (DD/DS SHOULD BE .LE. 1)

  MAXIMUM DD/DS =   0.00000
```

CORCON VERSION 2.00.00

TIME = 10800.00 CORCON-MOD2 STANDARD PROBLEM IT. NO. = 0

* * * * G A S G E N E R A T I O N * * * *

GAS EXITING POOL (INCLUDES FILM AND COOLANT)

SPECIES	GENERATION RATE MASS (KG/S)	GENERATION RATE MOLES (1/S)	CUMULATIVE RELEASE MASS (KG)	CUMULATIVE RELEASE MOLES (-)	SPECIES
C(G)	0.	0.	0.	0.	C(G)
CH4	0.	0.	0.	0.	CH4
CO	0.	0.	0.	0.	CO
CO2	0.	0.	0.	0.	CO2
C2H2	0.	0.	0.	0.	C2H2
C2H4	0.	0.	0.	0.	C2H4
C2H6	0.	0.	0.	0.	C2H6
H	0.	0.	0.	0.	H
H2	0.	0.	0.	0.	H2
H2O	0.	0.	0.	0.	H2O
N	0.	0.	0.	0.	N
NH3	0.	0.	0.	0.	NH3
N2	0.	0.	0.	0.	N2
O	0.	0.	0.	0.	O
O2	0.	0.	0.	0.	O2
OH	0.	0.	0.	0.	OH
CHO	0.	0.	0.	0.	CHO
CH2O	0.	0.	0.	0.	CH2O
CRO3(G)	0.	0.	0.	0.	CRO3(G)
FPMO2(G)	0.	0.	0.	0.	FPMO2(G)
FPMO3(G)	0.	0.	0.	0.	FPMO3(G)

CORCON VERSION 2.00.00

TIME = 10800.00 CORCON-MOD2 STANDARD PROBLEM IT. NO. = 0

* * * * G E O M E T R Y * * * *

BODY POINT	R COORDINATE (M)	Z COORDINATE (M)	STREAM LENGTH (M)	BODY ANGLE (DEG)	RAY ANGLE (DEG)	VOLUME (M3)	SURFACE AREA (M2)	VOID FRACTION (-)
1	0.000000	5.000000	0.000000	0.000	0.000	0.00000	0.00000	0.00000
2	.322222	5.000000	.322222	0.000	4.096	0.00000	.32618	0.00000
3	.644444	5.000000	.644444	0.000	8.150	0.00000	1.30473	0.00000
4	.966667	5.000000	.966667	0.000	12.124	0.00000	2.93564	0.00000
5	1.288889	5.000000	1.288889	0.000	15.983	0.00000	5.21892	0.00000
6	1.611111	5.000000	1.611111	0.000	19.699	0.00000	8.15457	0.00000
7	1.933333	5.000000	1.933333	0.000	23.250	0.00000	11.74258	0.00000
8	2.255556	5.000000	2.255556	0.000	26.622	0.00000	15.98295	0.00000
9	2.577778	5.000000	2.577778	0.000	29.806	0.00000	20.87569	0.00000
10	2.900000	5.000000	2.900000	0.000	32.800	0.00000	26.42079	0.00000
11	2.900000	5.000000	2.900000	0.000	0.000	0.00000	26.42079	0.00000
12	2.914231	4.998982	2.914266	8.182	32.933	.02702	26.68141	0.00000
13	2.928173	4.995949	2.928536	16.364	33.076	.10833	26.94329	0.00000
14	2.941542	4.990963	2.942604	24.545	33.224	.24325	27.20639	0.00000
15	2.954064	4.984125	2.957071	32.727	33.376	.42992	27.47065	0.00000
16	2.965486	4.975575	2.971339	40.909	33.528	.66524	27.73599	0.00000
17	2.975575	4.965486	2.985607	49.091	33.677	.94492	28.00229	0.00000
18	2.984125	4.954064	2.999875	57.273	33.821	1.26354	28.26943	0.00000
19	2.990963	4.941542	3.014143	65.455	33.957	1.61468	28.53725	0.00000
20	2.995949	4.928173	3.028411	73.636	34.081	1.99101	28.80561	0.00000
21	2.998982	4.914231	3.042678	81.818	34.192	2.38454	29.07432	0.00000
22	3.000000	4.900000	3.056946	87.955	34.287	2.78679	29.34322	0.00000
23	3.000000	4.832877	3.124069	90.000	34.698	4.68465	30.60846	0.00000
24	3.000000	4.765753	3.191193	90.000	35.118	6.58252	31.87371	0.00000
25	3.000000	4.698630	3.258316	90.000	35.547	8.48039	33.13895	0.00000
26	3.000000	4.631507	3.325439	90.000	35.984	10.37825	34.40420	0.00000
27	3.000000	4.564384	3.392563	90.000	36.432	12.27612	35.66944	0.00000
28	3.000000	4.497260	3.459686	90.000	36.889	14.17398	36.93468	0.00000
	3.000000	4.492618	OXIDE / METAL INTERFACE					
29	3.000000	4.430137	3.526809	90.000	37.356	16.07185	38.19993	0.00000
30	3.000000	4.363014	3.593933	90.000	37.833	17.96972	39.46517	0.00000
31	3.000000	4.295890	3.661056	90.000	38.320	19.86758	40.73042	0.00000
32	3.000000	4.228767	3.728179	90.000	38.819	21.76545	41.99566	0.00000
33	3.000000	4.161644	3.795302	90.000	39.328	23.66332	43.26091	0.00000
34	3.000000	4.094521	3.862426	90.000	39.848	25.56118	44.52615	0.00000
35	3.000000	4.027397	3.929549	90.000	40.381	27.45905	45.79139	0.00000
	3.000000	3.991278	METAL / COOLANT INTERFACE					
36	3.000000	3.960274	3.996672	90.000	40.925	29.35691	47.05664	0.00000
37	3.000000	3.893151	4.063796	90.000	41.481	31.25478	48.32188	0.00000
38	3.000000	3.826027	4.130919	90.000	42.050	33.15265	49.58713	0.00000
39	3.000000	3.758904	4.198042	90.000	42.631	35.05051	50.85237	0.00000
40	3.000000	3.691781	4.265165	90.000	43.226	36.94838	52.11761	0.00000
41	3.000000	3.624658	4.332289	90.000	43.834	38.84625	53.38266	0.00000
42	3.000000	3.557534	4.399412	90.000	44.456	40.74411	54.64810	0.00000
43	3.000000	3.490411	4.466535	90.000	45.092	42.64198	55.91335	0.00000

44	3.000000	3.423268	4.533659	90.000	45.742	44.53984	57.17859	0.00000
45	3.000000	3.356164	4.600782	90.000	46.407	46.[illegible]3771	58.44384	0.00000
46	3.000000	3.289041	4.667905	90.000	47.067	48.83558	59.70908	0.00000
47	3.000000	3.221918	4.735028	90.000	47.782	50.23344	60.97432	0.00000
48	3.000000	3.154795	4.802152	90.000	48.493	52.13131	62.23957	0.00000
49	3.000000	3.087671	4.869275	90.000	49.220	54.02918	63.50481	0.00000
50	3.000000	3.020548	4.936398	90.000	49.964	55.92704	64.77006	0.00000
51	3.000000	2.953425	5.003522	90.000	50.723	57.82491	66.03530	0.00000
52	3.000000	2.886301	5.070645	90.000	51.500	59.72277	67.30054	0.00000
53	3.000000	2.819178	5.137766	90.000	52.294	61.62064	68.56579	0.00000
54	3.000000	2.752055	5.204891	90.000	53.105	63.51851	69.83103	0.00000
55	3.000000	2.684932	5.272015	90.000	53.934	65.41637	71.09628	0.00000
56	3.000000	2.617808	5.339138	90.000	54.780	67.31424	72.36152	0.00000
57	3.000000	2.550685	5.406261	90.000	55.645	69.21211	73.62677	0.00000
58	3.000000	2.483562	5.473385	90.000	56.528	71.10997	74.89201	0.00000
59	3.000000	2.416438	5.540508	90.000	57.429	73.00784	76.15725	0.00000
60	3.000000	2.349315	5.607631	90.000	58.349	74.90570	77.42250	0.00000
61	3.000000	2.282192	5.674754	90.000	59.287	76.80357	78.68774	0.00000
62	3.000000	2.215068	5.741878	90.000	60.244	78.70144	79.95299	0.00000
63	3.000000	2.147945	5.809001	90.000	61.219	80.59930	81.21823	0.00000
64	3.000000	2.080822	5.876124	90.000	62.213	82.49717	82.48347	0.00000
65	3.000000	2.013699	5.943248	90.000	63.226	84.39504	83.74872	0.00000
66	3.000000	1.946575	6.010371	90.000	64.257	86.29290	85.01396	0.00000
67	3.000000	1.879452	6.077494	90.000	65.306	88.19077	86.27921	0.00000
68	3.000000	1.812329	6.144617	90.000	66.373	90.08863	87.54445	0.00000
	3.000000	1.782464	COOLANT / ATMSPHRE INTERFACE					
69	3.000000	1.745205	6.211741	90.000	67.458	91.98650	88.80970	1.00000
70	3.000000	1.678082	6.278864	90.000	68.560	93.88437	90.07494	1.00000
71	3.000000	1.610959	6.345987	90.000	69.679	95.78223	91.34018	1.00000
72	3.000000	1.543836	6.413111	90.000	70.815	97.68010	92.60543	1.00000
73	3.000000	1.476712	6.480234	90.000	71.966	99.57797	93.87067	1.00000
74	3.000000	1.409589	6.547357	90.000	73.133	101.47583	95.13592	1.00000
75	3.000000	1.342466	6.614480	90.000	74.314	103.37370	96.40116	1.00000
76	3.000000	1.275342	6.681604	90.000	75.509	105.27156	97.66640	1.00000
77	3.000000	1.208219	6.748727	90.000	76.717	107.16943	98.93165	1.00000
78	3.000000	1.141096	6.815850	90.000	77.937	109.06730	100.19689	1.00000
79	3.000000	1.073973	6.882974	90.000	79.169	110.96516	101.46214	1.00000
80	3.000000	1.006849	6.950097	90.000	80.410	112.86303	102.72738	1.00000
81	3.000000	.939726	7.017220	90.000	81.661	114.76090	103.99263	1.00000
82	3.000000	.872603	7.084343	90.000	82.920	116.65876	105.25787	1.00000
83	3.000000	.805479	7.151467	90.000	84.188	118.55663	106.52311	1.00000
84	3.000000	.738356	7.218590	90.000	85.457	120.45449	107.78836	1.00000
85	3.000000	.671233	7.285713	90.000	86.733	122.35236	109.05360	1.00000
86	3.000000	.604110	7.352837	90.000	88.012	124.25023	110.31885	1.00000
87	3.000000	.536986	7.419960	90.000	89.294	126.14809	111.58409	1.00000
88	3.000000	.469863	7.487083	90.000	90.576	128.04596	112.84933	1.00000
89	3.000000	.402740	7.554206	90.000	91.857	129.94383	114.11458	1.00000
90	3.000000	.335616	7.621330	90.000	93.136	131.84169	115.37982	1.00000
91	3.000000	.268493	7.688453	90.000	94.413	133.73956	116.64507	1.00000
92	3.000000	.201370	7.755576	90.000	95.685	135.63742	117.91031	1.00000
93	3.000000	.134247	7.822700	90.000	96.951	137.53529	119.17556	1.00000
94	3.000000	.067123	7.889823	90.000	98.211	139.43316	120.44080	1.00000
95	3.000000	.000000	7.956946	90.000	99.462	141.33102	121.70604	1.00000

CORCON VERSION 2.00.00

TIME = 10800.00 CORCON-MOD2 STANDARD PROBLEM IT. NO. = 0

* * * * H E A T T R A N S F E R R E S U L T S * * *

BODY POINT	ABLATION RATE (M/S)	FILM THICKNESS (M)	FILM FLOW (KG/S)	FILM VELOCITY (M/S)	REYNOLDS NUMBER (-)	REGIME	HT TRANS COEFF (W/M2-K)	INTERFACE TEMPERATURE (K)	CONVECTIVE FLUX (W/M2)	RADIATIVE FLUX (W/M2)
1	2.354E-04	3.154E-04	0.	0.	5.580	LAM.BUB.	502.998	2492.8	4.742E+05	9.716E+05
2	2.354E-04	3.154E-04	0.	0.	5.580	LAM.BUB.	502.998	2492.8	4.742E+05	9.716E+05
3	2.354E-04	3.154E-04	0.	0.	5.580	LAM.BUB.	502.998	2492.8	4.742E+05	9.716E+05
4	2.354E-04	3.154E-04	0.	0.	5.580	LAM.BUB.	502.998	2492.8	4.742E+05	9.716E+05
5	2.354E-04	3.154E-04	0.	0.	5.580	LAM.BUB.	502.998	2492.8	4.742E+05	9.716E+05
6	2.354E-04	3.154E-04	0.	0.	5.580	LAM.BUB.	502.998	2492.8	4.742E+05	9.716E+05
7	2.354E-04	3.154E-04	0.	0.	5.580	LAM.BUB.	502.998	2492.8	4.742E+05	9.716E+05
8	2.354E-04	3.154E-04	0.	0.	5.580	LAM.BUB.	502.998	2492.8	4.742E+05	9.716E+05
9	2.354E-04	3.154E-04	0.	0.	5.580	LAM.BUB.	502.998	2492.8	4.742E+05	9.716E+05
10	2.354E-04	3.154E-04	0.	0.	5.580	LAM.BUB.	502.998	2492.8	4.742E+05	9.716E+05
11	2.354E-04	3.154E-04	0.	0.	5.580	LAM.BUB.	502.998	2492.8	4.742E+05	9.716E+05
12	2.354E-04	3.153E-04	0.	0.	5.579	LAM.BUB.	503.030	2492.7	4.742E+05	9.714E+05
13	2.352E-04	3.153E-04	0.	0.	5.576	LAM.BUB.	503.126	2492.3	4.741E+05	9.706E+05
14	2.396E-04	3.121E-04	1.559E-03	2.377E+00	5.874	TRN.BUB.	534.945	2491.4	5.036E+05	9.690E+05
15	2.231E-04	4.400E-04	1.893E-02	2.038E+01	18.396	TRN.BUB.	427.591	2490.9	4.023E+05	9.680E+05
16	2.119E-04	5.529E-04	5.060E-02	4.320E+01	45.654	LAM.FLM.	356.864	2489.6	3.353E+05	9.658E+05
17	2.057E-04	6.130E-04	8.264E-02	6.357E+01	74.492	LAM.FLM.	321.859	2487.4	3.017E+05	9.617E+05
18	2.017E-04	6.521E-04	1.144E-01	8.231E+01	102.595	TRN.FLM.	304.119	2483.7	2.840E+05	9.550E+05
19	2.060E-04	6.837E-04	1.462E-01	1.001E+02	130.755	TRN.FLM.	347.921	2477.0	3.225E+05	9.428E+05
20	2.083E-04	7.129E-04	1.785E-01	1.170E+02	159.407	TRN.FLM.	387.114	2466.6	3.548E+05	9.244E+05
21	2.089E-04	7.416E-04	2.111E-01	1.329E+02	188.330	TRN.FLM.	421.719	2453.3	3.812E+05	9.019E+05
22	2.109E-04	7.712E-04	2.439E-01	1.475E+02	217.516	TRN.FLM.	451.796	2447.0	4.053E+05	8.900E+05
23	2.250E-04	9.108E-04	4.042E-01	2.071E+02	360.550	TRN.FLM.	558.861	2443.0	4.990E+05	8.829E+05
24	2.367E-04	1.024E-03	5.740E-01	2.616E+02	511.926	TRN.FLM.	646.753	2440.0	5.756E+05	8.778E+05
25	2.436E-04	1.156E-03	7.510E-01	3.031E+02	669.872	TRB.FLM.	700.644	2438.2	6.223E+05	8.747E+05
26	2.471E-04	1.311E-03	9.314E-01	3.316E+02	830.746	TRB.FLM.	726.234	2437.3	6.444E+05	8.733E+05
27	2.500E-04	1.455E-03	1.114E+00	3.572E+02	993.657	TRB.FLM.	748.235	2436.6	6.634E+05	8.720E+05
28	2.525E-04	1.591E-03	1.299E+00	3.808E+02	1158.339	TRB.FLM.	767.605	2436.0	6.801E+05	8.709E+05
			OXIDE	/ METAL	INTERFACE					
29	2.356E-04	1.844E-03	1.472E+00	3.726E+02	1312.999	TRB.FLM.	727.780	2407.4	6.269E+05	8.229E+05
30	2.372E-04	1.968E-03	1.646E+00	3.903E+02	1467.941	TRB.FLM.	741.437	2406.8	6.452E+05	8.218E+05
31	2.386E-04	2.087E-03	1.821E+00	4.070E+02	1623.922	TRB.FLM.	754.022	2406.2	6.456E+05	8.208E+05
32	2.402E-04	2.202E-03	1.997E+00	4.230E+02	1780.862	TRB.FLM.	765.705	2405.6	6.551E+05	8.199E+05
33	2.415E-04	2.314E-03	2.174E+00	4.382E+02	1936.694	TRB.FLM.	776.619	2405.1	6.641E+05	8.191E+05
34	2.427E-04	2.423E-03	2.352E+00	4.528E+02	2097.361	TRB.FLM.	786.868	2404.6	6.725E+05	8.183E+05
35	2.439E-04	2.529E-03	2.530E+00	4.669E+02	2256.812	TRB.FLM.	796.536	2404.1	6.803E+05	8.175E+05
			METAL	/ COOLANT	INTERFACE					
36	0.	4.963E-03	2.627E+00	2.470E+02	2342.923	TRB.FLM.	417.423	322.0	0.	0.
37	0.	4.963E-03	2.627E+00	2.470E+02	2342.923	TRB.FLM.	417.423	322.0	0.	0.
38	0.	4.963E-03	2.627E+00	2.470E+02	2342.923	TRB.FLM.	417.423	322.0	0.	0.
39	0.	4.963E-03	2.627E+00	2.470E+02	2342.923	TRB.FLM.	417.423	322.0	0.	0.
40	0.	4.963E-03	2.627E+00	2.470E+02	2342.923	TRB.FLM.	417.423	322.0	0.	0.
41	0.	4.963E-03	2.627E+00	2.470E+02	2342.923	TRB.FLM.	417.423	322.0	0.	0.
42	0.	4.963E-03	2.627E+00	2.470E+02	2342.923	TRB.FLM.	417.423	322.0	0.	0.
43	0.	4.963E-03	2.627E+00	2.470E+02	2342.923	TRB.FLM.	417.423	322.0	0.	0.

44	0.	4.963E-03	2.627E+00	2.470E+02	2342.923	TRB.FLM.	417.423	322.0	0.	0.
45	0.	4.963E-03	2.627E+00	2.470E+02	2342.923	TRB.FLM.	417.423	322.0	0.	0.
46	0.	4.963E-03	2.627E+00	2.470E+02	2342.923	TRB.FLM.	417.423	322.0	0.	0.
47	0.	4.963E-03	2.627E+00	2.470E+02	2342.923	TRB.FLM.	417.423	322.0	0.	0.
48	0.	4.963E-03	2.627E+00	2.470E+02	2342.923	TRB.FLM.	417.423	322.0	0.	0.
49	0.	4.963E-03	2.627E+00	2.470E+02	2342.923	TRB.FLM.	417.423	322.0	0.	0.
50	0.	4.963E-03	2.627E+00	2.470E+02	2342.923	TRB.FLM.	417.423	322.0	0.	0.
51	0.	4.963E-03	2.627E+00	2.470E+02	2342.923	TRB.FLM.	417.423	322.0	0.	0.
52	0.	4.963E-03	2.627E+00	2.470E+02	2342.923	TRB.FLM.	417.423	322.0	0.	0.
53	0.	4.963E-03	2.627E+00	2.470E+02	2342.923	TRB.FLM.	417.423	322.0	0.	0.
54	0.	4.963E-03	2.627E+00	2.470E+02	2342.923	TRB.FLM.	417.423	322.0	0.	0.
55	0.	4.963E-03	2.627E+00	2.470E+02	2342.923	TRB.FLM.	417.423	322.0	0.	0.
56	0.	4.963E-03	2.627E+00	2.470E+02	2342.923	TRB.FLM.	417.423	322.0	0.	0.
57	0.	4.963E-03	2.627E+00	2.470E+02	2342.923	TRB.FLM.	417.423	322.0	0.	0.
58	0.	4.963E-03	2.627E+00	2.470E+02	2342.923	TRB.FLM.	417.423	322.0	0.	0.
59	0.	4.963E-03	2.627E+00	2.470E+02	2342.923	TRB.FLM.	417.423	322.0	0.	0.
60	0.	4.963E-03	2.627E+00	2.470E+02	2342.923	TRB.FLM.	417.423	322.0	0.	0.
61	0.	4.963E-03	2.627E+00	2.470E+02	2342.923	TRB.FLM.	417.423	322.0	0.	0.
62	0.	4.963E-03	2.627E+00	2.470E+02	2342.923	TRB.FLM.	417.423	322.0	0.	0.
63	0.	4.963E-03	2.627E+00	2.470E+02	2342.923	TRB.FLM.	417.423	322.0	0.	0.
64	0.	4.963E-03	2.627E+00	2.470E+02	2342.923	TRB.FLM.	417.423	322.0	0.	0.
65	0.	4.963E-03	2.627E+00	2.470E+02	2342.923	TRB.FLM.	417.423	322.0	0.	0.
66	0.	4.963E-03	2.627E+00	2.470E+02	2342.923	TRB.FLM.	417.423	322.0	0.	0.
67	0.	4.963E-03	2.627E+00	2.470E+02	2342.923	TRB.FLM.	417.423	322.0	0.	0.
68	0.	4.963E-03	2.627E+00	2.470E+02	2342.923	TRB.FLM.	417.423	322.0	0.	0.

COOLANT / ATMSPHRE INTERFACE

```
                                        CORCON VERSION 2.00.00
TIME =  10800.00        CORCON-MOD2 STANDARD PROBLEM                                                    IT. NO. =   0
                                  * * * * P O O L   C O M P O S I T I O N * * * *

                        OXIDE          METAL          COOLANT

MASS OF LAYER        1.2153E+05     9.6405E+04     6.0000E+04

MASS OF SPECIES
        FEO          6.0000E+03                                    FEO
        UO2          1.0000E+05                                    UO2
        ZRO2         1.4000E+04                                    ZRO2
        FPOX         1.4927E+03                                    FPOX
        FPALKMET     3.8663E+01                                    FPALKMET
        FPHALOGN     1.5773E+00                                    FPHALOGN
        FE                          7.0000E+04                     FE
        CR                          1.0000E+04                     CR
        NI                          6.0000E+03                     NI
        ZR                          1.0000E+04                     ZR
        FPM                         4.0476E+02                     FPM
        H2OCLN                                     6.0000E+04      H2OCLN
```

```
                                                CORCON VERSION 2.00.00
  TIME =  10800.00        CORCON-MOD2 STANDARD PROBLEM                                                    IT. NO. =   0
                                    * * * * L A Y E R   P R O P E R T I E S * * * *

                                          OXIDE          METAL          COOLANT
  MASS                    (KG)          1.2153E+05     9.6405E+04     6.0000E+04
  DENSITY                (KG/M3)        8.4957E+03     6.8010E+03     9.6073E+02
  THERMAL EXPANSIVITY    (1/K)          3.2285E-05     2.7395E-05     3.7296E-04

  AVERAGE TEMPERATURE     (K)           2.5000E+03     2.5000E+03     3.2200E+02
  INTERFACE TEMPERATURE   (K)    2.4928E+03     2.5000E+03     2.3714E+03     3.2230E+02
  SOLIDUS TEMPERATURE     (K)           2.3182E+03     1.7588E+03     2.6816E+02
  LIQUIDUS TEMPERATURE    (K)           2.8054E+03     1.7688E+03     2.7816E+02
  SPECIFIC ENTHALPY      (J/KG)        -3.7671E+06     1.7729E+06    -1.5778E+07
  TOTAL ENTHALPY          (J)          -4.5783E+11     1.7092E+11    -9.4671E+11
  SPECIFIC HEAT         (J/KG K)        1.1412E+03     7.4604E+02     4.1706E+03

  VISCOSITY             (KG/M S)        8.1729E-03     4.0489E-03     5.5498E-04
  THERMAL CONDUCTIVITY  (W/M K)         2.6400E+00     4.7090E+01     6.0000E-01
  THERMAL DIFFUSIVITY    (M2/S)         2.7230E-07     9.2811E-06     1.4975E-07
  SURFACE TENSION        (N/M)          4.9095E-01     1.7696E+00     7.3000E-02
  EMISSIVITY              (-)           8.0000E-01     8.0000E-01     1.0000E+00

  SUPERFICIAL GAS VEL    (M/S)  3.2968E-01     0.             0.             0.
  BUBBLE RADIUS           (M)           1.1303E-02     1.1303E-02     5.7080E-03
  BUBBLE VELOCITY        (M/S)          3.3292E-01     3.3292E-01     2.3658E-01
  VOID FRACTION           (-)           7.1054E-15     0.             0.

  BOT CRUST THICKNESS     (M)           0.             0.             0.
  HT COEFF, LIQ TO BOT (W/M2 K)         2.0150E+05     1.8786E+02     7.6191E+02
  Z-AVE LIQ TEMPERATURE   (K)           2.5000E+03     2.5000E+03     3.2200E+02
  HT COEFF, LIQ TO TOP (W/M2 K)         1.0406E+01     1.2144E+04     3.7385E+03
  TOP CRUST THICKNESS     (M)           0.             0.             0.

  R-AVE LIQ TEMPERATURE   (K)           2.5002E+03     2.5005E+03     3.2200E+02
  HT COEFF, LIQ TO SID (W/M2 K)         2.4193E+04     1.5558E+04     1.0000E-10
  SIDE CRUST THICKNESS    (M)           4.6051E-04     8.5202E-04     0.

  DECAY HEAT              (W)           1.8851E+07     2.6998E+06     0.
  HEAT TO CONCRETE        (W)           5.3403E+07     1.3910E+07     0.
  HEAT OF REACTION        (W)           0.             0.             0.
  INTERLAYER HEAT FLOW    (W)                   0.             4.4150E+07    -3.1311E+04

* * * SOLLIQ * * *, METAL CONTAINS  10.5 PERCENT NON CR-FE-NI,  MELT RANGE MAY BE INACCURATE
********** POSSIBLE ERROR, EXECUTION CONTINUES AT CYCLE NUMBER   1, TIME =  1.08000E+04 **********

* * * SOLLIQ * * *, METAL CONTAINS  10.2 PERCENT NON CR-FE-NI,  MELT RANGE MAY BE INACCURATE
********** POSSIBLE ERROR, EXECUTION CONTINUES AT CYCLE NUMBER   2, TIME =  1.08300E+04 **********


************************************
* LAYER FLIP AT TIME = 1.18500E+04 *
************************************

*****************************************
* COOLANT DEPLETED AT TIME = 1.56600E+04 *
*****************************************
```

CORCON VERSION 2.00.00

TIME = 21600.00 CORCON-MOD2 STANDARD PROBLEM IT. NO. = 360

* * * * G E N E R A L S U M M A R Y * * * *

MELT AND COOLANT LAYERS

NUMBER OF LAYERS, NLYR = 2
CONFIGURATION, ILYR = 0
NO COOLANT PRESENT, ICOOL = 0

EXTREME CAVITY DIMENSIONS, WITH LOCATIONS

RADIAL			AXIAL		
MAXIMUM CAVITY RADIUS	(M) =	3.57805	DEEPEST POINT IN CAVITY	(M) =	5.55558
OUTSIDE RADIUS OF CONCRETE	(M) =	4.00000	MAXIMUM DEPTH OF CONCRETE	(M) =	7.00000
REMAINING THICKNESS	(M) =	.42195	REMAINING THICKNESS	(M) =	1.44442
CORRESPONDING BODY POINT	=	41	CORRESPONDING BODY POINT	=	1

APPROXIMATE OVERALL ENERGY BUDGET FOR DEBRIS
(SEE MANUAL FOR EXPLANATION AND CAVEATS)

INTERNAL (DECAY) SOURCE	(W) =	1.864E+07
CHEMICAL REACTION SOURCE	(W) =	6.353E+05
HEAT LOSS TO CONCRETE	(W) =	7.797E+06
HEATUP OF ABLATION PRODUCTS	(W) =	3.265E+05
HEAT LOSS FROM SURFACE (TO SURROUNDINGS)	(W) =	1.051E+07
CHANGE IN POOL ENTHALPY (SUMMATION OF M*DH/DT)	(W) =	8.460E+05

NUMERICAL CHECKS ON MASS AND ENERGY CONSERVATION

RELATIVE ERROR IN MASS = -7.95808E-13 RELATIVE ERROR IN ENTHALPY = -2.84217E-14

CHECK ON RECESSION CALCULATION (DD/DS SHOULD BE .LE. 1)

MAXIMUM DD/DS = .01432

CORCON VERSION 2.00.00

TIME = 21600.00 CORCON-MOD2 STANDARD PROBLEM IT. NO. = 360

* * * * G A S G E N E R A T I O N * * * *

GAS EXITING POOL (INCLUDES FILM AND COOLANT)

	GENERATION RATE		CUMULATIVE RELEASE		
SPECIES	MASS (KG/S)	MOLES (1/S)	MASS (KG)	MOLES (-)	SPECIES
C(G)	3.74925E-16	3.12151E-14	2.54533E-05	2.11917E-03	C(G)
CH4	1.56565E-05	9.75935E-04	3.94096E-01	2.45656E+01	CH4
CO	1.79189E-01	6.39723E+00	7.67223E+03	2.73907E+05	CO
CO2	3.21819E-01	7.31244E+00	4.01220E+03	9.11661E+04	CO2
C2H2	3.95833E-07	1.52022E-05	1.00195E+01	3.84807E+02	C2H2
C2H4	2.71117E-08	9.66426E-07	1.82339E-02	6.49968E-01	C2H4
C2H6	1.17939E-10	3.92224E-09	5.75910E-06	1.91527E-04	C2H6
H	7.09957E-07	7.04392E-04	8.64628E-01	8.57851E+02	H
H2	6.96898E-03	3.45718E+00	2.98056E+02	1.47860E+05	H2
H2O	7.17409E-02	3.98224E+00	6.08982E+04	3.38038E+06	H2O
N	0.	0.	0.	0.	N
NH3	0.	0.	0.	0.	NH3
N2	0.	0.	0.	0.	N2
O	6.10026E-13	3.81281E-11	1.04828E-06	6.55197E-05	O
O2	3.08102E-15	9.62855E-14	1.89351E-09	5.91744E-08	O2
OH	3.78449E-09	2.22522E-07	4.15694E-04	2.44421E-02	OH
CHO	3.23618E-08	1.11522E-06	5.17125E-03	1.78206E-01	CHO
CH2O	1.93415E-07	6.44154E-06	4.55185E-03	1.51596E-01	CH2O
CRO3(G)	2.01059E-16	2.01070E-15	1.78588E-10	1.78598E-09	CRO3(G)
FPMO2(G)	2.79703E-12	2.14600E-11	1.56000E-06	1.19690E-05	FPMO2(G)
FPMO3(G)	1.37715E-13	9.41086E-13	9.23614E-08	6.31157E-07	FPMO3(G)

CORCON VERSION 2.00.00

TIME = 21600.00 CORCON-MOD2 STANDARD PROBLEM IT. NO. = 360

* * * * G E O M E T R Y * * * *

BODY POINT	R COORDINATE (M)	Z COORDINATE (M)	STREAM LENGTH (M)	BODY ANGLE (DEG)	RAY ANGLE (DEG)	VOLUME (M3)	SURFACE AREA (M2)	VOID FRACTION (-)
1	0.000000	5.555581	0.000000	0.000	0.000	0.00000	0.00000	.03023
2	.362005	5.555581	.362005	0.000	4.096	0.00000	.41170	.03023
3	.724009	5.555581	.724009	0.000	8.150	0.00000	1.64679	.03023
4	1.086014	5.555581	1.086014	0.000	12.124	0.00000	3.70527	.03023
5	1.448018	5.555581	1.448018	0.000	15.983	0.00000	6.58716	.03023
6	1.810023	5.555581	1.810023	0.000	19.699	0.00000	10.29243	.03023
7	2.172027	5.555581	2.172027	0.000	23.250	0.00000	14.82110	.03023
8	2.534032	5.555581	2.534032	0.000	26.622	0.00000	20.17316	.03023
9	2.896036	5.555581	2.896036	0.000	29.806	0.00000	26.34862	.03023
10	2.900000	5.555581	2.900000	0.000	0.000	0.00000	26.42079	.03023
11	3.211960	5.484076	3.220050	23.820	32.800	2.09972	32.56617	.02799
12	3.223342	5.476186	3.233899	47.171	32.933	2.35635	32.84616	.02764
13	3.231683	5.461962	3.250389	62.264	33.076	2.82185	33.18055	.02702
14	3.239335	5.445616	3.268437	65.102	33.224	3.35944	33.54746	.02633
15	3.247047	5.428859	3.286884	66.732	33.376	3.91316	33.92336	.02563
16	3.254122	5.411190	3.305916	69.238	33.528	4.49965	34.31207	.02491
17	3.260570	5.393182	3.325044	70.870	33.677	5.09994	34.70356	.02419
18	3.266498	5.375529	3.343666	71.951	33.821	5.69061	35.08540	.02349
19	3.271836	5.358634	3.361384	74.537	33.957	6.25797	35.44935	.02283
20	3.275831	5.341853	3.378634	75.929	34.081	6.82291	35.80418	.02219
21	3.279650	5.327349	3.393632	76.297	34.192	7.31245	36.11307	.02163
22	3.282554	5.314413	3.406890	76.918	34.287	7.74996	36.38639	.02114
23	3.295654	5.259887	3.462967	68.494	34.698	9.60310	37.54529	.01907
24	3.318775	5.219026	3.509917	57.150	35.118	11.00717	38.52089	.01737
25	3.345621	5.182342	3.555375	33.831	35.547	12.28682	39.47263	.01580
	3.391046	5.171135	METAL / OXIDE INTERFACE					
26	3.391718	5.170969	3.602854	23.103	35.984	12.69227	40.47758	.02338
27	3.429889	5.146794	3.648036	46.497	36.432	13.57581	41.44586	.02287
28	3.454560	5.102925	3.698367	65.886	36.889	15.20882	42.53442	.02255
29	3.472812	5.049542	3.754784	74.127	37.356	17.22085	43.76222	.02232
30	3.486530	4.989505	3.816369	79.346	37.833	19.50459	45.10867	.02215
31	3.496273	4.923823	3.882769	79.932	38.320	22.01993	46.56531	.02203
32	3.509156	4.861609	3.946303	80.661	38.819	24.41791	47.96358	.02187
33	3.517517	4.793298	4.015124	83.920	39.328	27.06691	49.48279	.02177
34	3.523956	4.722311	4.086402	82.954	39.848	29.83127	51.05957	.02169
35	3.534391	4.655734	4.153792	81.934	40.381	32.43634	52.55390	.02157
36	3.543136	4.586740	4.223338	84.934	40.925	35.15068	54.10023	.02146
37	3.546945	4.511773	4.298402	88.206	41.481	38.11049	55.77222	.02142
38	3.547875	4.433443	4.376737	84.410	42.050	41.20720	57.51824	.02141
39	3.560121	4.367364	4.443941	83.078	42.631	43.82929	59.01894	.02126
40	3.564504	4.292372	4.519061	82.500	43.226	46.81859	60.70032	.02121
41	3.578046	4.226723	4.586092	102.667	43.834	49.44941	62.20443	.02106
	3.497843	4.120250	OXIDE / ATMSPHRE INTERFACE					
42	3.318428	3.882069	5.017587	120.121	44.456	62.32990	71.55316	1.00000

43	3.262628	3.752200	5.158937	99.360	45.092	66.74763	74.47556	1.00000
44	3.267999	3.684433	5.226915	94.789	45.742	69.01756	75.87025	1.00000
45	3.243838	3.584311	5.326027	104.449	46.407	72.21883	77.89784	1.00000
46	3.218442	3.492123	5.425512	116.871	47.087	75.37374	79.91757	1.00000
47	3.000000	3.221918	5.772971	109.477	47.782	83.58340	86.70546	1.00000
48	3.000000	3.154795	5.840094	90.000	48.493	85.48127	87.97070	1.00000
49	3.000000	3.087671	5.907218	90.000	49.220	87.37913	89.23595	1.00000
50	3.000000	3.020548	5.974341	90.000	49.964	89.27700	90.50119	1.00000
51	3.000000	2.953425	6.041464	90.000	50.723	91.17486	91.76644	1.00000
52	3.000000	2.886301	6.108588	90.000	51.500	93.07273	93.03168	1.00000
53	3.000000	2.819178	6.175711	90.000	52.294	94.97060	94.29692	1.00000
54	3.000000	2.752055	6.242834	90.000	53.105	96.86846	95.56217	1.00000
55	3.000000	2.684932	6.309957	90.000	53.934	98.76633	96.82741	1.00000
56	3.000000	2.617808	6.377081	90.000	54.780	100.66420	98.09266	1.00000
57	3.000000	2.550685	6.444204	90.000	55.645	102.56206	99.35790	1.00000
58	3.000000	2.483562	6.511327	90.000	56.528	104.45993	100.62315	1.00000
59	3.000000	2.416438	6.578451	90.000	57.429	106.35779	101.88839	1.00000
60	3.000000	2.349315	6.645574	90.000	58.349	108.25566	103.15363	1.00000
61	3.000000	2.282192	6.712697	90.000	59.287	110.15353	104.41888	1.00000
62	3.000000	2.215068	6.779820	90.000	60.244	112.05139	105.68412	1.00000
63	3.000000	2.147945	6.846944	90.000	61.219	113.94926	106.94937	1.00000
64	3.000000	2.080822	6.914067	90.000	62.213	115.84713	108.21461	1.00000
65	3.000000	2.013699	6.981190	90.000	63.226	117.74499	109.47985	1.00000
66	3.000000	1.946575	7.048314	90.000	64.257	119.64286	110.74510	1.00000
67	3.000000	1.879452	7.115437	90.000	65.306	121.54072	112.01034	1.00000
68	3.000000	1.812329	7.182560	90.000	66.373	123.43859	113.27559	1.00000
69	3.000000	1.745205	7.249683	90.000	67.458	125.33646	114.54083	1.00000
70	3.000000	1.678082	7.316807	90.000	68.560	127.23432	115.80608	1.00000
71	3.000000	1.610959	7.383930	90.000	69.679	129.13219	117.07132	1.00000
72	3.000000	1.543836	7.451053	90.000	70.815	131.03006	118.33656	1.00000
73	3.000000	1.476712	7.518177	90.000	71.966	132.92792	119.60181	1.00000
74	3.000000	1.409589	7.585300	90.000	73.133	134.82579	120.86705	1.00000
75	3.000000	1.342466	7.652423	90.000	74.314	136.72365	122.13230	1.00000
76	3.000000	1.275342	7.719546	90.000	75.509	138.62152	123.39754	1.00000
77	3.000000	1.208219	7.786670	90.000	76.717	140.51939	124.66278	1.00000
78	3.000000	1.141096	7.853793	90.000	77.937	142.41725	125.92803	1.00000
79	3.000000	1.073973	7.920916	90.000	79.169	144.31512	127.19327	1.00000
80	3.000000	1.006849	7.988040	90.000	80.410	146.21299	128.45852	1.00000
81	3.000000	.939726	8.055163	90.000	81.661	148.11085	129.72376	1.00000
82	3.000000	.872603	8.122286	90.000	82.920	150.00872	130.98901	1.00000
83	3.000000	.805479	8.189409	90.000	84.186	151.90658	132.25425	1.00000
84	3.000000	.738356	8.256533	90.000	85.457	153.80445	133.51949	1.00000
85	3.000000	.671233	8.323656	90.000	86.733	155.70232	134.78474	1.00000
86	3.000000	.604110	8.390779	90.000	88.012	157.60018	136.04998	1.00000
87	3.000000	.536986	8.457903	90.000	89.294	159.49805	137.31523	1.00000
88	3.000000	.469863	8.525026	90.000	90.576	161.39592	138.58047	1.00000
89	3.000000	.402740	8.592149	90.000	91.857	163.29378	139.84571	1.00000
90	3.000000	.335616	8.659273	90.000	93.136	165.19165	141.11096	1.00000
91	3.000000	.268493	8.726396	90.000	94.413	167.08951	142.37620	1.00000
92	3.000000	.201370	8.793519	90.000	95.685	168.98738	143.64145	1.00000
93	3.000000	.134247	8.860642	90.000	96.951	170.88525	144.90669	1.00000
94	3.000000	.067123	8.927766	90.000	98.211	172.78311	146.17194	1.00000
95	3.000000	.000000	8.994889	90.000	99.462	174.68098	147.43718	1.00000

CORCON VERSION 2.00.00

TIME = 21600.00 CORCON-MOD2 STANDARD PROBLEM IT. NO. = 360

****HEAT TRANSFER RESULTS****

BODY POINT	ABLATION RATE (M/S)	FILM THICKNESS (M)	FILM FLOW (KG/S)	FILM VELOCITY (M/S)	REYNOLDS NUMBER (-)	REGIME	HT TRANS COEFF (W/M2-K)	INTERFACE TEMPERATURE (K)	CONVECTIVE FLUX (W/M2)	RADIATIVE FLUX (W/M2)
1	1.620E-05	1.740E-04	0.	0.	.797	LAM.BUB.	911.811	1621.9	6.555E+04	3.395E+04
2	1.620E-05	1.740E-04	0.	0.	.797	LAM.BUB.	911.811	1621.9	6.555E+04	3.395E+04
3	1.620E-05	1.740E-04	0.	0.	.797	LAM.BUB.	911.811	1621.9	6.555E+04	3.395E+04
4	1.620E-05	1.740E-04	0.	0.	.797	LAM.BUB.	911.811	1621.9	6.555E+04	3.395E+04
5	1.620E-05	1.740E-04	0.	0.	.797	LAM.BUB.	911.811	1621.9	6.555E+04	3.395E+04
6	1.620E-05	1.740E-04	0.	0.	.797	LAM.BUB.	911.811	1621.9	6.555E+04	3.395E+04
7	1.620E-05	1.740E-04	0.	0.	.797	LAM.BUB.	911.811	1621.9	6.555E+04	3.395E+04
8	1.620E-05	1.740E-04	0.	0.	.797	LAM.BUB.	911.811	1621.9	6.555E+04	3.395E+04
9	1.620E-05	1.740E-04	0.	0.	.797	LAM.BUB.	911.811	1621.9	6.555E+04	3.395E+04
10	1.620E-05	1.740E-04	0.	0.	.797	LAM.BUB.	911.811	1621.9	6.555E+04	3.395E+04
11	1.518E-05	1.702E-04	0.	0.	.747	LAM.BUB.	931.778	1616.5	6.198E+04	3.125E+04
12	1.275E-05	1.592E-04	8.645E-04	2.358E+00	.794	TRN.BUB.	1209.320	1596.9	5.669E+04	2.161E+04
13	9.524E-06	1.955E-04	3.013E-03	6.675E+00	2.495	LAM.FLM.	1009.093	1589.9	4.023E+04	1.826E+04
14	8.829E-06	2.238E-04	4.966E-03	9.589E+00	4.102	LAM.FLM.	881.695	1590.5	3.568E+04	1.854E+04
15	8.422E-06	2.483E-04	6.847E-03	1.189E+01	5.643	LAM.FLM.	794.642	1591.3	3.280E+04	1.893E+04
16	7.959E-06	2.668E-04	8.695E-03	1.402E+01	7.150	LAM.FLM.	739.478	1590.8	3.018E+04	1.870E+04
17	7.668E-06	2.823E-04	1.047E-02	1.592E+01	8.593	LAM.FLM.	698.877	1590.7	2.844E+04	1.865E+04
18	7.475E-06	2.958E-04	1.215E-02	1.760E+01	9.953	LAM.FLM.	667.042	1590.8	2.721E+04	1.870E+04
19	7.129E-06	3.071E-04	1.369E-02	1.908E+01	11.198	LAM.FLM.	642.537	1589.8	2.556E+04	1.822E+04
20	6.953E-06	3.155E-04	1.514E-02	2.051E+01	12.370	LAM.FLM.	625.372	1589.4	2.466E+04	1.805E+04
21	6.889E-06	3.240E-04	1.639E-02	2.159E+01	13.368	LAM.FLM.	608.994	1589.7	2.415E+04	1.816E+04
22	6.810E-06	3.304E-04	1.747E-02	2.255E+01	14.243	LAM.FLM.	597.168	1589.6	2.367E+04	1.815E+04
23	7.687E-06	3.583E-04	2.236E-02	2.650E+01	18.153	LAM.FLM.	550.671	1596.7	2.570E+04	2.151E+04
24	9.108E-06	3.956E-04	2.714E-02	2.893E+01	21.879	LAM.FLM.	498.678	1608.0	2.892E+04	2.702E+04
25	1.171E-05	4.317E-04	3.295E-02	3.193E+01	26.353	LAM.FLM.	457.030	1627.2	3.529E+04	3.665E+04
			METAL	/ OXIDE	INTERFACE					
26	2.482E-05	7.740E-04	3.985E-02	2.125E+01	31.441	LAM.FLM.	254.897	1744.1	4.947E+04	1.030E+05
27	2.608E-05	6.537E-04	5.423E-02	3.386E+01	42.311	LAM.FLM.	301.803	1742.6	5.814E+04	1.021E+05
28	2.671E-05	6.063E-04	7.098E-02	4.744E+01	54.980	LAM.FLM.	325.423	1741.9	6.245E+04	1.016E+05
29	2.629E-05	6.371E-04	8.987E-02	5.686E+01	69.248	LAM.FLM.	309.697	1742.4	5.958E+04	1.019E+05
30	2.584E-05	6.743E-04	1.102E-01	6.564E+01	84.611	LAM.FLM.	292.582	1742.9	5.644E+04	1.022E+05
31	2.542E-05	7.118E-04	1.319E-01	7.420E+01	100.964	LAM.FLM.	277.190	1743.4	5.361E+04	1.025E+05
32	2.580E-05	7.490E-04	1.527E-01	8.133E+01	116.442	TRN.FLM.	291.145	1743.0	5.618E+04	1.023E+05
33	2.630E-05	7.806E-04	1.757E-01	8.956E+01	133.648	TRN.FLM.	309.750	1742.4	5.959E+04	1.019E+05
34	2.675E-05	8.137E-04	2.000E-01	9.763E+01	151.848	TRN.FLM.	327.037	1741.9	6.274E+04	1.016E+05
35	2.713E-05	8.457E-04	2.234E-01	1.046E+02	169.100	TRN.FLM.	341.119	1741.4	6.530E+04	1.013E+05
36	2.753E-05	8.736E-04	2.479E-01	1.121E+02	187.216	TRN.FLM.	356.390	1741.0	6.806E+04	1.010E+05
37	2.796E-05	9.018E-04	2.748E-01	1.203E+02	207.338	TRN.FLM.	372.705	1740.5	7.099E+04	1.007E+05
38	2.837E-05	9.316E-04	3.034E-01	1.285E+02	228.819	TRN.FLM.	388.491	1740.0	7.381E+04	1.004E+05
39	2.863E-05	9.606E-04	3.282E-01	1.343E+02	246.705	TRN.FLM.	398.626	1739.7	7.561E+04	1.002E+05
40	2.904E-05	9.820E-04	3.564E-01	1.425E+02	267.539	TRN.FLM.	414.414	1739.2	7.841E+04	9.992E+04
41	2.926E-05	1.010E-03	3.819E-01	1.479E+02	285.572	TRN.FLM.	423.124	1739.0	7.995E+04	9.976E+04
			OXIDE	/ ATMSPHRE	INTERFACE					

CORCON VERSION 2.00.00

TIME = 21600.00 CORCON-MOD2 STANDARD PROBLEM IT. NO. = 360

* * * * BULK METAL/GAS REACTION DURING TIMESTEP * * * *

OXIDES SPECIES NAMES	REACTANTS (MOLS)	PRODUCTS (MOLS)
FEO	0.	0.
MNO	0.	0.
ZRO2	0.	0.
CR2O3	0.	8.7179E+01
NIO	0.	0.
FPMO2	0.	0.
FPMO3	0.	0.
FE3O4	0.	0.
MN3O4	0.	0.

METALS SPECIES NAMES	REACTANTS (MOLS)	PRODUCTS (MOLS)
FE	1.4372E+06	1.4372E+06
CR	5.5872E+04	5.5697E+04
NI	1.0220E+05	1.0220E+05
ZR	0.	0.
FPM	4.1160E+03	4.1160E+03
MN	0.	0.
C(C)	0.	0.
X	0.	0.

GASES SPECIES NAMES	REACTANTS (MOLS)	PRODUCTS (MOLS)
C(G)	0.	9.2364E-13
CH4	0.	1.7055E-02
CO	0.	1.6974E+02
CO2	1.7002E+02	2.6906E-01
C2H2	0.	2.9635E-04
C2H4	0.	1.2413E-05
C2H6	0.	3.1997E-08
H	0.	2.0250E-02
H2	0.	9.1720E+01
H2O	9.2283E+01	5.1867E-01
N	0.	0.
NH3	0.	0.
N2	0.	0.
O	0.	1.1368E-09
O2	0.	2.8786E-12
OH	0.	6.5592E-06
CHO	0.	3.1491E-05
CH2O	0.	1.6975E-04
CRO3(G)	0.	6.0171E-14
FPMO2(G)	0.	6.4138E-10
FPMO3(G)	0.	2.8142E-11

NO. OF ITERATIONS = 4

CORCON VERSION 2.00.00

TIME = 21600.00 CORCON-MOD2 STANDARD PROBLEM IT. NO. = 360

* * * * FILM METAL/GAS REACTION DURING TIMESTEP * * * *

OXIDES			METALS			GASES		
SPECIES NAMES	REACTANTS (MOLS)	PRODUCTS (MOLS)	SPECIES NAMES	REACTANTS (MOLS)	PRODUCTS (MOLS)	SPECIES NAMES	REACTANTS (MOLS)	PRODUCTS (MOLS)
FEO	0.	0.	FE	1.4372E+06	1.4372E+06	C(G)	0.	1.2814E-14
MNO	0.	0.	CR	5.5697E+04	5.5674E+04	CH4	0.	1.2223E-02
ZRO2	0.	0.	NI	1.0220E+05	1.0220E+05	CO	0.	2.2181E+01
CR2O3	0.	1.1409E+01	ZR	0.	0.	CO2	2.2216E+01	2.2373E-02
NIO	0.	0.	FPM	4.1160E+03	4.1160E+03	C2H2	0.	1.5972E-04
FPMO2	0.	0.	MN	0.	0.	C2H4	0.	1.6580E-05
FPMO3	0.	0.	C(C)	0.	0.	C2H6	0.	8.5670E-08
FE3O4	0.	0.	X	0.	0.	H	0.	8.8160E-04
MN3O4	0.	0.				H2	0.	1.1995E+01
						H2O	1.2058E+01	3.7571E-02
						N	0.	0.
						NH3	0.	0.
						N2	0.	0.
						O	0.	7.0062E-12
						O2	0.	1.0004E-14
						OH	0.	1.1645E-07
						CHO	0.	1.9659E-06
						CH2O	0.	2.3500E-05
						CRO3(G)	0.	1.5023E-16
						FPMO2(G)	0.	2.4201E-12
						FPMO3(G)	0.	9.0466E-14

NO. OF ITERATIONS = 4

CORCON VERSION 2.00.00

TIME = 216[illegible]0.00 CORCON-MOD2 STANDARD PROBLEM IT. NO. = 360

* * * * P O O L C O M P O S I T I O N * * * *

	METAL	OXIDE	
MASS OF LAYER	8.9575E+04	2.0182E+05	
MASS OF SPECIES			
SIO2		2.7250E+04	SIO2
TIO2		1.3701E+02	TIO2
FEO		6.0000E+03	FEO
MNO		2.2835E+01	MNO
MGO		3.6536E+02	MGO
CAO		2.38[illegible]5E+04	CAO
NA2O		6.24[illegible]6E+01	NA2O
K2O		9.286[illegible]+02	K2O
FE2O3		1.0961E+03	FE2O3
AL2O3		2.7402E+03	AL2O3
UO2		1.0000E+05	UO2
ZRO2		2.7508E+04	ZRO2
CR2O3		1.0395E+04	CR2O3
FPOX		1.4927E+03	FPOX
FPALKMET		1.4788E-04	FPALKMET
FPHALOGN		6.0329E-06	FPHALOGN
FE	8.0276E+04		FE
CR	2.8948E+03		CR
NI	6.0000E+03		NI
FPM	4.0476E+02		FPM

CORCON VERSION 2.00.00

TIME = 21600.00 CORCON-MOD2 STANDARD PROBLEM IT. NO. = 360

* * * * L A Y E R P R O P E R T I E S * * * *

		METAL	OXIDE	
MASS	(KG)	6.9575E+04	2.0182E+05	
DENSITY	(KG/M3)	7.2257E+03	5.0385E+03	
THERMAL EXPANSIVITY	(1/K)	3.0857E-05	5.6159E-05	
AVERAGE TEMPERATURE	(K)	1.7565E+03	1.7728E+03	
INTERFACE TEMPERATURE	(K)	1.6219E+03	1.7720E+03	1.7669E+03
SOLIDUS TEMPERATURE	(K)	1.7677E+03	1.6075E+03	
LIQUIDUS TEMPERATURE	(K)	1.7777E+03	2.3259E+03	
SPECIFIC ENTHALPY	(J/KG)	9.9083E+05	-6.5283E+06	
TOTAL ENTHALPY	(J)	8.8754E+10	-1.3176E+12	
SPECIFIC HEAT	(J/KG K)	7.3304E+02	1.3259E+03	
VISCOSITY	(KG/M S)	6.9977E-03	6.2589E-02	
THERMAL CONDUCTIVITY	(W/M K)	4.7261E+01	3.8493E+00	
THERMAL DIFFUSIVITY	(M2/S)	8.9227E-06	5.7618E-07	
SURFACE TENSION	(N/M)	1.7975E+00	4.7785E-01	
EMISSIVITY	(-)	8.0000E-01	8.0000E-01	
SUPERFICIAL GAS VEL	(M/S)	9.6417E-03	1.0075E-02	1.1175E-02
BUBBLE RADIUS	(M)	2.0783E-02	2.1643E-02	
BUBBLE VELOCITY	(M/S)	4.5144E-01	4.6069E-01	
VOID FRACTION	(-)	2.2819E-02	2.1841E-02	
BOT CRUST THICKNESS	(M)	7.3964E-02	0.	
HT COEFF, LIQ TO BOT	(W/M2 K)	2.7254E+04	4.3899E+04	
Z-AVE LIQ TEMPERATURE	(K)	1.7709E+03	1.7728E+03	
HT COEFF, LIQ TO TOP	(W/M2 K)	2.8576E+04	4.6233E+04	
TOP CRUST THICKNESS	(M)	0.	0.	
R-AVE LIQ TEMPERATURE	(K)	1.7681E+03	1.7728E+03	
HT COEFF, LIQ TO SID	(W/M2 K)	5.5262E+04	5.3066E+03	
SIDE CRUST THICKNESS	(M)	3.0557E-01	0.	
DECAY HEAT	(W)	2.3880E+06	1.6247E+07	
HEAT TO CONCRETE	(W)	3.6381E+06	4.1592E+06	
HEAT OF REACTION	(W)	6.3528E+05	0.	
INTERLAYER HEAT FLOW	(W)	-1.2295E+06	1.0514E+07	

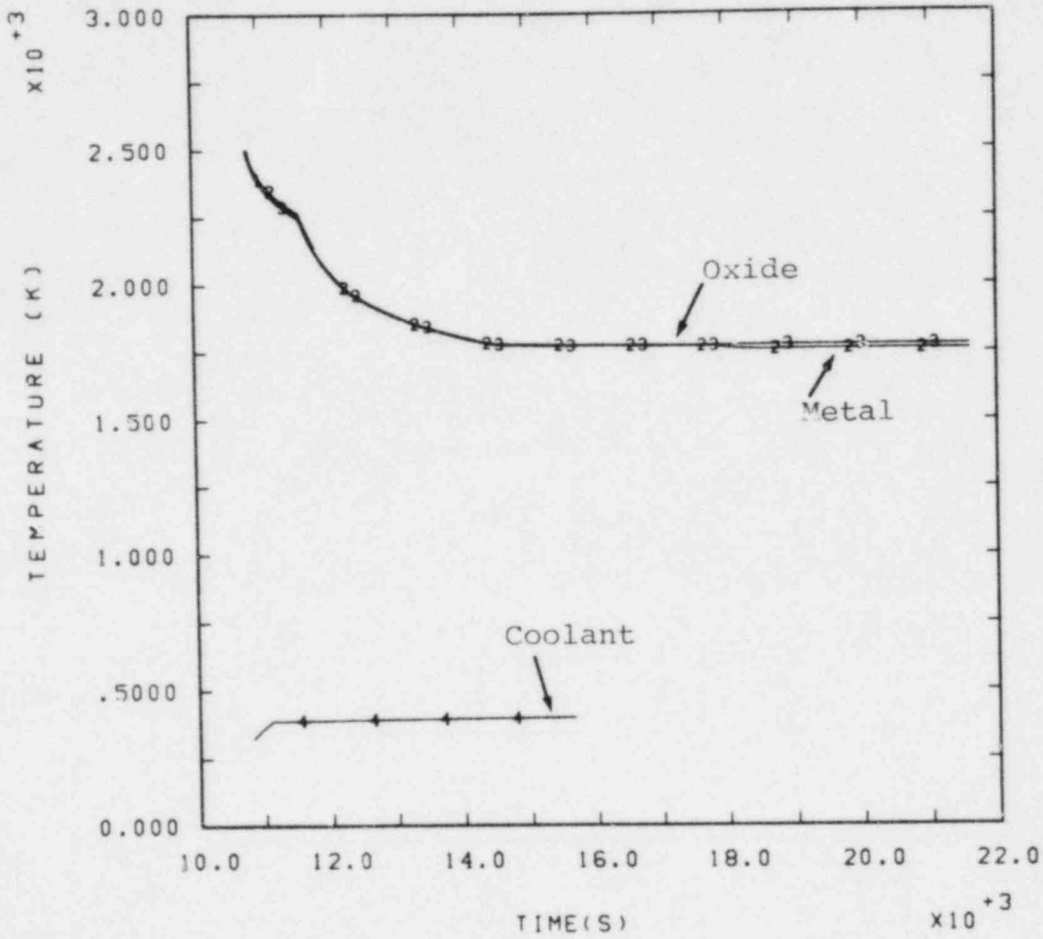

Figure 7.1 Layer Temperature Histories

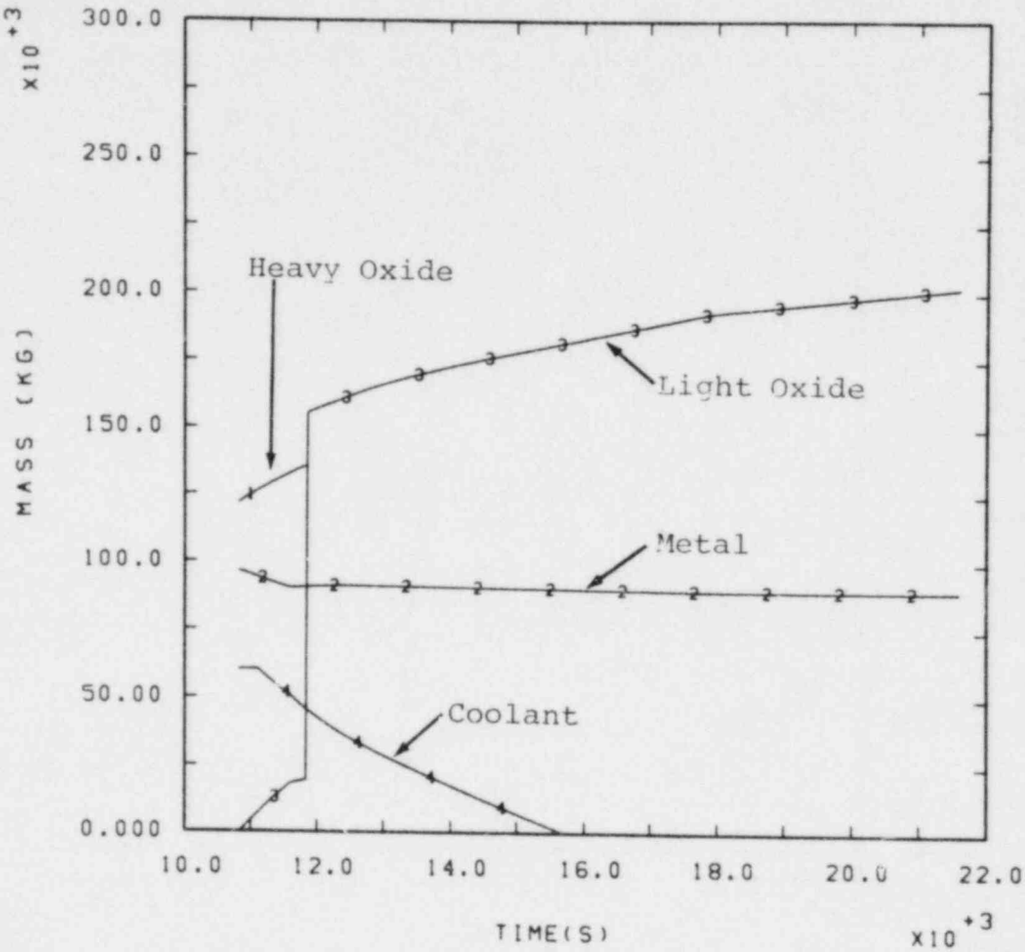

Figure 7.2 Layer Mass Histories

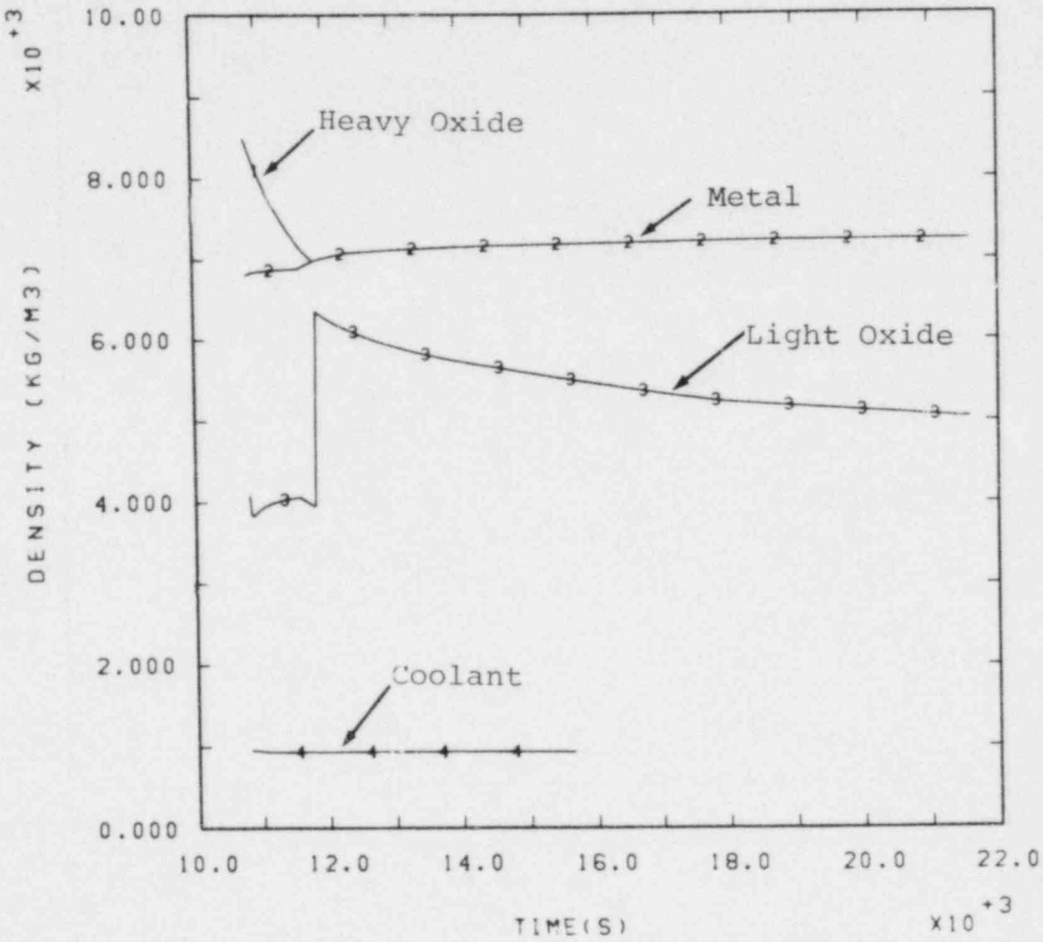

Figure 7.3 Layer Density Histories

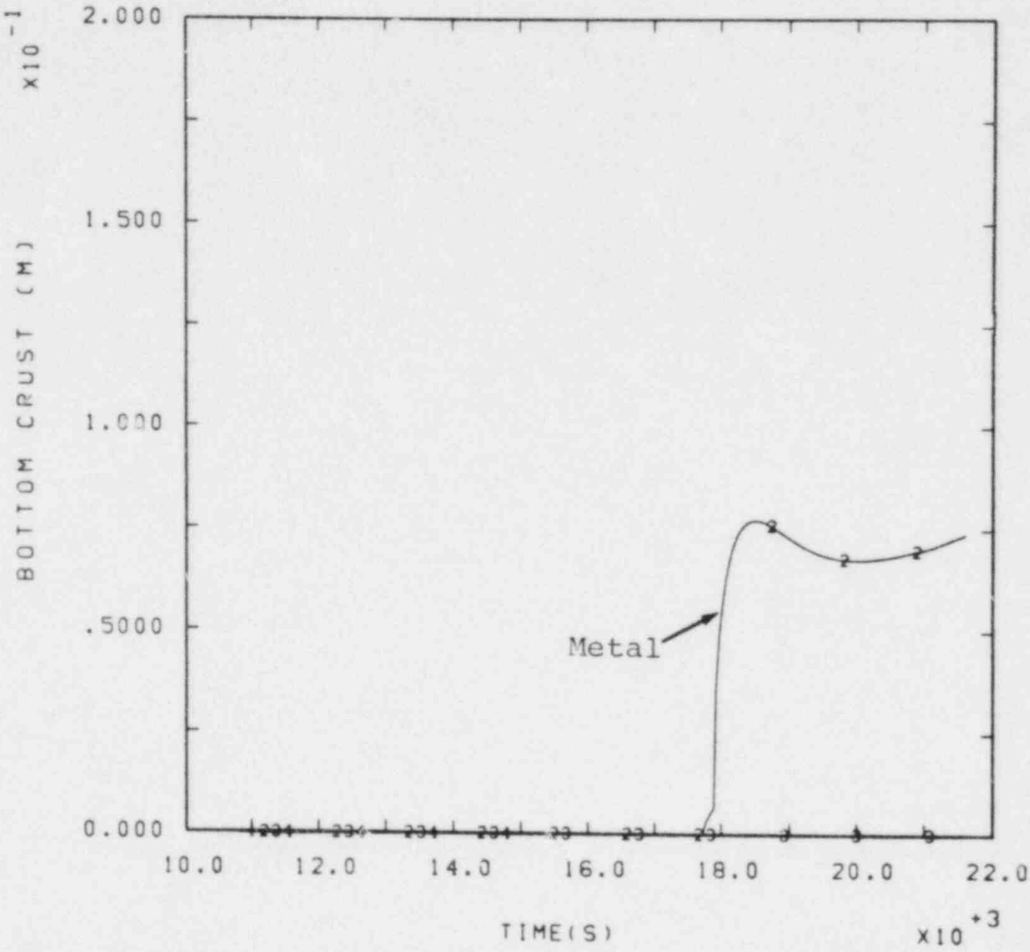

Figure 7.4 Layer Crust Thickness Histories

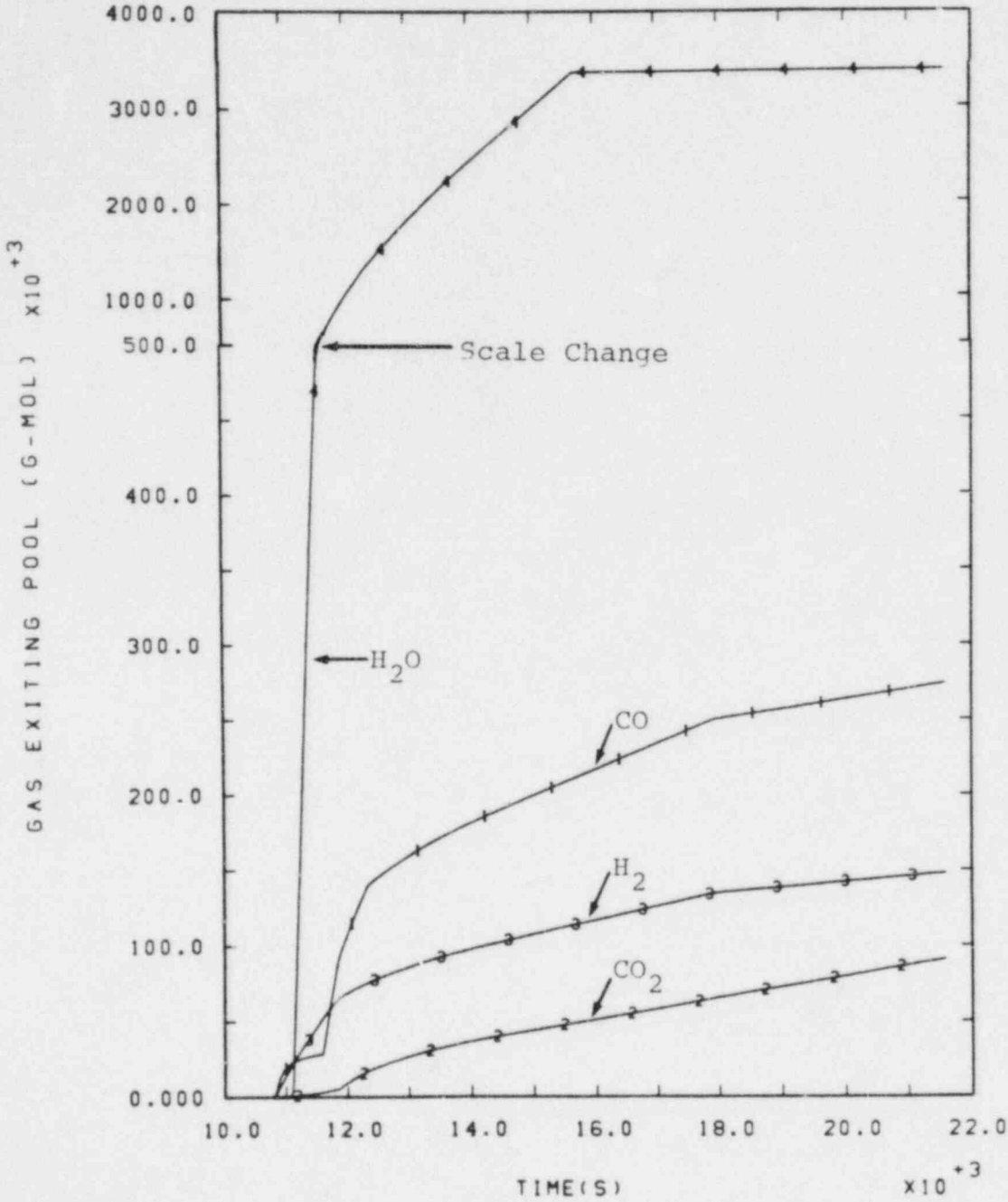

Figure 7.5 Cumulative Gas Generation, including Vaporized Coolant. Note scale change above 5×10^5 g-mole.

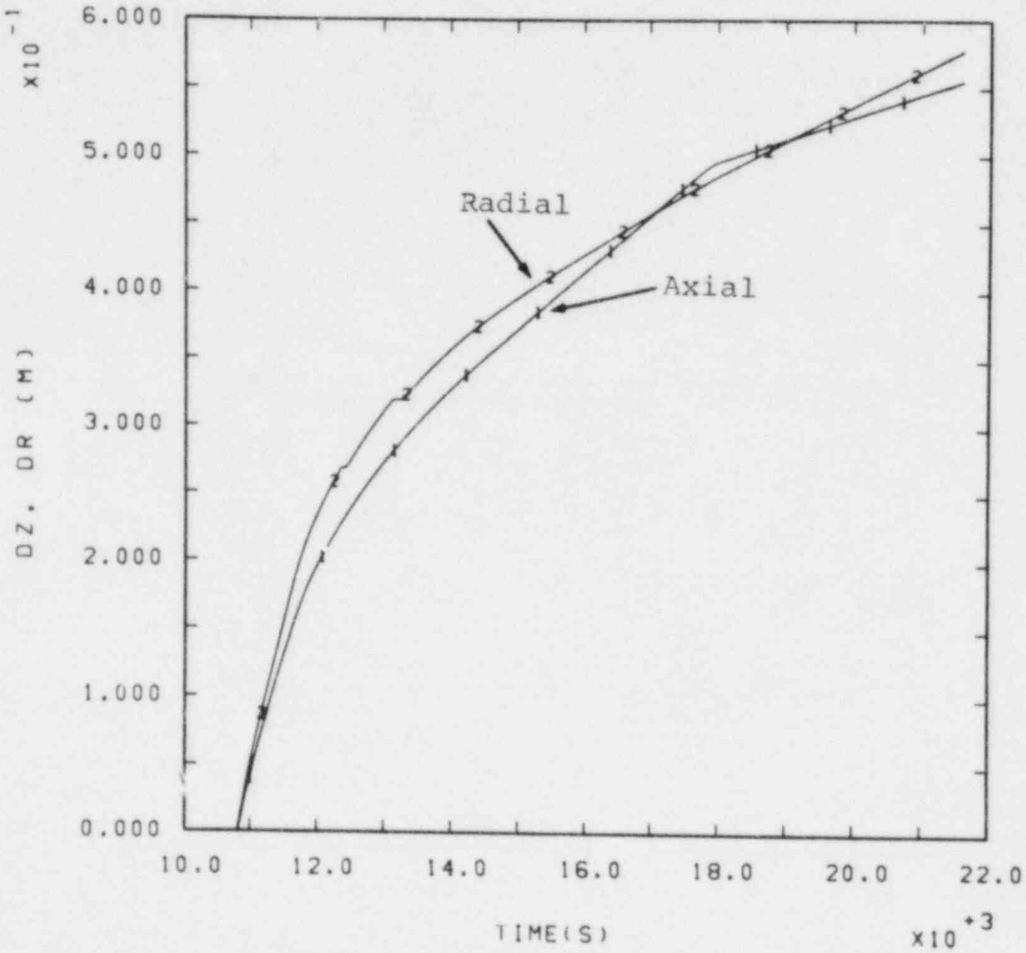

Figure 7.6 Maximum Concrete Erosion Histories

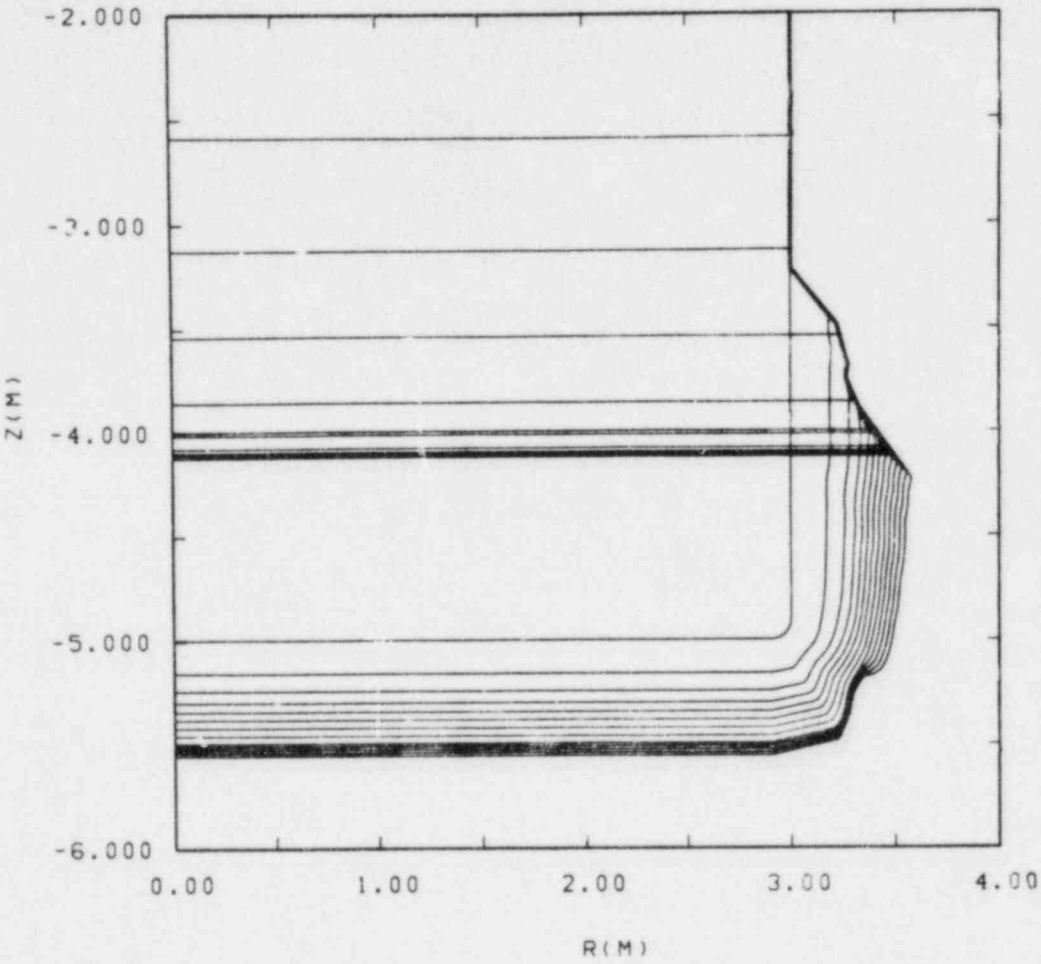

Figure 7.7 Shape of Axisymmetric Cavity at 900s Intervals

REFERENCES

1. Reactor Safety Study, NUREG-75-014 (WASH-1400), USNRC, 1975.

2. W. B. Murfin, A Preliminary Model for Core-Concrete Interactions, SAND77-0370, Sandia National Laboratories, Albuquerque, NM, October 1977.

3. J. F. Muir et al., CORCON-MOD1: An Improved Model for Molten-Core/Concrete Interactions, SAND80-2415, Sandia National Laboratories, Albuquerque, NM, 1981.

4. American National Standard Programming Language FORTRAN, ANSI X3.9-1978, American National Standards Institute, New York, NY, 1978.

5. V. K. Dhir, I. Catton, J. Castle, "Role of Taylor Instability on Sublimation of a Horizontal Slab of Dry Ice." Journal of Heat Transfer, V. 99, No. 3 August 1977, p. 411.

6. H. Alsmeyer, L. Barleon, J. Koster, I. Michael, V. Miller and M. Reimann, A Model Describing the Interaction of a Core Melt with Concrete, NUREG/TR-0039 (translation of KfK2395, Kernforschungszentrum Karlsruhe, F. R. Germany, October 1977), September 1978.

7. J. F. Muir, Response of Concrete to a High Heat Flux on One Surface, SAND77-1467, Sandia National Laboratories, Albuquerque, NM, 1977.

8. J. V. Beck and R. L. Knight, Users Manual for USINT, SAND79-1694, Sandia National Laboratories, Albuquerque, NM, 1979.

9. T. Y. Chu, Radiant Heat Evaluation of Concrete - a Study of the Erosion of Concrete due to Surface Heating, SAND77-0922, Sandia National Laboratories, Albuquerque, NM, 1978.

10. Light Water Reactor Safety Research Program Quarterly (or Semiannual) Report, Nuclear Fuel Cycle Program, Sandia National Laboratories, Albuquerque, NM.

a.	January - March 1976	SAND76-0363	September 1976
b.	October - December 1978	SAND79-0820	July 1979
c.	April - June 1979	SAND79-2057	April 1980
d.	January - March 1980	SAND80-1304 (1 of 4)	July 1980
e.	January - March 1981	SAND81-1216 (1 of 4)	July 1981

f. April - September 1981 SAND81-0006 February 1982
g. Oct 1981 - March 1982 SAND82-1572 December 1982
h. April - September 1982 SAND83-1576 October 1983

11. D. A. Powers et al., Exploratory Study of Molten Core Material/Concrete Interactions July 1975 - March 1977, SAND77-2042, Sandia National Laboratories, Albuquerque, NM, 1978.

12. Advanced Reactor Safety Research Quarterly Report July - September 1982, SAND82-0904 (3 of 4), Sandia National Laboratories, Albuquerque, NM, January 1984.

13. T. G. Theofanous and M. Saito, "An Assessment of Class-9 (Core-Melt) Accidents for PWR Dry-Containment Systems," Nuclear Engineering and Design, Volume 66, pp. 301-332, 1981.

14. G. A. Greene, private communication, March 1983.

15. D. P. Kelly, RADCYL: A Two-Dimensional Radiative Heat Transfer Program for a Cylindrical Enclosure with a Participating Atmosphere, SAND84-0116, Sandia National Laboratories, Albuquerque, NM, to be published.

16. K. D. Bergeron et al., User's Manual for CONTAIN, A Computer Code for Severe Nuclear Reactor Accident Containment Analysis, SAND84-1204, Sandia National Laboratories, Albuquerque, NM, to be published.

17. D. E. Bennett, Power Level-Burnup Parametric Study, memorandum to M. Berman, Sandia National Laboratories, Albuquerque, NM, September 10, 1979.

18. D. E. Bennett, SANDIA-ORIGEN User's Manual, SAND79-0299 (NUREG/CR-0987), Sandia National Laboratories, Albuquerque, NM, October 1979.

19. D. A. Powers, private communication, 1980.

20. V. V. Konsetov, "Heat Transfer during Bubbling of Gas Through Liquid," Int. J. Heat Mass Transfer, Vol. 9, pp. 1103-1108, 1966.

21. F. G. Blottner, Hydrodynamics and Heat Transfer Characteristics of Liquid Pools with Bubble Agitation, SAND79-1132 (NUREG/CR-0944), Sandia National Laboratories, Albuquerque, NM, November 1979.

22. T. Ginsberg and G. A. Greene, "BNL Program in Support of LWR Degraded Core Accident Analysis," in Proceedings of the U. S. Nuclear Regulatory Commission Tenth Water Reactor Safety Research Information Meeting, NUREG/CP-0041, Volume 2, pp. 364-395, 1983.

23. H. Werle, "Modelexperimente zum Kernschmelzen," Halbjahresbericht 1978/1, PNS 4332, 1978.

24. H. Werle, Enhancement of Heat Transfer between Two Horizontal Liquid Layer, by Gas Injection at the Bottom, KfK 3223, Kernforschungszentrum Karlsruhe, FRG, 1981.

25. J. Szekely, "Mathematical Model for Heat or Mass Transfer at the Bubble-Stirred Interface of Two Immiscible Fluids," International Journal of Heat and Mass Transfer, Volume 6, pp. 417-422, 1963.

26. A. E. Bergles et al., Two-Phase Flow and Heat Transfer in the Power and Process Industries, Chapter 7, Hermisphere Publishing Corporation, Washington, McGraw Hill, New York, 1981.

27. J. H. Keenan et al., Steam Tables, Thermodynamic Properties of Water Including Vapor, Liquid, and Solid Phases (International System of Units-S.I.), John Wiley and Sons, New York, 1978.

28. W. M. Rohsenow, "A Method of Correlating Heat Transfer for Surface Boiling of Liquids," Trans. ASME, Volume 74, pp. 969-976, 1952, as cited in Reference 27.

29. N. Zuber, "On Stability of Boiling Heat Transfer," Trans. ASME, Volume 80, pp.711-720, 1958, as cited in Reference 27.

30. N. Zuber et al., "The Hydrodynamic Crisis in Pool Boiling of Saturated and Subcooled Liquids," International Developments in Heat Transfer, Part II, pp. 230-235, ASME, New York, 1961, as cited in Reference 27.

31. W. H. Rohsenow, "Boiling," in Handbook of Heat Transfer, pp. 13-28, McGraw-Hill, New York, 1973, as cited in Reference 27.

32. H. J. Ivey, "Acceleration and the Critical Heat Flux in Pool Boiling," Chartered Mechanical Engineering, Volume 9, pp. 413-427, 1962, as cited in Reference 27.

33. P. J. Berenson, "Transition Boiling Heat Transfer from a Horizontal Surface," Journal of Heat Transfer, Volume 83, pp. 351-358, 1961, as cited in Reference 27.

34. W. H. McAdams, Heat Transmission, McGraw-Hill Book Co., New York, NY, 1954.

35. F. A. Kulacki and R. J. Goldstein, J. Fluid Mech., Volume 55, p. 271, 1975.

36. F. A. Kulacki and M. E. Nagle, J. Heat Transfer, Volume 97, p. 204, 1975.

37. F. A. Kulacki and A. A. Emara, Trans ANS Volume 22, p. 447, 1975.

38. R. T. Cole, Jr., "A Crust Formation and Refreezing Model for Molten-Fuel/Concrete Interactions Codes," Paper 12.5 in Proceedings, International Meeting on Light Water Reactor Severe Accident Evaluation, Cambridge, MA, 1983.

39. D. A. Powers and F. E. Arellano, Direct Observation of Melt Behavior During High Temperature Melt/Concrete Interactions, SAND81-1754 (NUREG/CR-2283), Sandia National Laboratories, Albuquerque, NM, January 1982.

40. H. Alsmeyer and M. Reimann, "On the Heat and Mass Transport Processes of a Horizontal Melting or Decomposing Layer under a Molten Pool," Nuclear Reactor Safety Heat Transfer, Winter Annual Meeting ASME, Atlanta, GA, pp 47-53, 1977.

41. A. S. Benjamin, "Core-Concrete Molten Pool Dynamics and Interfacial Heat Transfer," Proceedings of the ANS/ASME/NRC International Topical Meeting on Nuclear Reactor Thermal-Hydraulics, NUREG/CP-0014, Vol. 2, p. 1437, October 1980.

42. M. Lee, M. S. Kazimi, and G. Brown, "A Heat Transfer Model for the Corium/Concrete Interface," Paper 12.6 in Proceedings, International Meeting of Light Water Reactor Severe Accident Evaluation, Cambridge, MA, 1983.

43. J. Persh, A Procedure for Calculating the Boundary Layer Development in the Region of Transition from Laminar to Turbulent Flow, NAVORD Report 4438, March 1957.

44. R. W. Wooton and H. I. Avci, MARCH (Meltdown Accident Response Characteristics) Code Description and Users Manual, BMI-2064 (NUREG/CR-1711) Battelle Columbus Laboratories, Columbus, Ohio, October 1980.

45. F. B. Cheung, S. H. Chan, T. C. Chawla, and D. H. Cho, "Radiative Heat Transfer in a Heat Generating and Turbulently Convecting Fluid Layer," Int. J. Heat Mass Transfer 23, pp. 1313-1323, 1980.

46. Advanced Reactor Safety Research Quarterly Report July - September 1981, SAND81-1529 (3 of 4), Sandia National Laboratories, Albuquerque, NM, 1982.

47. K. C. Kwong, R. A. S. Beck, and T. C. Derbidge, CORCON Program Assistance, ACUREX Final Report FR-79-10/AS, ACUREX Corporation/Aerotherm Aerospace Systems Division, Mt. View, CA, July 1979.

48. F. H. Van Zeggeren and S. H. Storey, The Computation of Chemical Equilibrium, Cambridge University Press, Cambridge, MA, 1970.

49. G. B. Wallis, One-Dimensional, Two-Phase Flow, McGraw-Hill, Inc., New York, NY, 1969.

50. E. R. Hosler and J. W. Westwater, "Film Boiling on a Horizontal Plate," ARS Journal, pp. 553-558, April 1962.

51. W. L. Haberman and R. K. Morton, An Experimental Investigation of the Drag and Shape of Air Bubbles Rising in Various Liquids, DTMB-802, David Taylor Model Basin, Navy Dept., Washington, DC, (1953).

52. R. J. Andreini, J. S. Foster, and R. W. Callen, "Characterization of Gas Bubbles Injected into Molten Metals Under Laminar Flow Conditions," Metallurgical Transactions, Volume 8B, pp. 625-631, December 1977.

53. G. A. Greene, and T. Ginsberg, "BNL Program in Support of LWR Degraded Core Accident Analysis," in Proceedings of the U. S. Nuclear Regulatory Commission Ninth Water Reactor Safety Research Information Meeting, NUREG/CP-0024 Volume 3, 1982.

54. D. A. Powers, private communication, 1983.

55. D. A. Powers and A. W. Frazier, VISRHO: A Computer Subroutine for Estimating the Viscosity and Density of Complex Silicate Melts, SAND76-0649, Sandia National Laboratories, Albuquerque, NM (June 1977).

56. Core-Meltdown Experimental Review, SAND74-0382 (NUREG-0205), Sandia National Laboratories, Albuquerque, NM, March 1977.

57. R. C. Weast, Ed., Handbook of Chemistry and Physics, CRC Press, Inc., 1976.

58. JANAF Thermochemical Tables, Physicochemical Studies, DOW Chemical USA, Midland, Michigan (including supplements).

59. G. V. Samsonov, Ed., The Oxide Handbook, translated from Russian by C. N. Turton and T. I. Turton, IFI/Plenum Press, New York, 1973.

60. R. A. Robie, B. S. Hemingway, and J. R. Fisher, Thermodynamic Properties of Minerals, Geological Survey Bulletin 1452, U. S. Department of Interior, U. S. Government Printing Office, Washington, DC, 1978.

61. Y. S. Touloukian, Ed., Thermophysical Properties of Matter, The TPRC Data Series, Vols. 1-8, IFI/Plenum Press, New York, 1970.

62. J. Kendell and K. P. Monroe, "The Viscosity of Liquids. III Ideal Solution of Solids in Liquids," Journal of the American Chem. Soc., Volume 39, No. 9, p. 1802, September 1917.

63. H. R. Shaw, "Viscosities of Magmatic Silicate Liquids: An Empirical Method of Prediction," American Journal of Science, Volume 272, pp. 870-893, 1972.

64. Y. Bottinga and D. F. Weill, "The Viscosity of Magmatic Silicate Liquids: A Model for Calculation," American Journal of Science, Volume 272, pp. 438-475, 1972.

65. Y. Ogino, F. O. Borgmann, and M. G. Frohberg, "On the Viscosity of Liquid Iron," Japan Inst. of Metals Journ., Volume 37, p. 1230, 1973.

66. Kunitz, Journal General Physiology, Volume 9, p. 715 (1926).

67. J. E. Parrott and A. D. Stuckes, Thermal Conductivity of Solids, Pion Limited, London, 1975.

68. G. R. Speich, "Cr-Fe-Ni (Chromium-Iron-Nickel)," Metals Handbook, American Society for Metals, Metals Park, Ohio, Volume 8, p. 424, 1973.

69. D. A. Powers, private communication, March 1984.

70. D. P. Kelly and M. A. Ellis, umpublished sensitivity studies for CORCON-MOD1.

DISTRIBUTION:

Division of Technical Information & Document Control
USNRC Distribution Contractor
U. S. Nuclear Regulatory Commission
15700 Crabbs Branch Way
Rockville, MD 20850
275 copies for R3

U. S. Nuclear Regulatory Commission (17)
Office of Nuclear Regulatory Research
Washington, DC 20555
Attn: O. E. Bassett
S. B. Burson (5)
J. Costello
M. Cunningham
R. T. Curtis
C. Kelber
J. Larkins
T. Lee
R. Minogue
M. Silberberg
D. F. Ross
J. Telford
T. Walker

U. S. Nuclear Regulatory Commission (6)
Office of Nuclear Regulatory Regulation
Washington, DC 20555
Attn: W. R. Butler
A. R. Marchese
J. Rosenthal
Z. Rosztoczy
T. P. Speis
C. G. Tinkler

U. S. Department of Energy (2)
Operational Safety Division
P.O. Box 5400
Albuquerque, NM 87185
Attn: J. R. Roeder
D. K. Nowlin

U. S. Department of Energy
Office of Nuclear Safety Coordination
Washington, DC 20545
Attn: R. W. Barber

Argonne National Laboratory (3)
9700 South Cass Avenue
Argonne, IL 60439
Attn: L. Baker
Dae Cho
D. Pedersen

Brookhaven National Laboratory (4)
Upton, NY 11973
Attn: G. A. Greene
T. Ginsberg
T. Pratt
N. Tutu

Oak Ridge National Laboratory (3)
Post Office Box Y
Oak Ridge, TN 37830
Attn: T. Kress
S. Hodge
C. Hyman

Battelle Columbus Laboratory (3)
505 King Avenue
Columbus, OH 43201
Attn: R. Denning
P. Cybulskis
J. Gieseke

Battelle Pacific Northwest Laboratories
P. O. Box 999
Richland, WA 99352
Attn: F. E. Panisko

EG&G Idaho, Inc.
P. O. Box 1625
Idaho Falls, ID 83415
Attn: Ms. LaRene Smith

Los Alamos National Laboratory
P. O. Box 1663
Los Alamos, NM 87545
Attn: M. L. Stevenson

Prof. I. Caton
University of California
School of Eng. and Applied Science
Los Angeles, CA 90024

Massachusetts Institute of Technology (2)
Department of Nuclear Engineering
Cambridge, MA 02139
Attn: Prof. M. Kazimi
Mr. M. Lee

University of Wisconsin (3)
Nuclear Engineering Department
1500 Johnson Drive
Madison, WI 53706
Attn: Prof. M. L. Corradini
Prof. G. Moses
Mr. F. Gonzalez

Prof. R. Seale
University of Arizona
Department of Nuclear Engineering
Tuscon, AZ 85721

Electric Power Research Institute (4)
3412 Hillview Avenue
Palo Alto, CA 94303
Attn: G. Thomas
R. Vogel
D. Squarer
B. R. Sehgal

Bechtel Power Corporation
P. O. Box 3965
San Francisco, CA 94119
Attn: R. Tosetti

Westinghouse Electric Corporation (3)
Power Systems
Monroeville Nuclear Center
P. O. Box 355
Pittsburg, PA 15320
Attn: L. Hochreiter
L. Stahl
R. J. Lutz, Jr

Northeast Utilities
P.O. Box 270
Hartford, CN 06101
Attn: W. S. Chow

NUS Corporation (2)
4 Research Place
Rockville, MD 20850
Attn: P. J. Fulford
R. Sherry

Offshore Power System
8000 Arlington Expressway
Box 8000
Jacksonville, FL 32211
Attn: D. H. Walker

Tennessee Valley Authority
Civil Engineering Branch
400 West Summit Hill Drive, W9D224
Knoxville, TN 37902
Attn: R. O. Barnett, Chief

General Electric Company
175 Kurtner Avenue
Mail Code 766
San Jose, CA 95125
Attn: J. T. Teng

General Electric Co. ASRD
310 Deguigne Drive
P. O. Box 50H
Sunnyvale, CA 94086
Attn: Mr. Steven Lam

Power Authority State of New York
10 Columbus Circle
New York, NY 10019
Attn: Mr. Richard Deem

M. Fontana, Director
IDCOR Program
Technology for Energy Inc.
P. O. Box 22996
10770 Dutchtown Road
Knoxville, TN 37922

Technology for Energy Corporation
One Energy Center, Pellissippi Pkwy
Knoxville, TN 37922
Attn: H. A. Mitchell

Fauske & Associates, Inc. (2)
16W070 West 83rd Street
Burr Ridge, IL 60521
Attn: R. E. Henry
M. Plys

Ms. Cathy Anderson
Nuclear Safety Oversight Commission
1133 15th Street NW
Room 307
Washington, DC 20005

S. J. Niemczyk
Union of Concerned Scientists
1346 Connecticut Avenue NW
Suite 1101
Washington, DC 20036

AEC, Ltd.
Whiteshell Nuclear Research Establishment
Pinawa, Manitoba
Canada
Attn: D. Torgerson

United Kingdom Atomic Energy Authority (6)
Wigshaw Lane, Culcheth
Warrington WA3 4NE
England
Attn: F. Briscoe
M. R. Hayns
R. S. Peckover
F. Allen
F. Abbey
A. R. Edwards

United Kingdom Atomic Energy Authority (2)
Risley
Warrington WA3 6AT
Cheshire
England
Attn: B. Cowking
D. Hicks

United Kingdom Atomic Energy Authority
Culham Laboratory
Abingdon, Oxon OX14 3DB
England
Attn: Dr. B. D. Turland

Atomic Energy Establishment
Winfrith
Dorchester, Dorset DT2 8DH
England
Attn: Dr. A. T. D. Butland

Dr. R. J. Stubbs
HMNII, HSE
Thames House North
Millbank
London SW1P 4QJ
England

Berkley Nuclear Laboratory (2)
Berkley GL13 9PB
Gloucestershire
England
Attn: N. E. Buttery
J. E. Antill

Gesellshaft fuer Reaktorsicherheit (GRS) mbH (2)
Forschungsgelaende
8046 Garching
Federal Republic of Germany
Attn: H. L. Jahn
E. F. Hicken

Gesellshaft fuer Reaktorsicherheit (GRS) mbH (2)
Glockengasse 2
5000 Koeln 1
Federal Republic of Germany
Attn: Dr. K. Bracht
Dr. M. V. Banaschik

Kernforschungszentrum Karlsruhe (15)
Postfach 3640
D-7500 Karlsruhe 1
Federal Republic of Germany
Attn: Dr. J. P. Hosemann (PNS-PL)
Dr. H. Alsmeyer (IRB)
Dr. M. Reimann (IRB)
Dr. R. Cole (IRB) (10)
Dr. S. Hagen (IT-CP)
Dr. Heusener (PSB)

Kraftwerk Union (2)
Hammerbacher Strasse 12 & 14
Postfach 3220
D-8520 Erlangen 2
Federal Republic of Germany
Attn: Dr. M. Peehs
Dr. K. Hassmann

Prof. F. Mayinger
Technische Universitaet Hannover
3000 Hannover 1
Federal Republic of Germany

Dr. Reinecke
Ingenieurbuero fuer Rechnung und Entwicklung (IVA)
Kurzer Kamp 12
D-3016 Seelze 2
Federal Republic of Germany

B. Tolley
Dir. of Research, Science, and Education
CEC
Rue de la Loi 200
1049 Brussels
Belgium

Swedish State Power Board
El-Och Vaermeteknik
Sweden
Attn: E. Ahlstroem

Dr. Watanabe
Power Reactor Nuclear Fuel Development Corporation
Fast Breeder Reactor Development Project
9-13, 1-Chome, Akasaka
Minato-Ku, Tokyo
Japan

1633 D. P. Kelly
6000 E. H. Beckner
6400 A. W. Snyder
6411 V. L. Behr
6411 R. D. Gasser
6411 F. E. Haskin
6412 A. L. Camp
6420 J. V. Walker
6421 T. R. Schmidt
6422 D. A. Powers (5)
6422 J. E. Brockmann
6422 E. R. Copus
6422 J. E. Gronager
6422 W. Tarbell
6423 P. S. Pickard
6423 K. Muramatsu
6425 W. J. Camp
6425 D. R. Bradley
6425 M. Pilch
6427 M. Berman
6440 D. A. Dahlgren
6442 W. A. von Riesemann
6444 S. L. Thompson (7)
6444 P. N. Demmie
6444 J. M. McGlaun
6444 R. M. Summers
6444 J. L. Orman
6444 S. W. Webb
6445 J. H. Linebarger

6446 L. L. Bonzon
6447 D. L. Berry
6449 K. D. Bergeron
6449 P. R. Shire
3141 C. M. Ostrander (5)
3151 W. L. Garner
8024 M. A. Pound

NRC FORM 335 (2-84) NRCM 1102, 3201, 3202

U.S. NUCLEAR REGULATORY COMMISSION

BIBLIOGRAPHIC DATA SHEET

SEE INSTRUCTIONS ON THE REVERSE

1. REPORT NUMBER (Assigned by TIDC, add Vol. No., if any)
NUREG/CR-3920
SAND84-1246

2. TITLE AND SUBTITLE
CORCON-MOD2: A COMPUTER PROGRAM FOR ANALYSIS OF MOLTEN-CORE CONCRETE INTERACTIONS

3. LEAVE BLANK

4. DATE REPORT COMPLETED
MONTH: August YEAR: 1984

5. AUTHOR(S)
R. K. Cole, Jr.
D. P. Kelly
M. A. Ellis

6. DATE REPORT ISSUED
MONTH: August YEAR: 1984

7. PERFORMING ORGANIZATION NAME AND MAILING ADDRESS (Include Zip Code)
Thermal/Hydraulic Analysis Division 6444
Sandia National Laboratories
P. O. Box 5800
Albuquerque, NM 87185

8. PROJECT/TASK/WORK UNIT NUMBER

9. FIN OR GRANT NUMBER
A-1019

10. SPONSORING ORGANIZATION NAME AND MAILING ADDRESS (Include Zip Code)
Division of Accident Evaluation
Office of Nuclear Regulatory Research
U. S. Nuclear Regulatory Commission
Washington, DC 20555

11a. TYPE OF REPORT
Technical

b. PERIOD COVERED (Inclusive dates)

12. SUPPLEMENTARY NOTES

13. ABSTRACT (200 words or less)

CORCON is a computer code for modelling the interactions between molten core materials and concrete, such as might occur following a core meltdown accident in a Light Water Reactor. It may also be applied to experiments which simulate such accident conditions. The code predicts the behavior of the system, including heat transfer, concrete ablation, cavity shape change, and gas generation. The first version, CORCON-MOD1, was released in 1981. This report is a complete users' manual and reference for the updated version, CORCON-MOD2. The major changes are the inclusion of models for solidification of the melt and for its (non-explosive) interactions with coolant water. In addition, a number of improvements have been made in response to experience with CORCON-MOD1. The new code remains compatible with the old in the sense that MOD2 will accept any input data set which was accepted by MOD1.

14. DOCUMENT ANALYSIS — a. KEYWORDS/DESCRIPTORS

b. IDENTIFIERS/OPEN-ENDED TERMS

15. AVAILABILITY STATEMENT

16. SECURITY CLASSIFICATION
(This page) Uncl
(This report) Uncl

17. NUMBER OF PAGES
193

18. PRICE

120555078877 1 1AN1R3
US NRC
ADM-DIV OF TIDC
POLICY & PUB MGT BR-PDR NUREG
W-501
WASHINGTON DC 20555